Nonlinear Dynamics **23:** 105–164, 2000.

Bifurcations in Nonlinear Discontinuous Systems

R. I. LEINE, D. H. VAN CAMPEN, and B. L. VAN DE VRANDE
Department of Mechanical Engineering, Eindhoven University of Technology, P.O. Box 513, 5600 MB Eindhoven, The Netherlands

(Received: 1 June 1999; accepted: 22 March 2000)

Abstract. This paper treats bifurcations of periodic solutions in discontinuous systems of the Filippov type. Furthermore, bifurcations of fixed points in non-smooth continuous systems are addressed. Filippov's theory for the definition of solutions of discontinuous systems is surveyed and jumps in fundamental solution matrices are discussed. It is shown how jumps in the fundamental solution matrix lead to jumps of the Floquet multipliers of periodic solutions. The Floquet multipliers can jump through the unit circle causing discontinuous bifurcations. Numerical examples are treated which show various discontinuous bifurcations. Also infinitely unstable periodic solutions are addressed.

Keywords: Bifurcations, stick-slip vibrations, discontinuous systems, non-smooth systems.

1. Introduction

This paper studies bifurcations in discontinuous dynamical systems. A dynamical system can be expressed as a set of first-order ordinary differential equations. Before proceeding we should clarify what we mean with the term '*discontinuous dynamical system*' [50].

1.1. Discontinuous Systems

Physical systems can often operate in different modes, and the transition from one mode to another can sometimes be idealized as an instantaneous, discrete transition. Since the time scale of the transition from one mode to another is often much smaller than the scale of the dynamics of the individual modes, it may be very advantageous to model the transitions as being instantaneous. The mathematical modeling of physical systems therefore leads to discontinuous dynamical systems, which switch between different modes, where the dynamics in each mode is given by a different set of differential equations.

Discontinuous dynamical systems can be divided into three types according to their degree of discontinuity:

1. Non-smooth continuous systems with a discontinuous Jacobian, like systems with purely elastic one-sided supports. Those systems have a continuous vector field but the vector field is non-smooth.
2. Systems described by differential equations with a discontinuous right-hand side, also called *Filippov systems* (Section 2). The vector field of those systems is discontinuous. Examples are systems with visco-elastic supports and dry friction.
3. Systems which expose discontinuities (or jumps) in the state, like impacting systems with velocity reversals. The latter category of systems will not be treated in this paper for reasons to be clarified.

In all three cases, a kind of switching is involved and those systems are therefore often called *switching systems* or *differential equations with switching conditions* [14]. In the field of Systems and Control theory, the term *hybrid system* is frequently used for systems composed of continuous differential equations and discrete event parts [7]. Nowadays, the term *hybrid system* is used for any system which expose a mixed continuous and discrete nature, even if the system is not controlled [24].

1.2. Literature Survey

The amount of publications on discontinuous systems is vast. We will only survey the literature in the mathematical and mechanical field.

The mathematical literature is mainly concerned with existence and uniqueness of solutions of discontinuous differential equations. The fundamental work of Filippov [17, 18] extends a discontinuous differential equation to a differential inclusion (see Section 2). More recent results on differential inclusions can be found in [4, 8]. Deimling and Szilagyi [12], Fečkan [15] and Kunze and Küpper [29] treat dry friction problems as differential inclusions and address existence of periodic solutions. Aizerman and Gantmakher [1] derived jumping conditions of fundamental solution matrices (see Section 3) and their results were extended to systems with a discontinuous state by Müller [34]. Contemporary literature in the field of control theory focuses on hybrid systems and complementarity systems, which encompasses also Filippov systems [24, 50].

Publications from a mechanical point of view are mainly concerned with dry friction/stick-slip oscillations and impact. An extensive literature review on dry friction models can be found in [3, 26]. Dynamics of impacting systems (not treated in this paper) is reviewed in depth by Brogliato [7]. Pfeiffer and Glocker [22, 42] apply the theory of Linear Complementarity to multibody systems with impact and friction. Non-existence of solutions of impacting systems is discussed in [7, 21].

During the last decades many textbooks about bifurcation theory for smooth systems appeared and bifurcations of smooth vector fields are well understood [23, 30, 47]. However, little is known about bifurcations of discontinuous vector fields.

Andronov et al. [2] treat periodic solutions of discontinuous systems. They revealed many aspects of discontinuous systems and addressed periodic solutions with sliding modes (Section 2) but did not treat periodic solutions in discontinuous systems with regard to Floquet theory.

Many publications deal with bifurcations in discontinuous Filippov systems. Published bifurcation diagrams were often constructed from data obtained by brute force techniques and only show stable branches of periodic solutions [5, 6, 11, 20, 25, 29, 39, 43, 48, 52] (this list is far from complete). Bifurcation diagrams calculated with path-following techniques show bifurcations to unstable periodic solutions but the bifurcations behave as conventional bifurcations in smooth systems [49, 51].

Dankowicz and Nordmark [11] study bifurcations of stick-slip oscillations but the applied friction model, with internal states which allow for history and rate dependence, yields a non-smooth continuous system. A small number of publications show non-conventional bifurcations in discontinuous Filippov systems [13, 53]. Yoshitake and Sueoka [53] also address Floquet theory and remark that the Floquet multipliers ‘jump’ at the bifurcation point.

The work of Feigin [16] and di Bernardo et al. [9, 10] studies non-conventional bifurcation in Filippov systems and refers to those bifurcations as ‘C-bifurcations’ (Section 6). Non-

conventional bifurcations of non-smooth discrete mappings were also addressed by Nusse and Yorke [38].

Another type of non-conventional bifurcation is the 'grazing bifurcation', which occurs in impacting systems. Bifurcations in impacting systems are studied in [7, 19, 27, 32, 37, 41].

Numerical methods to calculate periodic solutions in discontinuous systems can be found in [14, 31, 33, 45].

1.3. Objective and Scope

The theory of bifurcations in smooth dynamical systems is well developed. This is not the case for bifurcations in discontinuous dynamical systems. Many practical problems in engineering are related to vibrations caused or influenced by physical discontinuities. A mathematical model of the physical system may fall in one of the three classes of discontinuous dynamical systems mentioned previously depending on the way of modeling. This urges for a description of the bifurcation behaviour of discontinuous dynamical systems. Existence of solutions for systems with a discontinuous state is not guaranteed. This complicates the study of bifurcations of systems with a discontinuous state. In this sense Filippov systems are less complex as existence of solutions is guaranteed (under some conditions, see Section 2). We will therefore confine our study to Filippov systems and non-smooth continuous systems (which can be regarded as a subclass of Filippov systems). Filippov systems embrace systems with dry friction and compliant impact but not systems with impact between rigid bodies. Filippov systems arise also in models of electrical circuits with (ideal) diode elements, controlled systems with encoders and in other scientific fields. In this paper, however, we will focus on mechanical systems although the results apply to Filippov systems in general. Bifurcations of periodic solutions of Filippov systems are closely related to bifurcations of fixed points in non-smooth continuous systems (discontinuous Jacobian). We will therefore also address bifurcations of fixed points in non-smooth continuous systems and study the relation of those bifurcations to bifurcations of periodic solutions in Filippov systems.

Filippov systems expose non-conventional bifurcations, which we will call *discontinuous bifurcations*. The basic idea is that Floquet multipliers of Filippov systems can jump when a parameter of the system is varied. If a Floquet multiplier jumps through the unit circle in the complex plane a discontinuous bifurcation is encountered. The paper explains how the discontinuous bifurcations come into being through jumps of the fundamental solution matrix and shows how discontinuous bifurcations are related to conventional bifurcations in smooth systems.

The paper contains an introductory part (Sections 2 and 3) which surveys the theory of Filippov and of Aizerman and Gantmakher. It then proceeds with an investigation of bifurcations in discontinuous dynamical systems which is the actual body of the paper.

2. Filippov Theory

2.1. The Construction of a Solution

A dynamical system is usually expressed as the following set of ordinary differential equations

$$\dot{\underset{\sim}{x}}(t) = \underset{\sim}{f}(t, \underset{\sim}{x}(t)), \quad \underset{\sim}{x}(t) \in \mathbb{R}^n, \tag{2.1}$$

where $\underset{\sim}{x}$ is the n-dimensional state vector and $\underset{\sim}{f}(t, \underset{\sim}{x}(t))$ is the set of right-hand sides describing the time derivative of the state vector. A dot $(\dot{})$ denotes differentiation with respect to

time t. We will assume that $\underset{\sim}{f}(t, \underset{\sim}{x})$ is linearly bounded [8], i.e. there exists positive constants γ and c such that

$$\|\underset{\sim}{f}(t, \underset{\sim}{x})\| \leq \gamma \|\underset{\sim}{x}\| + c, \quad \forall (t, \underset{\sim}{x}). \tag{2.2}$$

If the vector field is smooth, that is $\underset{\sim}{f}$ is continuously differentiable up to any order both in $\underset{\sim}{x}$ and t, then a solution $\underset{\sim}{x}(t)$ of the system (2.1) exists for any given initial condition and is globally unique. In fact, smoothness of the vector field is not a necessary condition for existence and uniqueness of the solution (cf. [8, theorem 1.1, p. 178]). Existence and uniqueness of solutions is guaranteed for non-smooth continuous systems if $\underset{\sim}{f}(t, \underset{\sim}{x})$ is linearly bounded (2.2) and locally Lipschitz, i.e. there exists a constant $L > 0$ such that

$$\|\underset{\sim}{f}(t, \underset{\sim}{x}) - \underset{\sim}{f}(t, \underset{\sim}{y})\| \leq L\|\underset{\sim}{x} - \underset{\sim}{y}\|, \quad \forall \underset{\sim}{x}, \underset{\sim}{y} \in \mathbb{R}^n.$$

However, differential equations stemming from physical systems may be discontinuous, i.e. the right-hand side $\underset{\sim}{f}$ can be discontinuous in $\underset{\sim}{x}$. The theory of Filippov [17, 18] gives a generalized[1] definition of the solution of differential equations which incorporates systems with a discontinuous right-hand side. The solution $\underset{\sim}{x}(t)$ in the sense of Filippov to a differential equation with a discontinuous right-hand side (also called Filippov systems, see Section 1) is continuous in time. Systems with a discontinuous solution, i.e. 'jumps' in $\underset{\sim}{x}(t)$ at certain time instances t (e.g. systems with impact between rigid bodies), are not described by the theory of Filippov. Filippov's theory will be briefly outlined in this section.

Consider the nonlinear system with discontinuous right-hand side

$$\dot{\underset{\sim}{x}}(t) = \underset{\sim}{f}(t, \underset{\sim}{x}(t)) = \begin{cases} \underset{\sim}{f}_-(t, \underset{\sim}{x}(t)), & \underset{\sim}{x} \in V_-, \\ \underset{\sim}{f}_+(t, \underset{\sim}{x}(t)), & \underset{\sim}{x} \in V_+, \end{cases} \tag{2.3}$$

with the initial condition

$$\underset{\sim}{x}(t = 0) = \underset{\sim}{x}_0. \tag{2.4}$$

The state-space $\mathbb{R}^n$ is split into two subspaces V_- and V_+ by a hyper-surface Σ such that $\mathbb{R}^n = V_- \cup \Sigma \cup V_+$. The hyper-surface Σ is defined by a scalar indicator function $h(\underset{\sim}{x}(t))$. The subspaces V_- and V_+ and hyper-surface Σ can be formulated as

$$\begin{aligned} V_- &= \{\underset{\sim}{x} \in \mathbb{R}^n \mid h(\underset{\sim}{x}(t)) < 0\}, \\ \Sigma &= \{\underset{\sim}{x} \in \mathbb{R}^n \mid h(\underset{\sim}{x}(t)) = 0\}, \\ V_+ &= \{\underset{\sim}{x} \in \mathbb{R}^n \mid h(\underset{\sim}{x}(t)) > 0\}. \end{aligned} \tag{2.5}$$

The normal $\underset{\sim}{n}$ perpendicular to the hyper-surface Σ is given by

$$\underset{\sim}{n} = \underset{\sim}{n}(\underset{\sim}{x}(t)) = \text{grad}(h(\underset{\sim}{x}(t))). \tag{2.6}$$

We assume that the indicator function $h(\underset{\sim}{x}(t))$ is chosen such that it always holds that $\underset{\sim}{n}(\underset{\sim}{x}(t)) \neq \underset{\sim}{0}$.

The right-hand side $\underset{\sim}{f}(t, \underset{\sim}{x})$ is assumed to be discontinuous but such that it is piecewise continuous and smooth on V_- and V_+ and discontinuous on Σ. The function $\underset{\sim}{f}_-(t, \underset{\sim}{x})$ is

[1] Note: 'generalized' in the sense that the definition holds for a larger class of differential equations.

therefore assumed to be C^1 on $V_- \cup \Sigma$ and $\underset{\sim}{f}_+(t, \underset{\sim}{x})$ is assumed to be C^1 on $V_+ \cup \Sigma$. It is not required that $\underset{\sim}{f}_-(t, \underset{\sim}{x})$ and $\underset{\sim}{f}_+(t, \underset{\sim}{x})$ agree on Σ. The system described by (2.3) does not define $\underset{\sim}{f}(t, \underset{\sim}{x}(t))$ if $\underset{\sim}{x}(t)$ is on Σ. We can overcome this problem with the set-valued extension $\underset{\sim}{F}(t, \underset{\sim}{x})$

$$\dot{\underset{\sim}{x}}(t) \in \underset{\sim}{F}(t, \underset{\sim}{x}(t)) = \begin{cases} \underset{\sim}{f}_-(t, \underset{\sim}{x}(t)), & \underset{\sim}{x} \in V_-, \\ \overline{\text{co}}\{\underset{\sim}{f}_-(t, \underset{\sim}{x}(t)), \underset{\sim}{f}_+(t, \underset{\sim}{x}(t))\}, & \underset{\sim}{x} \in \Sigma, \\ \underset{\sim}{f}_+(t, \underset{\sim}{x}(t)), & \underset{\sim}{x} \in V_+, \end{cases} \tag{2.7}$$

where $\overline{\text{co}}(A)$ denotes the smallest closed convex set containing A. The convex set with two derivatives $\underset{\sim}{f}_-$ and $\underset{\sim}{f}_+$ can be cast in

$$\overline{\text{co}}\{\underset{\sim}{f}_-, \underset{\sim}{f}_+\} = \{(1-q)\underset{\sim}{f}_- + q\underset{\sim}{f}_+, \forall q \in [0,1]\}. \tag{2.8}$$

The parameter q is a parameter which defines the convex combination and has no physical meaning. The extension (or convexification) of a discontinuous system (2.3) into a convex differential inclusion (2.7) is known as *Filippov's convex method*.

Existence of solutions of (2.7) can be guaranteed with the notion of upper semi-continuity of set-valued functions.

DEFINITION 2.1 (Upper semi-continuity). A set-valued function $\underset{\sim}{F}(\underset{\sim}{x})$ is upper semi-continuous in $\underset{\sim}{x}$ if for $\underset{\sim}{y} \to \underset{\sim}{x}$

$$\sup_{\underset{\sim}{a} \in \underset{\sim}{F}(\underset{\sim}{y})} \inf_{\underset{\sim}{b} \in \underset{\sim}{F}(\underset{\sim}{x})} \|\underset{\sim}{a} - \underset{\sim}{b}\| \to 0.$$

The following theorem is proven in [4, theorem 3, p. 98]):

THEOREM 2.1 (Existence of solution of a differential inclusion). *Let $\underset{\sim}{F}$ be a set-valued function. We assume that $\underset{\sim}{F}$ is upper semi-continuous, closed, convex and bounded for all $\underset{\sim}{x} \in \mathbb{R}^n$. Then, for each $\underset{\sim}{x}_0 \in \mathbb{R}^n$ there exists a $\tau > 0$ and an absolutely continuous function $\underset{\sim}{x}(t)$ defined on $[0, \tau]$, which is a solution of the initial value problem*

$$\dot{\underset{\sim}{x}} \in \underset{\sim}{F}(t, \underset{\sim}{x}(t)), \quad \underset{\sim}{x}(0) = \underset{\sim}{x}_0.$$

Filippov's convex method together with the above existence theorem defines the *solution in the sense of Filippov* for a discontinuous differential equation.

DEFINITION 2.2 (Solution in the sense of Filippov). An absolute continuous function $\underset{\sim}{x}(t) : [0, \tau] \to \mathbb{R}^n$ is said to be a solution of $\dot{\underset{\sim}{x}}(t) = \underset{\sim}{f}(t, \underset{\sim}{x})$ (2.3) in the sense of Filippov if for almost all[2] $t \in [0, \tau]$ holds

$$\dot{\underset{\sim}{x}}(t) \in \underset{\sim}{F}(t, \underset{\sim}{x}(t)),$$

where $\underset{\sim}{F}(t, \underset{\sim}{x}(t))$ is the closed convex hull of all the limits of $\underset{\sim}{f}(t, \underset{\sim}{x}(t))$.

[2] *For almost all t* means except for a set t of measure 0.

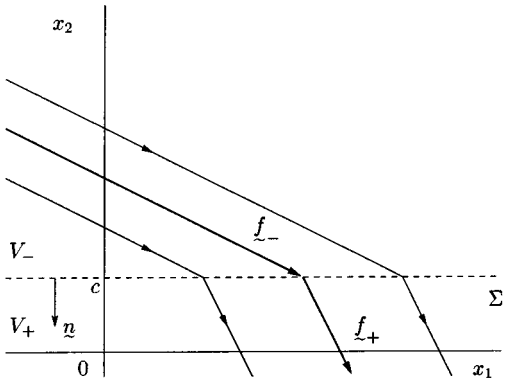

Figure 1. Transversal intersection.

Remarks. If $\underline{x}(t)$ is in a region where the vector field is continuous, $\underline{x}(t) \in V$, then of course must hold $\underset{\sim}{F}(t, \underline{x}(t)) = \{\underset{\sim}{f}(t, \underline{x}(t))\}$. If the solution $\underline{x}(t)$ slides along a surface of discontinuity, $\underline{x}(t) \in \Sigma$, then $\dot{\underline{x}}(t) \in \underset{\sim}{F}(t, \underline{x}(t))$. However, $\dot{\underline{x}}(t)$ is not defined at time instances where the solution arrives at a hyper-surface of discontinuity Σ or leaves Σ. The set of t for which $\underline{x}(t)$ arrives or leaves Σ is of measure zero.

It was assumed in (2.2) that $\underset{\sim}{f}(t, \underline{x})$ is linearly bounded. In addition $\underset{\sim}{F}(t, \underline{x}(t))$ is assumed to be bounded on values $(t, \underline{x})$ for which $\underset{\sim}{F}$ is set-valued. Consequently, $\underset{\sim}{F}(t, \underline{x}(t))$ is linearly bounded, i.e. there exist positive constants γ and c such that for all $t \in [0, \infty)$ and $\underline{x} \in \mathbb{R}^n$ holds:

$$\|\underset{\sim}{F}(t, \underline{x})\| \leq \gamma \|\underline{x}\| + c.$$

Solutions $\underline{x}(t)$ to (2.7) therefore exist on $[0, \infty)$ [4, 8] but uniqueness is not guaranteed.

A complication of discontinuous Filippov systems is the possibility of 'accumulation points' [18, 24]. At an accumulation point, an infinite number of mode switches occurs in a finite time. We will not address this phenomenon in this paper and we will assume that no accumulation points occur.

Solutions of differential inclusions do not have to be unique. Obviously, the solution of the IVP (initial value problem) where $\underline{x}_0 \notin \Sigma$ is locally unique, because $\underset{\sim}{f}_-(t, \underline{x})$ and $\underset{\sim}{f}_+(t, \underline{x})$ are C^1. Uniqueness problems of IVP for initial conditions on Σ will be illustrated in the following examples which show three basic ways in which the vector field around Σ can behave.

EXAMPLE 2.1. Consider the discontinuous system

$$\begin{aligned} \dot{x}_1 &= 4 + 2\ \mathrm{sgn}(x_2 - c), \\ \dot{x}_2 &= -4 + 2\ \mathrm{sgn}(x_2 - c), \end{aligned} \tag{2.9}$$

which can be extended to a set-valued vector field at $\Sigma = \{x_2 = c\}$ by replacing 'sgn(x)' with 'Sgn(x)' and '$=$' with '$\in$'. We take $h = c - x_2$ as indicator function which defines the subspaces V_- and V_+ by (2.5). The normal $\underline{n}$ to Σ is given by $\underline{n} = [0, -1]^{\mathrm{T}}$. The vector field (Figure 1) is pushing the solution to Σ in the space $V_- = \{x_2 > c\}$ and pushing from Σ in the space $V_+ = \{x_2 < c\}$. A solution of (2.9) with an initial condition in V_- will after some

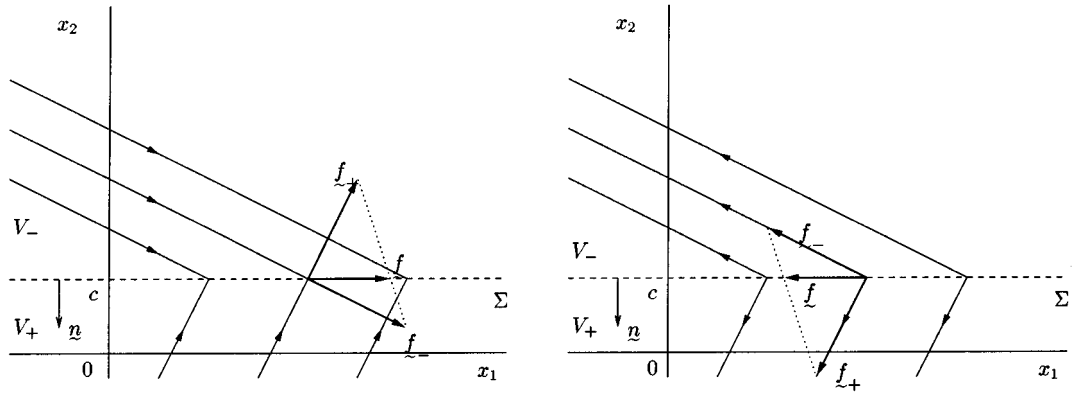

(a) Attraction sliding mode. (b) Repulsion sliding mode.

Figure 2. Sliding modes.

time hit Σ, cross it transversally and proceed in V_+. This is called a transversal intersection. Note that the word 'transversal' refers to the *solution* which is transversal to Σ and does not refer to the vector field $\underset{\sim}{f}$. Any solution of (2.9) with an initial condition in V_-, exposing a transversal intersection, therefore exists and is unique. A necessary condition for a transversal intersection at Σ is

$$\underset{\sim}{n}^{\mathrm{T}}\underset{\sim}{f}_-(t, \underset{\sim}{x}(t))\underset{\sim}{n}^{\mathrm{T}}\underset{\sim}{f}_+(t, \underset{\sim}{x}(t)) > 0, \quad \underset{\sim}{x}(t) \in \Sigma, \tag{2.10}$$

where $\underset{\sim}{n}^{\mathrm{T}}\underset{\sim}{f}_-$ and $\underset{\sim}{n}^{\mathrm{T}}\underset{\sim}{f}_+$ are the projections of $\underset{\sim}{f}_-$ and $\underset{\sim}{f}_+$ on the normal to the hyper-surface Σ.

The vector field could also push the solution to Σ in both V_- and V_+. This will be demonstrated in the following example.

EXAMPLE 2.2. Consider the system

$$\begin{aligned} \dot{x}_1 &= 4 + 2\ \mathrm{sgn}(x_2 - c), \\ \dot{x}_2 &= 2 - 4\ \mathrm{sgn}(x_2 - c), \end{aligned} \tag{2.11}$$

with the phase plane depicted in Figure 2a. The solution will hit Σ but cannot leave it and will therefore move along the plane Σ. This is often called a *sliding mode*. Because the hyper-surface attracts the solution, we call this an *attraction sliding mode*. During the sliding mode the solution will continue along Σ with time derivative $\underset{\sim}{f}$ given by

$$\underset{\sim}{f} = \alpha\underset{\sim}{f}_+ + (1 - \alpha)\underset{\sim}{f}_- \tag{2.12}$$

with

$$\alpha = \frac{\underset{\sim}{n}^{\mathrm{T}}\underset{\sim}{f}_-}{\underset{\sim}{n}^{\mathrm{T}}(\underset{\sim}{f}_- - \underset{\sim}{f}_+)}.$$

The scalar α can be regarded as the value for q that chooses one $\underset{\sim}{f} \in \underset{\sim}{F}$ such that it lies along Σ. The solution of (2.11), being an attraction sliding mode, exists and is unique in forward time. An attraction sliding mode at Σ occurs if

$$\underset{\sim}{n}^{\mathrm{T}}\underset{\sim}{f}_-(t, \underset{\sim}{x}(t)) > 0 \quad \text{and} \quad \underset{\sim}{n}^{\mathrm{T}}\underset{\sim}{f}_+(t, \underset{\sim}{x}(t)) < 0, \quad \underset{\sim}{x}(t) \in \Sigma, \tag{2.13}$$

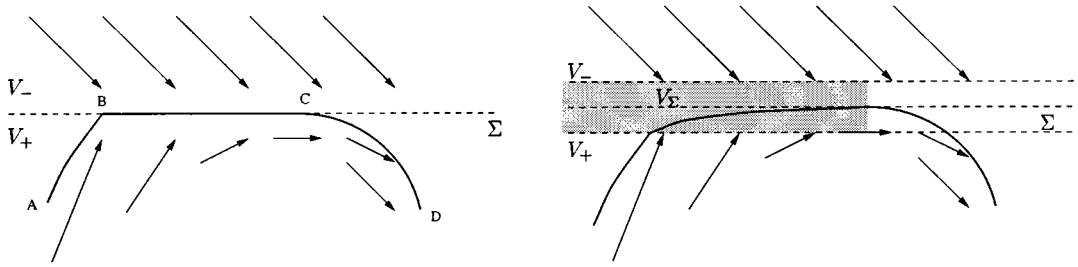

(a) Exact sliding mode (b) Numerical approximation

Figure 3. Numerical approximation of a sliding mode.

where the inequality signs depend of course on the choice of h (in this case $h(\underset{\sim}{x}) > 0$ in V_+ and $h(\underset{\sim}{x}) < 0$ in V_-).

The third possible case (Figure 2b) is illustrated by the following example.

EXAMPLE 2.3. Consider the system

$$\begin{aligned} \dot{x}_1 &= -4 - 2\ \mathrm{sgn}(x_2 - c), \\ \dot{x}_2 &= -2 + 4\ \mathrm{sgn}(x_2 - c). \end{aligned} \tag{2.14}$$

Note that this vector field is the vector field of (2.11) in reverse time. Here the solutions are diverging from Σ. A solution which starts close to Σ will move away from it. But a solution emanating on Σ can stay on Σ, obeying Filippov's solution, or leave Σ by entering either V_- or V_+. This type of vector field around the hyper-surface is addressed as *repulsion sliding mode* as the vector field is repulsing from Σ. The IVP with initial condition on Σ has three possible solutions. The solution still exists but is not unique in forward time.

The set-valued function $\underset{\sim}{F}$ in the differential inclusion (2.7) is the smallest closed convex set that contains the discontinuous function $\underset{\sim}{f}$ of (2.3). If $\underset{\sim}{F}$ obeys condition (2.10) at a point on Σ then there is no selection from $\underset{\sim}{F}$ which lies along Σ. We conclude that the solution of the differential inclusion (2.7) with $\underset{\sim}{x}_0 \in \Sigma$ is locally unique in forward time if (2.10) or (2.13) holds.

Filippov's theory will turn out to be very important to understand periodic solutions where part of the orbit is a sliding mode.

2.2. Numerical Approximation

The vector field of Figure 3a pushes the solution which starts in point A to the hyper-surface Σ at point B in finite time. The solution then slides along Σ and leaves Σ when the vector field in the space V_+ becomes parallel to Σ. The solution will then bend off at point C, i.e. the point at which the vector field is parallel to Σ, and reaches point D. This scenario is the attraction sliding mode. The solution from A to D is unique. If we consider the solution in backward time, that is from D to A, then the vector field reverses and the sliding mode will be of the repulsion type. The reverse solution is clearly not unique. This insight is essential to understand bifurcations of periodic solutions with sliding modes which will be treated in Section 6.

If we try to integrate such a scenario numerically we are faced with a difficulty: a Runge–Kutta algorithm, for example, will have collocation points in both V_- and V_+ between B and C. The integration algorithm will find the correct solution but it will take an enormous amount of integration points.

Instead, we construct a 'band' or 'boundary layer' around Σ, namely the space V_Σ, to allow for an efficient numerical approximation (Figure 3b). In the space V_Σ, the vector field is such that the solution is pushed to the middle of the band, i.e. to Σ. The space V_Σ ends when the vector field in V_+ or V_- becomes parallel to Σ. The width of V_Σ should be taken small to yield a good approximation.

As an alternative, the discontinuous vector field is often approximated by a smoothened vector field. For instance $\operatorname{sgn}(x)$ can be approximated by $\frac{2}{\pi}\arctan(\varepsilon x)$. The smooth approximation normally yields a good approximation for large values of ε although difficulties can be expected at repulsion sliding modes. It should be noted that the smooth approximation always has existence and uniqueness of solutions whereas this is not the case for the discontinuous system. The main disadvantage is however the fact that the smoothing method yields stiff differential equations which are expensive to solve. The method proposed here is far more efficient, as is pointed out in [31] where the two methods are compared.

3. Fundamental Solution Matrix

In this section the discontinuous behaviour of fundamental solution matrices of discontinuous systems is discussed and applied to two examples.

3.1. Jumping Conditions

We will derive how the fundamental solution matrix $\underline{\Phi}$ jumps if the trajectory $\underset{\sim}{x}(t)$ crosses a hyper-surface Σ, on which the vector field is discontinuous. Consider the nonlinear system (2.7) with discontinuous right-hand side as described in Section 2. Assume that at a certain point in time, say t_p, the trajectory $\underset{\sim}{x}(t)$ will cross Σ. With the definition of the indicator function (2.5) we obtain $h(\underset{\sim}{x}(t_p)) = 0$. At this hyper-surface there are two derivatives $\underset{\sim}{f}_{p-}$ and $\underset{\sim}{f}_{p+}$, where

$$\underset{\sim}{f}_{p+} = \underset{\sim}{f}(t_p^+, \underset{\sim}{x}(t_p^+)), \quad \underset{\sim}{f}_{p-} = \underset{\sim}{f}(t_p^-, \underset{\sim}{x}(t_p^-)). \tag{3.1}$$

We first consider only transversal intersections. Uniqueness of the solution is therefore assured. In order to assure a transversal intersection, we assume that the projections of the derivatives $\underset{\sim}{f}_{p-}$ and $\underset{\sim}{f}_{p+}$ on the normal $\underset{\sim}{n}$ have the same sign

$$\underset{\sim}{n}^{\mathrm{T}} \underset{\sim}{f}_{p-} \underset{\sim}{n}^{\mathrm{T}} \underset{\sim}{f}_{p+} > 0. \tag{3.2}$$

Equation (3.2) assures that the trajectory leaves the hyper-surface and stays on the hyper-surface at one point of time and not on an interval of time (i.e. the trajectory *crosses* the hyper-surface).

An infinitesimal disturbance $\delta\underset{\sim}{x}_0$ on the initial condition will cause a disturbance $\delta\underset{\sim}{x}(t)$ on the state $\underset{\sim}{x}(t)$. The fundamental solution matrix $\underline{\Phi}(t, t_0)$ relates $\delta\underset{\sim}{x}(t)$ to $\delta\underset{\sim}{x}_0$,

$$\delta\underset{\sim}{x}(t) = \underline{\Phi}(t, t_0)\delta\underset{\sim}{x}_0 + O(\|\underset{\sim}{x}_0\|^2). \tag{3.3}$$

The dependence of $\underline{\Phi}(t, t_0)$ on $\underset{\sim}{x}_0$ has been omitted for brevity. Let the trajectory start in the subspace V_-, that is $\underset{\sim}{x}_0 \in V_-$. Suppose the trajectory crosses the hyper-surface Σ at $t = t_p$. The system is continuous on the interval $D = \{t \in \mathbb{R} \mid t_0 \leq t \leq t_p\}$. The fundamental solution matrix will also be continuous on the interior of D. The time evolution of the fundamental solution matrix on the *interior* of D can be obtained from the initial value problem

$$\dot{\underline{\Phi}}(t, t_0) = \frac{\partial \underset{\sim}{f}(t, \underset{\sim}{x}(t))}{\partial \underset{\sim}{x}} \underline{\Phi}(t, t_0), \quad \underline{\Phi}(t_0, t_0) = \underline{\Phi}_0 = \underline{I}, \quad t_0, t \in D. \tag{3.4}$$

Equation (3.4) is called the *variational equation* [40]. The Jacobian $\partial \underset{\sim}{f} / \partial \underset{\sim}{x}$ is not uniquely defined on the border of D at $t = t_p$ where $\underset{\sim}{x}(t_p)$ is located on the hyper-surface Σ. This causes a jump (or discontinuity) in the fundamental solution matrix. We will derive an expression for the jump in Section 3.2. For the moment we will assume that we know how the fundamental solution matrix jumps and we assume that we can express the jump with a matrix $\underline{S}$, which maps the fundamental solution matrix just before the jump, $\underline{\Phi}(t_{p-}, t_0)$, to the fundamental solution matrix just after the jump, $\underline{\Phi}(t_{p+}, t_0)$, as

$$\underline{\Phi}(t_{p+}, t_0) = \underline{S}\, \underline{\Phi}(t_{p-}, t_0), \tag{3.5}$$

where $\underline{\Phi}(t_{p-}, t_0) = \lim_{t \uparrow t_p} \underline{\Phi}(t, t_0)$. On D the fundamental solution matrix can be obtained from integrating the variational equation (3.4) which gives for $\underline{\Phi}(t_{p-}, t_0)$

$$\underline{\Phi}(t_{p-}, t_0) = \int_{t_0}^{t_p} \dot{\underline{\Phi}}(t, t_0)\, \mathrm{d}t + \underline{I}. \tag{3.6}$$

The fundamental solution matrix after the jump can then be obtained by (3.5) where $\underline{S}$ should of course be known. The trajectory enters the subspace V_+ (as transversality was assumed) at $t = t_p$, and traverses V_+ during the interval $G = \{t \in \mathbb{R} \mid t_p \leq t \leq t_q\}$. We can now construct the fundamental solution matrix on G after the jump as

$$\underline{\Phi}(t_q, t_0) = \underline{\Phi}(t_q, t_{p+}) \underline{\Phi}(t_{p+}, t_0) = \left(\int_{t_p}^{t_q} \dot{\underline{\Phi}}(t, t_0)\, \mathrm{d}t + \underline{I} \right) \underline{\Phi}(t_{p+}, t_0). \tag{3.7}$$

If the fundamental solution matrix is known on G, then we can express $\underline{\Phi}(t_{p+}, t_0)$ by the right time limit to the jump as $\underline{\Phi}(t_{p+}, t_0) = \lim_{t \downarrow t_p} \underline{\Phi}(t, t_0)$.

We name the matrix $\underline{S}$ the *saltation matrix* because it describes the jump by mapping $\underline{\Phi}(t_{p-}, t_0)$ to $\underline{\Phi}(t_{p+}, t_0)$ with (3.5). The saltation matrix can be regarded as a fundamental solution matrix from time t_{p-} to t_{p+}

$$\underline{S} = \underline{\Phi}(t_{p+}, t_{p-}). \tag{3.8}$$

Substitution of (3.5) in (3.7) yields $\underline{\Phi}(t_q, t_0) = \underline{\Phi}(t_q, t_{p+}) \underline{S}\, \underline{\Phi}(t_{p-}, t_0)$.

The construction of saltation matrices (or jump conditions) is due to [1] and is explained in Section 3.2.

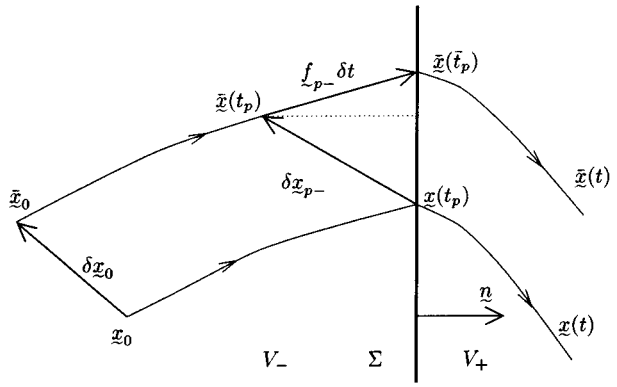

Figure 4. Construction of δt for autonomous Σ.

3.2. Construction of Saltation Matrices

The saltation matrix will be derived by inspecting the nonlinear dynamical system in the neighborhood of the occurrence of a discontinuity. Consider a trajectory $\underset{\sim}{x}(t)$ starting from $\underset{\sim}{x}_0$ (Figure 4) and a disturbed trajectory $\bar{\underset{\sim}{x}}(t)$ which is due to an initial disturbance

$$\bar{\underset{\sim}{x}}_0 = \underset{\sim}{x}_0 + \delta\underset{\sim}{x}_0. \tag{3.9}$$

The disturbed trajectory stays $\delta t = \bar{t}_p - t_p$ longer (if $\delta t > 0$) or shorter (if $\delta t < 0$) in V_- before hitting the hyper-surface Σ. The differences between the disturbed and undisturbed trajectories at the crossings are denoted by

$$\delta\underset{\sim}{x}_{p-} = \bar{\underset{\sim}{x}}(t_p) - \underset{\sim}{x}(t_p), \qquad \delta\underset{\sim}{x}_{p+} = \bar{\underset{\sim}{x}}(\bar{t}_p) - \underset{\sim}{x}(\bar{t}_p). \tag{3.10}$$

We can express the undisturbed and disturbed trajectories in a first-order Taylor expansion

$$\underset{\sim}{x}(\bar{t}_p) \approx \underset{\sim}{x}(t_p) + \underset{\sim}{f}_{p+}\delta t, \qquad \bar{\underset{\sim}{x}}(\bar{t}_p) \approx \underset{\sim}{x}(t_p) + \delta\underset{\sim}{x}_{p-} + \underset{\sim}{f}_{p-}\delta t. \tag{3.11}$$

Equations (3.11) are inserted into (3.10)

$$\begin{aligned}\delta\underset{\sim}{x}_{p+} = \bar{\underset{\sim}{x}}(\bar{t}_p) - \underset{\sim}{x}(\bar{t}_p) &\approx \underset{\sim}{x}(t_p) + \delta\underset{\sim}{x}_{p-} + \underset{\sim}{f}_{p-}\delta t - (\underset{\sim}{x}(t_p) + \underset{\sim}{f}_{p+}\delta t)\\ &\approx \delta\underset{\sim}{x}_{p-} + \underset{\sim}{f}_{p-}\delta t - \underset{\sim}{f}_{p+}\delta t.\end{aligned} \tag{3.12}$$

The disturbed trajectory satisfies the indicator function (2.5). We apply a Taylor series expansion up to the first-order terms [34] (where the normal $\underset{\sim}{n}$ is defined by (2.6)

$$\begin{aligned}0 = h(\bar{\underset{\sim}{x}}(\bar{t}_p)) &\approx h(\underset{\sim}{x}(t_p) + \delta\underset{\sim}{x}_{p-} + \underset{\sim}{f}_{p-}\delta t)\\ &\approx \underbrace{h(\underset{\sim}{x}(t_p))}_{=0} + \underset{\sim}{n}^{\mathrm{T}}(\delta\underset{\sim}{x}_{p-} + \underset{\sim}{f}_{p-}\delta t)\\ &\approx \underset{\sim}{n}^{\mathrm{T}}(\delta\underset{\sim}{x}_{p-} + \underset{\sim}{f}_{p-}\delta t).\end{aligned} \tag{3.13}$$

From (3.13) we can express the variation δt in terms of $\delta\underset{\sim}{x}_{p-}$

$$\delta t = -\frac{\underset{\sim}{n}^{\mathrm{T}}\delta\underset{\sim}{x}_{p-}}{\underset{\sim}{n}^{\mathrm{T}}\underset{\sim}{f}_{p-}}. \tag{3.14}$$

The dependence between the variation δt and $\delta \underset{\sim}{x}_{p-}$ can be envisaged from Figure 4. Due to the variation $\delta \underset{\sim}{x}_{p-}$ the disturbed trajectory after a time t_p does not lie exactly on the (fixed) surface Σ. The disturbed trajectory has to stay a time δt longer/shorter in V_-, covering an additional distance $\underset{\sim}{f}_{p-}\delta t$, to reach Σ. We infer from Figure 4 that the vectors $\delta \underset{\sim}{x}_{p-}$ and $\underset{\sim}{f}_{p-}\delta t$ are related by

$$\underset{\sim}{n}^{\mathrm{T}} \underset{\sim}{f}_{p-}\delta t = -\underset{\sim}{n}^{\mathrm{T}}\delta \underset{\sim}{x}_{p-}, \tag{3.15}$$

from which we can derive (3.14).

Combining (3.12) and (3.14) gives

$$\delta \underset{\sim}{x}_{p+} = \delta \underset{\sim}{x}_{p-} + (\underset{\sim}{f}_{p+} - \underset{\sim}{f}_{p-})\frac{\underset{\sim}{n}^{\mathrm{T}}\delta \underset{\sim}{x}_{p-}}{\underset{\sim}{n}^{\mathrm{T}}\underset{\sim}{f}_{p-}}. \tag{3.16}$$

We have now expressed the variation $\delta \underset{\sim}{x}_{p+}$ in the variation $\delta \underset{\sim}{x}_{p-}$. The saltation matrix relates $\delta \underset{\sim}{x}_{p+}$ to $\delta \underset{\sim}{x}_{p-}$

$$\delta \underset{\sim}{x}_{p+} = \underline{S}\delta \underset{\sim}{x}_{p-}. \tag{3.17}$$

We obtain the saltation matrix from (3.16) as $\underline{S} = \underline{\Phi}(t_{p+}, t_{p-})$ as

$$\underline{S} = \underline{I} + \frac{(\underset{\sim}{f}_{p+} - \underset{\sim}{f}_{p-})\underset{\sim}{n}^{\mathrm{T}}}{\underset{\sim}{n}^{\mathrm{T}}\underset{\sim}{f}_{p-}}. \tag{3.18}$$

The inverse of the saltation matrix $\underline{S}^{-1} = \underline{\Phi}(t_{p-}, t_{p+})$ is given by (for non-singular $\underline{S}$)

$$\underline{S}^{-1} = \underline{I} + \frac{(\underset{\sim}{f}_{p-} - \underset{\sim}{f}_{p+})\underset{\sim}{n}^{\mathrm{T}}}{\underset{\sim}{n}^{\mathrm{T}}\underset{\sim}{f}_{p+}}. \tag{3.19}$$

The saltation matrix $\underline{S}$ becomes singular if $\underset{\sim}{n}^{\mathrm{T}}\underset{\sim}{f}_{p+} = 0$ which will not happen if the transversality condition (3.2) is fulfilled.

The saltation matrix was derived in this section for an autonomous indicator function $h(\underset{\sim}{x}(t))$. Non-autonomous systems can give rise to non-autonomous indicator functions. However, non-autonomous time periodic systems can be transformed into autonomous systems having autonomous indicator functions. Alternatively, one can derive the saltation matrix for a non-autonomous indicator function $h(t, \underset{\sim}{x}(t))$ [1, 18, 34]. The saltation matrix for a non-autonomous indicator function is given by

$$\underline{S} = \underline{I} + \frac{(\underset{\sim}{f}_{p+} - \underset{\sim}{f}_{p-})\underset{\sim}{n}^{\mathrm{T}}}{\underset{\sim}{n}^{\mathrm{T}}\underset{\sim}{f}_{p-} + \frac{\partial h}{\partial t}(t_p, \underset{\sim}{x}(t_p))}. \tag{3.20}$$

3.3. Example I: The Stick-slip System

To demonstrate the above theory we will study a one-dimensional system with dry friction that possesses a stick-slip periodic solution.

Consider a mass m attached to inertial space by a spring k and damper c (Figure 5a). The mass is riding on a driving belt, that is moving at a constant velocity v_{rel}. A friction force F

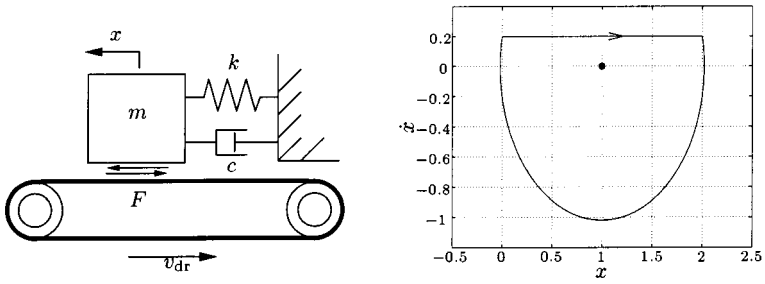

(a) system (b) Phase portrait.

Figure 5. 1–DOF model with dry friction.

acts between the mass and belt which is dependent on the relative velocity (see Appendix A.1 for the parameter values). The state equation of this autonomous system reads as

$$\dot{\underset{\sim}{x}} = \underset{\sim}{f}(\underset{\sim}{x}) = \begin{bmatrix} \dot{x} \\ -\frac{k}{m}x - \frac{c}{m}\dot{x} + \frac{F}{m} \end{bmatrix}, \tag{3.21}$$

where $\underset{\sim}{x} = [x \;\; \dot{x}]^{\mathrm{T}}$ and F is given by a signum model with static friction point

$$F = \begin{cases} F(v_{\mathrm{rel}}) = -F_{\mathrm{slip}} \operatorname{sgn} v_{\mathrm{rel}}, & v_{\mathrm{rel}} \neq 0 \;\; \text{slip}, \\ F(x, \dot{x}) = \min(|F_{\mathrm{ex}}|, F_{\mathrm{stick}}) \operatorname{sgn}(F_{\mathrm{ex}}), & v_{\mathrm{rel}} = 0 \;\; \text{stick}, \end{cases} \tag{3.22}$$

with $F_{\mathrm{ex}}(x, \dot{x}) = kx + c\dot{x}$. The maximum static friction force is denoted by F_{stick} and $v_{\mathrm{rel}} = \dot{x} - v_{\mathrm{dr}}$ is the relative velocity. Friction model (3.22) should be understood such that only a transition from stick to slip can take place if $|F_{\mathrm{ex}}|$ exceeds F_{stick}.

This model permits explicit solutions for $c = 0$ due to its simplicity but it is not directly applicable in numerical analysis. Instead, an adjoint switch model will be studied, which was discussed in [31]. The state equation for the switch model reads as

$$\dot{\underset{\sim}{x}} = \begin{cases} \begin{bmatrix} \dot{x} \\ -\frac{k}{m}x - \frac{c}{m}\dot{x} - \frac{F_{\mathrm{slip}}}{m} \operatorname{sgn} v_{\mathrm{rel}} \end{bmatrix}, & |v_{\mathrm{rel}}| > \eta \text{ or } |F_{\mathrm{ex}}| > F_{\mathrm{stick}}, \\ \begin{bmatrix} v_{\mathrm{dr}} \\ -v_{\mathrm{rel}}\sqrt{\frac{k}{m}} \end{bmatrix}, & |v_{\mathrm{rel}}| < \eta \text{ and } |F_{\mathrm{ex}}| < F_{\mathrm{stick}}. \end{cases} \tag{3.23}$$

A region of near-zero velocity is defined as $|v_{\mathrm{rel}}| < \eta$ where $\eta \ll v_{\mathrm{dr}}$. The space $\mathbb{R}^2$ is divided in three subspaces V, W and D as indicated in Figure 6. The small parameter η is enlarged in Figure 6 to make D visible.

A stable stick-slip periodic solution of this system exists and is depicted in Figure 5b together with the equilibrium point $(x, \dot{x}) = (1, 0)$. As this system is autonomous, the hyper-surfaces are not dependent on time. It can be seen that the state traverses V (the slip phase) and D (the stick phase). If the state leaves V and enters D, the hyper-surface Σ_α is crossed with normal $\underset{\sim}{n}_\alpha = [0 \;\; 1]^{\mathrm{T}}$ where $h_\alpha(x, \dot{x}) = \dot{x} - v_{\mathrm{dr}}$. Likewise, if the state leaves D and enters V again, the hyper-surface Σ_β is crossed with normal $\underset{\sim}{n}_\beta = [1 \;\; 0]^{\mathrm{T}}$ where $h_\beta(x, \dot{x}) = kx + cv_{\mathrm{dr}} - F_{\mathrm{stick}}$.

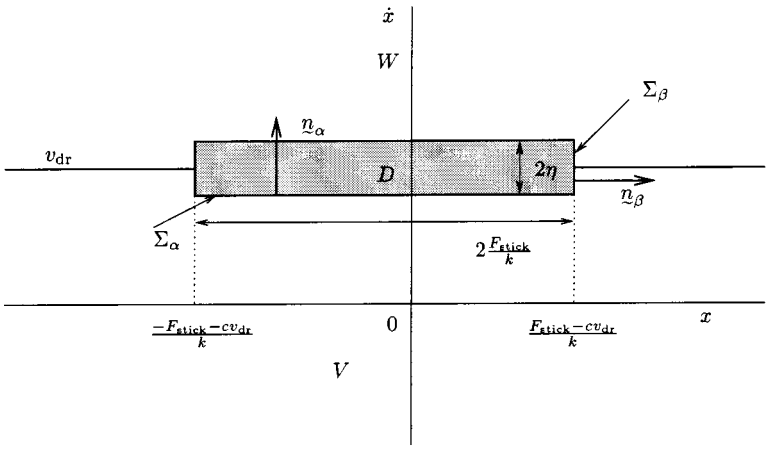

Figure 6. Definition of subspaces V, W and D.

Let us assume that the trajectory crosses Σ_α at $t = t_\alpha$ and Σ_β at $t = t_\beta$. We can now construct the saltation matrices $\underset{\sim}{S}_\alpha$ and $\underset{\sim}{S}_\beta$. The right-hand sides of (3.23) at $t = t_\alpha$ for $\lim \eta \downarrow 0$ are

$$\underset{\sim}{f}_{\alpha-} = \begin{bmatrix} v_{\mathrm{dr}} \\ \ddot{x}_{\alpha-} \end{bmatrix}, \qquad \underset{\sim}{f}_{\alpha+} = \begin{bmatrix} v_{\mathrm{dr}} \\ 0 \end{bmatrix}. \tag{3.24}$$

The saltation matrix $\underset{\sim}{S}_\alpha$ yields

$$\underset{\sim}{S}_\alpha = \underline{I} + \frac{(\underset{\sim}{f}_{\alpha+} - \underset{\sim}{f}_{\alpha-})\underset{\sim}{n}_\alpha^{\mathrm{T}}}{\underset{\sim}{n}_\alpha^{\mathrm{T}}\underset{\sim}{f}_{\alpha-}} = \begin{bmatrix} 1 & 0 \\ 0 & 0 \end{bmatrix}, \tag{3.25}$$

which is independent of any system parameter.

Conducting the same for $\underset{\sim}{S}_\beta$ yields

$$\underset{\sim}{f}_{\beta-} = \begin{bmatrix} v_{\mathrm{dr}} \\ 0 \end{bmatrix}, \qquad \underset{\sim}{f}_{\beta+} = \begin{bmatrix} v_{\mathrm{dr}} \\ -\frac{\Delta F}{m} \end{bmatrix}, \tag{3.26}$$

with $\Delta F = F_{\mathrm{stick}} - F_{\mathrm{slip}}$. Substitution yields $\underset{\sim}{S}_\beta$

$$\underset{\sim}{S}_\beta = \underline{I} + \frac{(\underset{\sim}{f}_{\beta+} - \underset{\sim}{f}_{\beta-})\underset{\sim}{n}_\beta^{\mathrm{T}}}{\underset{\sim}{n}_\beta^{\mathrm{T}}\underset{\sim}{f}_{\beta-}} = \begin{bmatrix} 1 & 0 \\ -\frac{\Delta F}{m v_{\mathrm{dr}}} & 1 \end{bmatrix}. \tag{3.27}$$

Note that the saltation matrix $\underset{\sim}{S}_\alpha$ is singular causing the fundamental solution matrix to be singular. The physical meaning of this is that the trajectory is uniquely mapped from $\underset{\sim}{x}_0$ in V to $\underset{\sim}{x}(t)$ in D but the inverse mapping does not exist. If different trajectories enter the stick phase, they all pass the same states on the stick phase and leave the stick phase from the same state $\underset{\sim}{x}_\beta$. So, if the trajectory enters the stick phase, knowledge about its initial state is lost. The fundamental solution matrix for the periodic solution of system (3.23) is plotted in Figure 7. Jumps at $t = t_\alpha$ and $t = t_\beta$ in the fundamental solution matrix can be clearly distinguished.

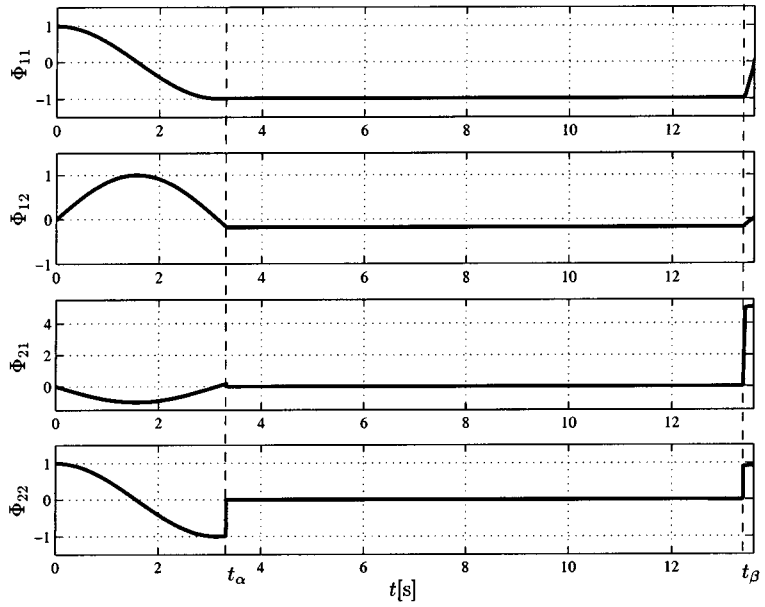

Figure 7. Fundamental solution matrix.

3.4. Example II: The Discontinuous Support

As a second example we will consider a mass-spring system with a discontinuous support (Figure 8a). The support is massless, has a spring stiffness k_f and damping coefficient c_f, which makes the support a first-order system. The displacement of the mass relative to the equilibrium position is denoted by x and of the support by y. The system has two possible modes: the mass is in contact with the support or the mass is not in contact with the support. Let f_c denote the contact force between mass and support. The following contact conditions holds:

$$\text{no contact:} \qquad x < y \text{ and } f_c = 0,$$

$$\text{contact:} \qquad x = y \text{ and } f_c = k_f y + c_f \dot{y} = k_f x + c_f \dot{x} \geq 0.$$

The support, being a first-order system, relaxes to the equilibrium state, $y = 0$, if the mass is not in contact with the support. If we assume that the relaxation time of the support is much smaller than the time between two contact events, we can neglect the free motion of the support. It is therefore assumed that the support is at rest at the moment that contact is made. This assumption reduces the system to a second-order equation. The motion of the mass is given by

$$\text{no contact:} \qquad m\ddot{x} + kx = f_0 \cos \omega t,$$

$$\text{contact:} \qquad m\ddot{x} + c_f \dot{x} + (k + k_f)x = f_0 \cos \omega t. \tag{3.28}$$

The mass comes in contact with the support if the displacement becomes zero, $x = 0$. The mass looses contact with the support if the contact force becomes zero, $f_c = k_f x + c_f \dot{x} = 0$. We introduce the state-vector $\underset{\sim}{x} = [\, x \;\; \dot{x} \,]^{\mathrm{T}}$ and define the following two indicator functions:

$$h_\alpha(x, \dot{x}) = x, \qquad h_\beta(x, \dot{x}) = k_f x + c_f \dot{x}. \tag{3.29}$$

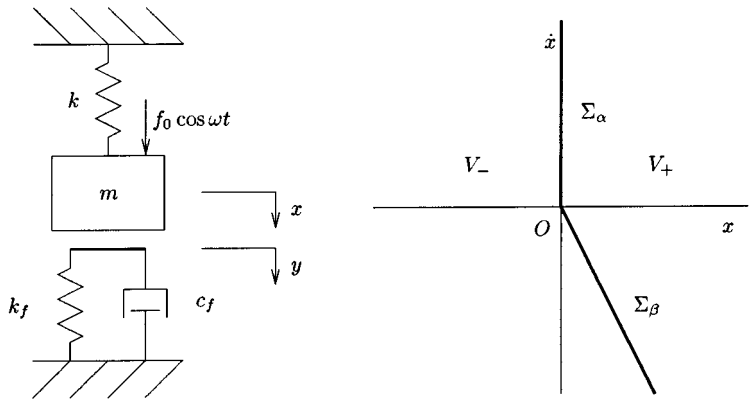

Figure 8. Mass with discontinuous support.

The indicator functions define the subspaces V_- and V_+

$$V_- = \{\underset{\sim}{x} \in \mathbb{R}^2 \mid h_\alpha(x, \dot{x}) < 0 \vee h_\beta(x, \dot{x}) < 0\} \quad \text{(no contact)},$$
$$V_+ = \{\underset{\sim}{x} \in \mathbb{R}^2 \mid h_\alpha(x, \dot{x}) > 0 \wedge h_\beta(x, \dot{x}) > 0\} \quad \text{(contact)}.$$

The hyper-surface Σ, which divides the state-space $\mathbb{R}^2$ in the subspaces V_- and V_+, consist of the conjunction of two surfaces Σ_α and Σ_β (Figure 8b). The hyper-surfaces Σ_α and Σ_β are defined by

$$\Sigma_\alpha = \{\underset{\sim}{x} \in \mathbb{R}^2 \mid h_\alpha(x, \dot{x}) = 0, h_\beta(x, \dot{x}) \geq 0\},$$
$$\Sigma_\beta = \{\underset{\sim}{x} \in \mathbb{R}^2 \mid h_\alpha(x, \dot{x}) \geq 0, h_\beta(x, \dot{x}) = 0\}, \tag{3.30}$$

and have the normals $\underset{\sim}{n}_\alpha = [1 \;\; 0]^{\mathrm{T}}$ and $\underset{\sim}{n}_\beta = [k_f \;\; c_f]^{\mathrm{T}}$. Remark that the hyper-surface Σ is non-smooth at the origin.

The state equation of this non-autonomous discontinuous system reads as

$$\dot{\underset{\sim}{x}}(t) = \underset{\sim}{f}(t, \underset{\sim}{x}(t)) = \begin{cases} \underset{\sim}{f}_-(t, \underset{\sim}{x}(t)) & \underset{\sim}{x} \in V_-, \\ \underset{\sim}{f}_+(t, \underset{\sim}{x}(t)) & \underset{\sim}{x} \in V_+, \end{cases} \tag{3.31}$$

with

$$\underset{\sim}{f}_-(t, \underset{\sim}{x}) = \begin{bmatrix} \dot{x} \\ -\dfrac{k}{m}x + \dfrac{f_0}{m}\cos \omega t \end{bmatrix},$$
$$\underset{\sim}{f}_+(t, \underset{\sim}{x}) = \begin{bmatrix} \dot{x} \\ -\dfrac{k + k_f}{m}x - \dfrac{c_f}{m}\dot{x} + \dfrac{f_0}{m}\cos \omega t \end{bmatrix}. \tag{3.32}$$

System (3.31), which is discontinuous for $\underset{\sim}{x} \in \Sigma$, can be extended to a differential inclusion with Filippov's convex method as described in Section 2.

We first consider the contact event, which is the transition from the mode without contact to the mode with contact. Let us assume that trajectory $\underset{\sim}{x}(t)$ crosses Σ, leaving V_- and entering

V_+, at $t = t_\alpha$. The trajectory crosses therefore the Σ_α part of Σ at this instance. We can now construct the saltation matrix $\underline{S}_\alpha$ of the contact event. The right-hand sides at the instance t_α are

$$\underset{\sim}{f}_{\alpha-} = \begin{bmatrix} \dot{x}_\alpha \\ -\frac{k}{m}x_\alpha + \frac{f_0}{m}\cos\omega t_\alpha \end{bmatrix},$$

$$\underset{\sim}{f}_{\alpha+} = \begin{bmatrix} \dot{x}_\alpha \\ -\frac{k+k_f}{m}x_\alpha - \frac{c_f}{m}\dot{x}_\alpha + \frac{f_0}{m}\cos\omega t_\alpha \end{bmatrix}. \tag{3.33}$$

The saltation matrix $\underline{S}_\alpha$ yields

$$\underline{S}_\alpha = \underline{I} + \frac{(\underset{\sim}{f}_{\alpha+} - \underset{\sim}{f}_{\alpha-})\underset{\sim}{n}_\alpha^{\mathrm{T}}}{\underset{\sim}{n}_\alpha^{\mathrm{T}}\underset{\sim}{f}_{\alpha-}} = \underline{I} + \begin{bmatrix} 0 & 0 \\ -\frac{c_f}{m} & 0 \end{bmatrix} = \begin{bmatrix} 1 & 0 \\ -\frac{c_f}{m} & 1 \end{bmatrix}. \tag{3.34}$$

We now consider the transition from the mode with contact to the mode without contact. Let us assume that the trajectory crosses Σ, leaving V_+ and entering V_-, at $t = t_\beta$. The trajectory crosses therefore the Σ_β part of Σ at this instance. Consequently, the following holds

$$f_c = k_f x_\beta + c_f \dot{x}_\beta = 0. \tag{3.35}$$

We can now construct the saltation matrix $\underline{S}_\beta$. The right-hand sides at the instance t_β are

$$\underset{\sim}{f}_{\beta-} = \begin{bmatrix} \dot{x}_\beta \\ -\frac{k+k_f}{m}x_\beta - \frac{c_f}{m}\dot{x}_\beta + \frac{f_0}{m}\cos\omega t_\beta \end{bmatrix},$$

$$\underset{\sim}{f}_{\beta+} = \begin{bmatrix} \dot{x}_\beta \\ -\frac{k}{m}x_\beta + \frac{f_0}{m}\cos\omega t_\beta \end{bmatrix}. \tag{3.36}$$

If we substitute (3.35) in (3.36), then the latter equations appear to be identical, $\underset{\sim}{f}_{\beta-} = \underset{\sim}{f}_{\beta+}$. Consequently, $\underline{S}_\beta$ is simply the identity matrix, $\underline{S}_\beta = \underline{I}$.

The results show that the saltation matrices $\underline{S}_\alpha$ and $\underline{S}_\beta$ are not dependent on the support stiffness k_f. The saltation matrix $\underline{S}_\alpha$ is affected, however, by the ratio $\frac{c_f}{m}$. The physical interpretation must be sought in the discontinuity of the contact force f_c. The spring force before the contact event, kx, is equal to the spring force after the contact event, $(k + k_f)x$, because contact is made when $x = 0$. But the damping force before the contact event, being zero, is not equal to the damping force after the contact event, $c_f\dot{x}$. The contact force f_c will be continuous for the transition from contact to no-contact, which is the reason that $\underline{S}_\beta$ is equal to the identity matrix.

If the damping coefficient c_f is set to zero, the system reduces to a second-order system with discontinuous stiffness. In this case, the hyper-surfaces Σ_α and Σ_β do not form an angle and Σ is a smooth hyper-plane. The saltation matrices $\underline{S}_\alpha$ and $\underline{S}_\beta$ are both equal to the identity matrix in this case. It can be concluded that the jumps in the fundamental solution matrix are not caused by the discontinuous stiffness but by the discontinuous damping term.

4. Non-Smooth Analysis

The method of linear approximation is developed in this section and applied to Jacobian matrices and saltation matrices. Linear approximation is compared with the generalized differential of Clarke. The non-smooth analysis tools developed in this section will be used to study bifurcation points of non-smooth systems in Section 5.

4.1. Linear Approximations at the Discontinuity

Discontinuities in the vector field $\underset{\sim}{f}$ cause jumps in the fundamental solution matrix as was shown in the Section 3. The discontinuous differential equation is therefore often approximated by a continuous differential equation. The approximation can be chosen to be smooth, which is called the 'smoothing method' [31], but this is not necessary. The approximation should at least yield a continuous differential equation and be asymptotic.

We employ a special approximation in the sequel for analytical purposes. The jump of the vector field $\underset{\sim}{f}$ is approximated by a linear variation of $\underset{\sim}{f}$ from $\underset{\sim}{f}_-$ to $\underset{\sim}{f}_+$ in a thin space around the hyper-surface of discontinuity. We should keep in mind that a smooth (or continuous) approximation does not necessarily describe all solutions of the discontinuous system. This is for instance the case when a the discontinuous system exposes a repulsion sliding mode which implies non-uniqueness of solutions. The smooth or continuous approximation has uniqueness of solutions and can therefore not describe the behaviour at the repulsion sliding mode.

It will be shown that this linear approximation of the vector field at the hyper-surface of discontinuity also yields a linear variation of the saltation matrix. The linear approximation at the discontinuity is suitable for analytical purposes, due to its simplicity, and will prove to be an important tool in the bifurcation analysis of discontinuous systems. In Section 4.2 we will show that the concept of linear approximation is identical to the generalized derivative.

Consider again the discontinuous system 2.3 where the indicator equation h defines the hyper-surface of discontinuity Σ and with the subspaces V_- and V_+ and hyper-surface Σ defined by (2.5). In the following we will briefly denote a function $\underset{\sim}{g}(t, \underset{\sim}{x}(t))$ by $\underset{\sim}{g}$.

The hyper-surface Σ, on which $\underset{\sim}{f}$ is discontinuous, will now be replaced by a thin space $\tilde{\Sigma}$ with thickness ε. If ε approaches zero, then the space $\tilde{\Sigma}$ becomes infinitely thin. The discontinuous vector field $\underset{\sim}{f}$ is replaced by a continuous vector field $\underset{\sim}{\tilde{f}}$. The vector field $\underset{\sim}{\tilde{f}}$ in $\tilde{\Sigma}$ varies linearly from $\underset{\sim}{f}_-$ to $\underset{\sim}{f}_+$ to ensure continuity.

$$\dot{\underset{\sim}{x}}(t) = \underset{\sim}{\tilde{f}} = \begin{cases} \underset{\sim}{f}_-, & \underset{\sim}{x} \in \tilde{V}_-, \\ (\underset{\sim}{f}_+ - \underset{\sim}{f}_-)\frac{h}{\varepsilon} + \underset{\sim}{f}_-, & \underset{\sim}{x} \in \tilde{\Sigma}, \\ \underset{\sim}{f}_+, & \underset{\sim}{x} \in \tilde{V}_+, \end{cases} \tag{4.1}$$

with

$$\begin{aligned} \tilde{V}_- &= \{\underset{\sim}{x} \in \mathbb{R}^n \mid h(\underset{\sim}{x}(t)) < 0\}, \\ \tilde{\Sigma} &= \{\underset{\sim}{x} \in \mathbb{R}^n \mid 0 \leq h(\underset{\sim}{x}(t)) \leq \varepsilon\}, \\ \tilde{V}_+ &= \{\underset{\sim}{x} \in \mathbb{R}^n \mid h(\underset{\sim}{x}(t)) > \varepsilon\}. \end{aligned} \tag{4.2}$$

Clearly, the vector field $\tilde{\underset{\sim}{f}}$ is continuous and converges asymptotically to $\underset{\sim}{f}$ as $\varepsilon \downarrow 0$. The Jacobian of $\tilde{\underset{\sim}{f}}$ follows from (4.1) and (2.6) to be

$$\underline{\tilde{J}}(t, \underset{\sim}{x}(t); \mu) = \begin{cases} \underline{J}_-, & \underset{\sim}{x} \in \tilde{V}_-, \\ (\underset{\sim}{f}_+ - \underset{\sim}{f}_-)\frac{\underset{\sim}{n}^{\mathrm{T}}}{\varepsilon} + (\underline{J}_+ - \underline{J}_-)\frac{h}{\varepsilon} + \underline{J}_-, & \underset{\sim}{x} \in \tilde{\Sigma}, \\ \underline{J}_+, & \underset{\sim}{x} \in \tilde{V}_+, \end{cases} \tag{4.3}$$

and is in fact not properly defined on the borders between $\tilde{V}_-, \tilde{V}_+$ and $\tilde{\Sigma}$ as $\tilde{\underset{\sim}{f}}$ is not necessarily smooth. This will not turn out to be problematic. Remark that system (4.1) is a non-smooth continuous system, which has existence and uniqueness of solutions (cf. [8, theorem 1.1, p. 178]).

We are interested in bifurcations of periodic solutions of discontinuous systems. The fundamental solution matrix of a discontinuous system can jump as we elaborated in Section 3. A periodic solution can be regarded as a fixed point of a Poincaré map $P(\underset{\sim}{x})$ on a Poincaré section. The derivative of the Poincaré map $DP(\underset{\sim}{x})$ can therefore also jump as it is directly related to the fundamental solution matrix [40]. We assume the Poincaré map itself to be locally continuous at the fixed point. As periodic solutions are fixed points of $P(\underset{\sim}{x})$ we will also study bifurcations of fixed points of non-smooth systems. Having periodic solutions in mind we will study only fixed points of continuous vector fields with discontinuous Jacobians. We consider therefore continuous but non-smooth *mappings*:

1. Bifurcations of fixed points: the vector field is

   (a) continuous: $\underset{\sim}{f}_-(t, \underset{\sim}{x}(t)) = \underset{\sim}{f}_+(t, \underset{\sim}{x}(t))$ if $\underset{\sim}{x}(t) \in \Sigma$;
   (b) non-smooth: $\underline{J}_-(t, \underset{\sim}{x}(t)) \neq \underline{J}_+(t, \underset{\sim}{x}(t))$ if $\underset{\sim}{x}(t) \in \Sigma$.

2. Bifurcations of periodic solutions:

   (a) the Poincaré map $P(\underset{\sim}{x})$ is continuous in $\underset{\sim}{x}$;
   (b) the derivative $DP(\underset{\sim}{x})$ of the Poincaré map is non-smooth, which yields $\underset{\sim}{f}_- \neq \underset{\sim}{f}_+$ if $\underset{\sim}{x}(t) \in \Sigma$.

Remarks. The statement that only continuous mappings will be considered is too restrictive. Poincaré mappings are in general discontinuous (for example the Lorenz system, [23] page 313). We will mainly consider mappings which are continuous in a sufficiently large neighborhood around the fixed point of the mapping. In Section 6.6, however, an example will be given where the Poincaré map is discontinuous at the fixed point, which results in infinitely unstable periodic solutions. Note that this is a sliding mode problem for which (3.2) does not hold.

We now study how the saltation matrix changes as the trajectory $\underset{\sim}{x}(t)$ is crossing the space $\tilde{\Sigma}$ from $\tilde{V}_-$ to $\tilde{V}_+$ (Figure 9), that is $\underset{\sim}{x}(t)$ crosses the hyper-surface $\tilde{\Sigma}$ *transversally* (2.10). Neighbouring trajectories of $\underset{\sim}{x}(t)$ will also cross $\tilde{\Sigma}$ transversally. Uniqueness of solutions in forward and backward time (cf. [8, theorem 1.1, p. 178]) assures that the neigbouring trajectories do not join with $\underset{\sim}{x}(t)$. We denote the state at the border of $\tilde{V}_-$ and $\tilde{\Sigma}$ by $\underset{\sim}{x}_0$ at time t_0. We denote the state at the border of $\tilde{V}_+$ and $\tilde{\Sigma}$ by $\underset{\sim}{x}_1$ at time t_1. Let the trajectory

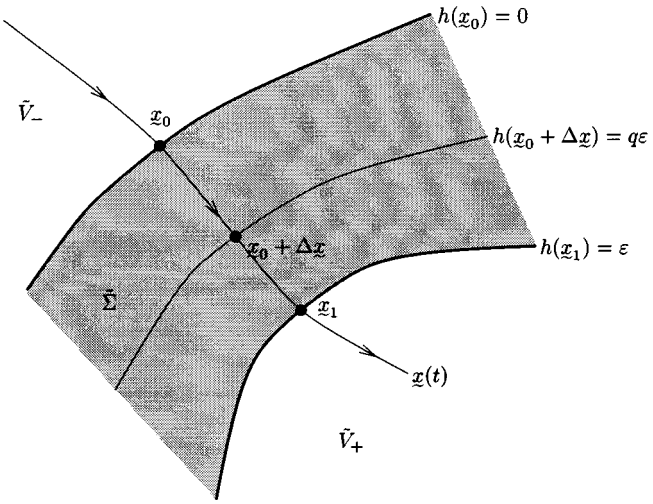

Figure 9. Linear approximation over a hyper-surface.

starting from $\underline{x}_0$ travel a distance $\Delta\underline{x}$ in $\tilde{\Sigma}$ during a time Δt. The following holds

$$\begin{aligned} &t_0 \leq t_0 + \Delta t \leq t_1, \\ &\Delta\underline{x}(t_0) = \underline{0}, \\ &\underline{x}_1 = \underline{x}_0 + \Delta\underline{x}(t_1). \end{aligned} \tag{4.4}$$

We expand the indicator function $h(\underline{x})$ as a Taylor approximation around $\underline{x}_0$,

$$h(\underline{x}_0 + \Delta\underline{x}) = h(\underline{x}_0) + \frac{\partial h}{\partial \underline{x}^{\mathrm{T}}}\Delta\underline{x} + O(\Delta\underline{x}^2). \tag{4.5}$$

The indicator function should be chosen such that it always holds that $\partial h/\partial \underline{x}^{\mathrm{T}} \neq \underline{0}$. As ε approaches zero, the space $\tilde{\Sigma}$ becomes infinitely thin and $\Delta\underline{x} \downarrow \underline{0}$ and $\Delta t \downarrow 0$. It therefore suffices to take only the linear term into account in the Taylor approximation of (4.5) as $\varepsilon \downarrow 0$. It follows from the definition of $\tilde{V}_-$ in (4.2) that

$$h(\underline{x}_0) = 0, \quad h(\underline{x}_1) = \varepsilon. \tag{4.6}$$

We assume that the indicator function in $\tilde{\Sigma}$ has values between 0 and ε

$$0 = h(\underline{x}_0) \leq h(\underline{x}_0 + \Delta\underline{x}) \leq h(\underline{x}_1) = \varepsilon \tag{4.7}$$

and assume that the indicator function in $\tilde{\Sigma}$ increases monotonically from 0 to ε when t is increased from t_0 to t_1. This assumption holds when $\tilde{\Sigma}$ is infinitely small. Consequently, due to monotonicity and the omission of higher-order terms it is allowed to express the indicator function for $\varepsilon \downarrow 0$ as a linear function of a variable $q(t)$

$$h(\underline{x}_0 + \Delta\underline{x}(t)) = q(t)\varepsilon, \tag{4.8}$$

where $0 \leq q(t) \leq 1$ on $t_0 \leq t \leq t_1$. The variable $q(t)$ is a parameterization of the transversal trajectory $\underline{x}(t)$ in the space $\tilde{\Sigma}$, where $q(t_0) = 0$ corresponds to $\underline{x}(t_0)$ on the border between $\tilde{V}_-$ and $\tilde{\Sigma}$ and $q(t_1) = 1$ corresponds to $\underline{x}(t_1)$ on the border between $\tilde{\Sigma}$ and $\tilde{V}_+$. The value

of $q(t)$ is found from (4.8) with $\underset{\sim}{x}(t) = \underset{\sim}{x}_0 + \Delta\underset{\sim}{x}(t) \in \tilde{\Sigma}$. Similarly, we express the distance $\Delta\underset{\sim}{x}(t_0 + \Delta t)$ as a Taylor approximation up to the linear term with $\Delta t \downarrow 0$ for $\varepsilon \downarrow 0$

$$\Delta\underset{\sim}{x}(t_0 + \Delta t) = \int_{t_0}^{t_0+\Delta t} \underset{\sim}{\tilde{f}}\, \mathrm{d}t = \underset{\sim}{f}_- \Delta t + O(\Delta t^2). \tag{4.9}$$

Substitution of (4.6) and (4.8) in (4.5) yields $q(t_0 + \Delta t)\varepsilon = \underset{\sim}{n}^{\mathrm{T}} \underset{\sim}{f}_- \Delta t$ for $\varepsilon \downarrow 0$. We will omit the dependence of q on t in the sequel.

The Jacobian can be approximated for small ε and bounded $\underset{\sim}{\tilde{f}}$ by

$$\underline{\tilde{J}}(t_0 + \Delta t, \underset{\sim}{x}_0 + \Delta\underset{\sim}{x}(t)) = \frac{1}{\varepsilon}(\underset{\sim}{f}_+ - \underset{\sim}{f}_-)\underset{\sim}{n}^{\mathrm{T}} + O(1), \tag{4.10}$$

which becomes *large* for $\varepsilon \downarrow 0$ and $\underset{\sim}{f}_+ \neq \underset{\sim}{f}_-$. We can now construct the saltation matrix $\underline{\tilde{S}} = \underline{\Phi}(t_0 + \Delta t, t_0)$ for $\varepsilon \downarrow 0$ from the previous results

$$\begin{aligned} \underline{\tilde{S}} = \underline{I} + \int_{t_0}^{t_0+\Delta t} \underline{\tilde{J}}(t, \underset{\sim}{x}(t))\, \underline{\Phi}(t_0 + \Delta t, t_0)\, \mathrm{d}t \;&=\; \underline{I} + (\underset{\sim}{f}_+ - \underset{\sim}{f}_-)\frac{\underset{\sim}{n}^{\mathrm{T}}}{\varepsilon}\Delta t + O(\Delta t) \\ &=\; \underline{I} + q\frac{(\underset{\sim}{f}_+ - \underset{\sim}{f}_-)\underset{\sim}{n}^{\mathrm{T}}}{\underset{\sim}{n}^{\mathrm{T}}\underset{\sim}{f}_-} + O(\Delta t). \end{aligned} \tag{4.11}$$

The saltation matrix $\underline{\tilde{S}}$ converges therefore for $\varepsilon \downarrow 0$ to the set

$$\underline{\tilde{S}} = \left\{ \underline{I} + q\frac{(\underset{\sim}{f}_+ - \underset{\sim}{f}_-)\underset{\sim}{n}^{\mathrm{T}}}{\underset{\sim}{n}^{\mathrm{T}}\underset{\sim}{f}_-}, \forall\, 0 \leq q \leq 1 \right\} = \{\underline{I} + q(\underline{S} - \underline{I}), \forall\, 0 \leq q \leq 1\}, \tag{4.12}$$

where $\underline{S}$ is the saltation matrix over Σ given by (3.18). The saltation matrix therefore behaves linearly over $\tilde{\Sigma}$ if $\varepsilon \downarrow 0$. The derivation is given for autonomous h but the same result could have been obtained for non-autonomous h.

For fixed points we have $\underset{\sim}{f}_- = \underset{\sim}{f}_+$ and the Jacobian on $\tilde{\Sigma}$ is therefore given by

$$\underline{\tilde{J}}(t, \underset{\sim}{x}_0 + \Delta\underset{\sim}{x}(t)) = (\underline{J}_+ - \underline{J}_-)q(t) + \underline{J}_-. \tag{4.13}$$

If $\varepsilon \downarrow 0$, then the space $\tilde{\Sigma}$ reduces to the hyper-surface Σ and the Jacobian on Σ becomes set-valued. The set-valued Jacobian is given by

$$\underline{\tilde{J}}(t, \underset{\sim}{x}) = \{(\underline{J}_+ - \underline{J}_-)q + \underline{J}_-, \forall\, 0 \leq q \leq 1\}, \quad \underset{\sim}{x} \in \Sigma. \tag{4.14}$$

The linear approximation with $\varepsilon > 0$ smoothens a non-smooth continuous vector field and replaces a discontinuous vector field by a non-smooth continuous vector field.

4.2. Generalized Differentials

The concept of *linear approximation* is closely related with the subdifferential of Clarke [8], also called *generalized differential*.

Consider a scalar continuous piecewise differentiable function $f(x)$ with a kink at one value of x, such as $f(x) = |x|$ (Figure 10a). The derivative $f'(x)$ is defined by the tangent

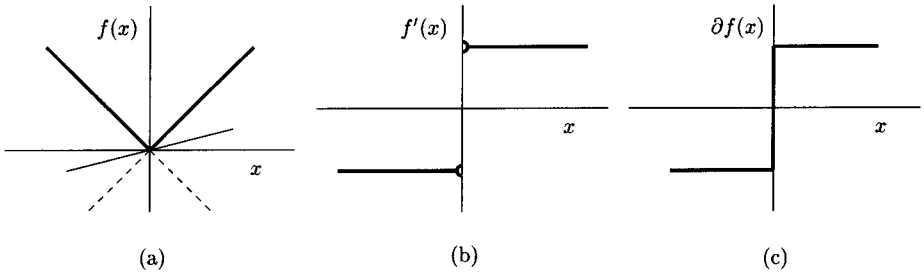

Figure 10. Function (a), classical derivative (b) and generalized derivative (c).

line to the graph of f when the graph is smooth at x. Although the function is not absolutely differentiable at every point x, it possesses a left and right derivative defined as

$$f'_-(x) = \lim_{y \uparrow x} \frac{f(y) - f(x)}{y - x}, \quad f'_+(x) = \lim_{y \downarrow x} \frac{f(y) - f(x)}{y - x}. \tag{4.15}$$

The *generalized derivative* of f at x is declared as *any* value $f'_q(x)$ included between its left and right derivatives. Such an intermediate value can be expressed as a convex combination of the left and right derivatives,

$$f'_q(x) = (1 - q) f'_- + q f'_+(x), \quad 0 \leq q \leq 1. \tag{4.16}$$

Geometrically, a generalized derivative is the slope of *any* line drawn through the point $(x, f(x))$ and between the left and right tangent lines (drawn by dashed lines in Figure 10a). The set of all the generalized derivatives of f at x, more generally the convex hull of the derivative extremes, is called the *generalized differential* of f at x

$$\begin{aligned} \partial f(x) &= \overline{\text{co}}\{f'_-(x), f'_+(x)\} \\ &= \{f'_q(x) \mid f'_q(x) = (1 - q) f'_-(x) + q f'_+(x), \forall q \mid 0 \leq q \leq 1\}. \end{aligned} \tag{4.17}$$

The generalized differential is the set of all the slopes of all the lines included in the cone bounded by the left and right tangent lines and is a closed convex set. Alternatively, it consists in closing the graph of $f'(x)$ at the points where it is discontinuous (Figures 10b and 10c). In non-smooth analysis, the generalized differential is used to define a local extremum of f at x by $0 \in \partial f$, which is the generalized form of $f'(x) = 0$ in smooth analysis [8].

In Section 4.1 the concept of linear approximation was introduced with approximation parameter ε. Considering the limit of ε going to zero, it was shown that the Jacobian behaves on the hyper-surface as (4.13) and the saltation matrix as (4.12) or in terms of the fundamental solution matrix

$$\underline{\tilde{\Phi}} = \{(1 - q)\underline{\Phi}_- + q\underline{\Phi}_+, \forall\, 0 \leq q \leq 1\}. \tag{4.18}$$

The Jacobian of linear approximation $\underline{\tilde{J}}$ can be regarded as the generalized Jacobian in the sense of Clarke, that is, the generalized differential of the vector field $\underset{\sim}{f}$ with respect to the state $\underset{\sim}{x}$,

$$\underline{\tilde{J}} = \partial_{\underset{\sim}{x}} \underset{\sim}{f}. \tag{4.19}$$

Similarly, the generalized fundamental solution matrix can be defined as the generalized differential of the solution $\underset{\sim}{x}(t)$ with respect to the initial condition $\underset{\sim}{x}_0$,

$$\underline{\tilde{\Phi}}(t, t_0) = \partial_{\underset{\sim}{x}_0} \underset{\sim}{x}(t). \tag{4.20}$$

We conclude that the approximation of the vector field by a linear approximation, as outlined in the previous section, converges for the Jacobian and fundamental solution matrix to their generalized differential forms.

5. Bifurcations of Fixed Points

In this section, we will study bifurcations of fixed points occurring in *non-smooth continuous systems*. It will be shown that a bifurcation in non-smooth systems can be discontinuous, in the sense that an eigenvalue jumps over the imaginary axis under the variation of a parameter. We will try to compare the bifurcations found in non-smooth systems with bifurcations of smooth systems. Bifurcations of fixed points will be used as a stepping stone to bifurcations of periodic solutions in discontinuous systems in Section 6.

5.1. Smooth Systems

We study bifurcations of fixed points of autonomous systems which depend on one single parameter μ:

$$\dot{\underset{\sim}{x}} = \underset{\sim}{f}(\underset{\sim}{x}, \mu). \tag{5.1}$$

Let n denote the dimension of the system. The system (5.1) is called *smooth* if it is differentiable up to any order in both $\underset{\sim}{x}$ and μ. Fixed points of (5.1) are solutions of the algebraic equations

$$\underset{\sim}{0} = \underset{\sim}{f}(\underset{\sim}{x}, \mu). \tag{5.2}$$

The continuous curves of solutions of (5.2) under variation of μ are called *branches*. The branches of smooth systems are continuous and smooth but can split into one or more other branches or can fold at bifurcation points. Seydel [47] defines a *bifurcation point* in the following way:

DEFINITION 5.1 (Bifurcation point [47]). A *bifurcation point* (with respect to μ) is a solution $(\underset{\sim}{x}^*, \mu^*)$, where the number of fixed points or (quasi-)periodic solutions changes when μ passes μ^*.

The definition is to be understood that also the number of fixed points and (quasi-)periodic solutions at the point under consideration have to be taken into account. Consider for instance the bifurcation diagram depicted in Figure 14a; there are two fixed points for $\mu < 0$, one fixed point for $\mu = 0$ (which is the point under consideration) and two fixed points for $\mu > 0$. The point $(x, \mu) = (0, 0)$ is therefore a bifurcation point because the number of fixed points changes at this point for varying μ (the change is: 2–1–2). We conclude that if branches intersect, then their intersection point must be a bifurcation point.

Another example is the saddle-node (or turning point) bifurcation depicted in Figure 13a: there are zero fixed points for $\mu < 0$, one fixed point for $\mu = 0$ and two fixed points for $\mu > 0$. One could be tempted to think that a bifurcation occurs if the slope of the branch becomes vertical. A counter example is the system

$$\dot{x} = f(x, \mu) = \mu - x^3.$$

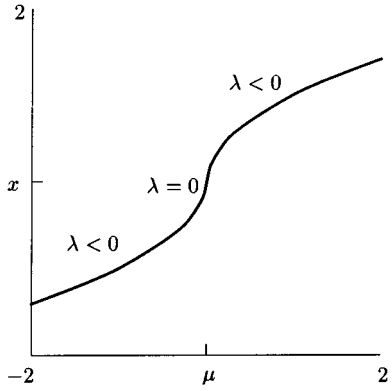

Figure 11. Hysteresis point.

The Jacobian is $\underline{J}(x, \mu) = -3x^2$ and therefore $\underline{J}(0, 0) = 0$. Furthermore, $f_{,\mu} \neq 0$ so the slope at $(0, 0)$ is vertical. But if we study the bifurcation diagram in Figure 11, then we see that $(0, 0)$ is not a bifurcation point according to Definition 5.1. Such a point is called a hysteresis point ([47]). Remark that the hysteresis effect is caused by the fact that $\partial^2 f(0, 0)/\partial x^2 = 0$.

A bifurcation diagram can be misleading. Two branches can cross each other in the two-dimensional bifurcation diagram without intersecting in the multi-dimensional space. Such a point is not a bifurcation point. The problem is caused by the projection of the multi-dimensional state-parameter space on the two-dimensional bifurcation diagram. Note that this is never a problem if $n = 1$.

Many bifurcations in the sense of Definition 5.1 expose a topological change of the phase portrait of the system as its parameter passes the bifurcation point. This brings us to the following definition for a bifurcation taken from Kuznetsov [30]:

DEFINITION 5.2 (Topological equivalence [30]). A dynamical system $\dot{\underset{\sim}{x}} = \underset{\sim}{f}(\underset{\sim}{x})$, $\underset{\sim}{x} \in \mathbb{R}^n$, is topologically equivalent in a region $U \subset \mathbb{R}^n$ to a dynamical system $\dot{\underset{\sim}{y}} = \underset{\sim}{g}(\underset{\sim}{y})$, $\underset{\sim}{y} \in \mathbb{R}^n$, in a region $V \subset \mathbb{R}^n$ if there is a homeomorphism $h : \mathbb{R}^n \to \mathbb{R}^n$, $h(U) = V$, mapping trajectories of the first system in U onto trajectories of the second system in V, preserving the direction of time.

Remark. A homeomorphism is an invertible map such that both the map and its inverse are continuous.

DEFINITION 5.3 (Bifurcation [30]). The appearance of a topologically nonequivalent phase portrait under variation of parameters is called a *bifurcation*.

A third definition of a bifurcation is given by Guckenheimer and Holmes [23], which does not exclude hysteresis points from being a bifurcation point. This is regarded as unsatisfactory and the definition of [23] will therefore not be used.

Definitions 5.1 and 5.3 are consistent with each other for all the examples of smooth continuous systems given in this paper in the sense that a bifurcation appears at a bifurcation point. Although Definitions 5.1, 5.2 and 5.3 were originally defined for smooth continuous systems, we can apply them to non-smooth or discontinuous systems. For periodic solutions of discontinuous systems, Definitions 5.1 and 5.3 can be inconsistent with each other. A

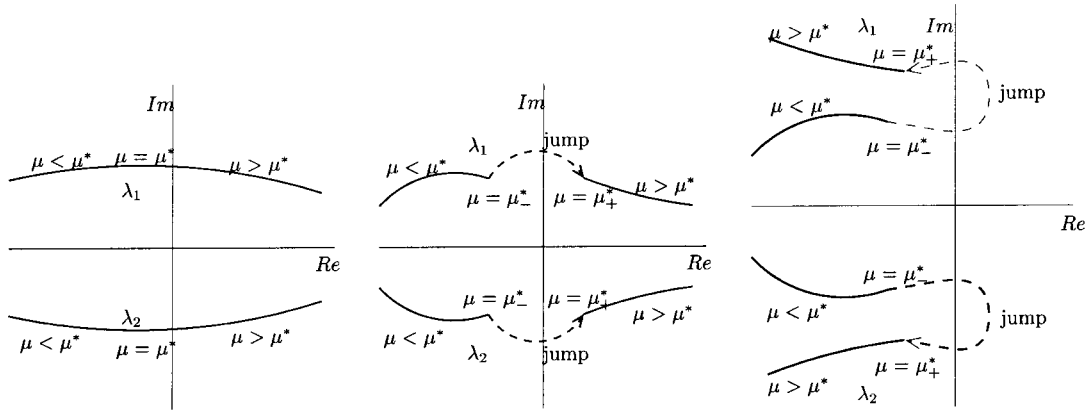

(a) continuous bifurcation

(b) discontinuous bifurcation; single crossing

(c) discontinuous bifurcation; double crossing

Figure 12. Eigenvalue paths at a bifurcation.

bifurcation in the sense of Definition 5.3 is not always a bifurcation in the sense of Definition 5.1. But a bifurcation in the sense of Definition 5.1 is always a bifurcation in the sense of Definition 5.3. With the aim to study non-smooth and discontinuous systems in mind, we will take Definition 5.1 as the definition for bifurcation in this paper.

Fixed points of smooth systems can expose the following bifurcations: (a) saddle-node bifurcation, (b) transcritical bifurcation, (c) pitchfork bifurcation or (d) Hopf bifurcation. Bifurcations (a–c) are static bifurcations, at which only branches of fixed points meet, and (d) is a dynamic bifurcation of a fixed point where a branch of periodic solutions is created at the bifurcation point. The Jacobian matrices of smooth systems are smooth continuous functions of the state vector and parameter. The eigenvalues of the Jacobian matrix will therefore also depend continuously (but not necessarily smooth) on the parameter. A bifurcation of a fixed point of a smooth system occurs when one eigenvalue (or a pair) passes the imaginary axis when a parameter is varied. The scenario is depicted in Figure 12a where a pair of complex conjugated eigenvalues pass the imaginary axis when a parameter μ is varied and a Hopf bifurcation occurs at some critical value $\mu = \mu^*$. The bifurcations occurring in smooth systems are called *continuous bifurcations* in this paper because the eigenvalues behave continuously.

5.2. Discontinuous Bifurcation: The Basic Idea

Non-smooth continuous systems possess hyper-surfaces on which the vector field is non-smooth. Let $\underset{\sim}{x}$ be a fixed point of (5.1) at some value for μ and let Σ be a hyper-surface which divides the state-space in the smooth subspaces V_- and V_+. If $\underset{\sim}{x}$ is not on Σ, then we can find a single-valued Jacobian matrix $\underline{J}(\underset{\sim}{x}, \mu)$. If $\underset{\sim}{x}$ is on Σ then there are two Jacobian matrices $\underline{J}_-(\underset{\sim}{x}, \mu)$ and $\underline{J}_+(\underset{\sim}{x}, \mu)$ on either side of Σ associated with the vector field in V_- and V_+. Assume that we vary μ such that the fixed point $\underset{\sim}{x}$ moves from V_- to V_+ via Σ. Let $\underset{\sim}{x}_\Sigma$ denote the unique fixed point on Σ for $\mu = \mu_\Sigma$. The Jacobian matrix $\underline{J}(\underset{\sim}{x}, \mu)$ varies as μ is varied and is discontinuous at $\mu = \mu_\Sigma$ for which $\underset{\sim}{x} = \underset{\sim}{x}_\Sigma$. Loosely speaking, we say that $\underline{J}(\underset{\sim}{x}, \mu)$ 'jumps' at $\mu = \mu_\Sigma$ from $\underline{J}_-(\underset{\sim}{x}_\Sigma, \mu_\Sigma)$ to $\underline{J}_+(\underset{\sim}{x}_\Sigma, \mu_\Sigma)$. A jump of the Jacobian matrix under the influence of a parameter implies a jump of the eigenvalues. In Section 4 we elaborated how we can define a 'generalized Jacobian' $\underline{\tilde{J}}(\underset{\sim}{x}, \mu)$ which is set-valued at

$(\underset{\sim}{x}_\Sigma, \mu_\Sigma)$. The generalized Jacobian is the closed convex hull of $\underset{\sim}{J}_-(\underset{\sim}{x}, \mu)$ and $\underset{\sim}{J}_+(\underset{\sim}{x}, \mu)$ at $(\underset{\sim}{x}_\Sigma, \mu_\Sigma)$,

$$\begin{aligned}\tilde{\underset{\sim}{J}}(\underset{\sim}{x}_\Sigma, \mu_\Sigma) &= \overline{\text{co}}\{\underset{\sim}{J}_-(\underset{\sim}{x}_\Sigma, \mu_\Sigma), \underset{\sim}{J}_+(\underset{\sim}{x}_\Sigma, \mu_\Sigma)\} \\ &= \{(1-q)\underset{\sim}{J}_-(\underset{\sim}{x}_\Sigma, \mu_\Sigma) + q\underset{\sim}{J}_+(\underset{\sim}{x}_\Sigma, \mu_\Sigma), \forall q \mid 0 \le q \le 1\}. \end{aligned} \tag{5.3}$$

In fact, (5.3) defines *how* the Jacobian 'jumps' at Σ. To be more precise, (5.3) gives the set of values which the generalized Jacobian can attain on Σ. From the set-valued generalized Jacobian we can obtain the set-valued eigenvalues. We can look upon $\text{eig}(\tilde{\underset{\sim}{J}}(\underset{\sim}{x}_\Sigma, \mu_\Sigma))$ together with (5.3) as if it gives a *unique* path of eigenvalues 'during' the jump as q is varied from 0 to 1. It is important to realize that for smooth systems the eigenvalues are single-valued functions of the parameter μ and that the eigenvalues are set-valued functions in μ for non-smooth systems. An eigenvalue can pass the imaginary axis while varying μ, leading to a smooth bifurcation, but it can also cross the imaginary axis during its jump along a path defined by the generalized Jacobian. Examples will be given in the next subsections where jumps of eigenvalues over the imaginary axis lead to non-classical bifurcations. We will name a bifurcation associated by a jump of an eigenvalue (or pair of them) over the imaginary axis a *discontinuous bifurcation*. A typical scenario of a discontinuous bifurcation is depicted in Figure 12b where the unique path of a pair of complex conjugated eigenvalues on the jump is indicated by the dashed lines. The path depends on the Jacobian matrices $\underset{\sim}{J}_-(\underset{\sim}{x}_\Sigma, \mu_\Sigma)$ and $\underset{\sim}{J}_+(\underset{\sim}{x}_\Sigma, \mu_\Sigma)$. The possibility of the eigenvalues to become set-valued greatly complicates the bifurcation behaviour as the eigenvalue could also cross the imaginary axis multiple times during its jump. This is depicted in Figure 12c where a pair of complex conjugated eigenvalues cross the imaginary axis twice during the jump. One can suggest that for this case there exists a discontinuous bifurcation which is a combination of two classical Hopf bifurcations. Other combinations would also be possible, like Hopf – saddle-node, saddle-node – saddle-node, etc. The discontinuous bifurcation can therefore be a single crossing bifurcation which behaves very much like a conventional smooth bifurcation, or it can be a multiple crossing bifurcation being far more complex.

We call the type of bifurcation, at which set-valued eigenvalues cross the imaginary axis, a discontinuous bifurcation because the eigenvalues behave discontinuous at the bifurcation point.

DEFINITION 5.4 (Discontinuous bifurcation). A bifurcation point, as defined by Definition 5.1, is called a *discontinuous bifurcation point* if the eigenvalues at the bifurcation point are set-valued and contain a value on the imaginary axis.

A treatise of some discontinuous bifurcations of fixed points will be given in the next subsections. For each of the continuous bifurcations (a)-(d) we try to find a similar discontinuous (single crossing) bifurcation occurring in a non-smooth continuous system. The non-smooth system should be as simple as possible and will therefore be chosen as a piecewise-linear continuous function. First the continuous bifurcation is briefly treated, and then its discontinuous counterpart is discussed. The insight in discontinuous bifurcations of fixed points of non-smooth continuous systems is important in its own right but will also be of value for the understanding of bifurcations of periodic solutions of discontinuous systems in Section 6.

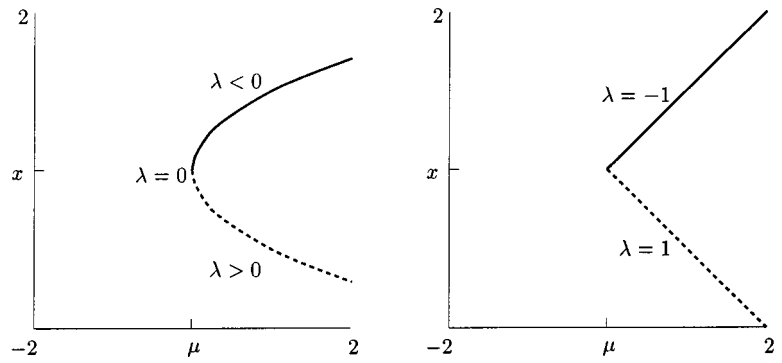

(a) smooth (b) discontinuous

Figure 13. Saddle-node bifurcation.

5.3. SADDLE-NODE BIFURCATION

The smooth scalar system

$$\dot{x} = f(x, \mu) = \mu - x^2 \tag{5.4}$$

has two fixed points $x = \pm\sqrt{\mu}$ for $\mu > 0$. The Jacobian $\underline{J} = -2x$ becomes singular at $x = 0$. There exists a bifurcation at $(x, \mu) = (0, 0)$ in the $x - \mu$ space (Figure 13a), which is known as a saddle-node bifurcation point. The upper branch is stable (solid line) and the lower one unstable (dashed line). At a continuous saddle-node bifurcation, $f_{,\mu}$ does not belong to the range of the matrix $\underline{J}$ (cf. theorem 3.1 in [30]). Hence the matrix $[\underline{J}|f_{,\mu}]$ has rank n. This can be geometrically interpreted as stating that the *continuation problem* is unique, i.e. we can follow the branch up to the bifurcation and continue uniquely on the other part of the branch. However, the fact that the continuation problem is unique does not necessarily imply that $\left[\underline{J}|f_{,\mu}\right]$ has full rank.

We now replace the term x^2 by $|x|$ which yields a non-smooth system:

$$\dot{x} = f(x, \mu) = \mu - |x|, \tag{5.5}$$

which has again two fixed points $x = \pm\mu$ for $\mu > 0$ with the generalized set-valued Jacobian $\underline{\tilde{J}}(x, \mu) = -\operatorname{Sgn} x$ and $f_{,\mu}(x, \mu) = 1$. The linear approximation of the Jacobian $\underline{\tilde{J}}(x, \mu)$ at $(x, \mu) = (0, 0)$ takes the form

$$\underline{\tilde{J}}(0, 0) = \{-2q + 1, \forall\, 0 \leq q \leq 1\}, \tag{5.6}$$

which becomes singular at $q = 1/2$. The bifurcation diagram is depicted in Figure 13b and looks similar to the one for the continuous version. Again there is a stable branch and an unstable branch but they now meet at an acute angle. From inspection of the bifurcation diagram we see that a static bifurcation (in the sense of Definition 5.1) exists at $(x, \mu) = (0, 0)$. We also conclude that the single eigenvalue on the bifurcation point is set-valued, i.e. $\lambda = [-1, 1]$. Where for the smooth case the eigenvalue passed the origin, the set-valued eigenvalue of the non-smooth system 'jumps' over the imaginary axis through the origin. For this reason, we will call the point $(x, \mu) = (0, 0)$ a *discontinuous* bifurcation point. The matrix $[\underline{\tilde{J}}(0, 0)|f_{,\mu}(0, 0)]$ for $q = 1/2$ has rank n similar to the smooth case. However,

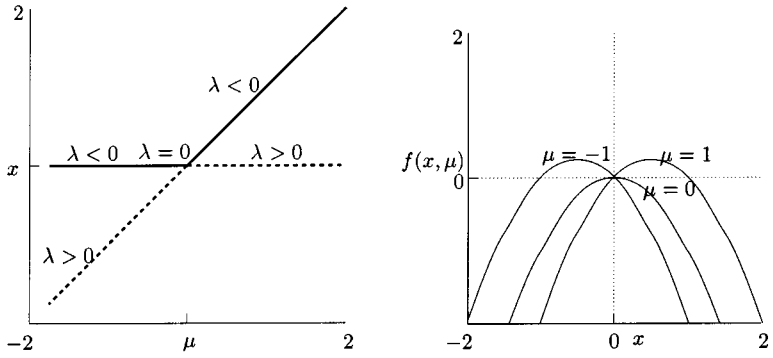

Figure 14. Transcritical bifurcation, smooth.

it seems awkward to conclude from this that the continuation problem (i.e. the possibility to follow the branch after the bifurcation point) is unique because the slope of the branch is not properly defined on the non-smooth bifurcation point.

The jump of the eigenvalue and the acute conjunction of branches are properties of discontinuous bifurcations which we will also encounter for bifurcations of periodic solutions.

It should be noted that, if we smoothen the non-smooth system with a particular arctangent function

$$\dot{x} \approx \mu - \frac{2}{\pi}\arctan(\varepsilon x)x \approx \mu - \frac{2}{\pi}\varepsilon x^2 + O(x^4),$$

the resulting bifurcation will be a continuous saddle-node bifurcation for all ε as can be seen from the expansion around the bifurcation point ($x = 0$). Whether *every* smoothing function will reveal a saddle-node bifurcation is not clear. But still, the discontinuous bifurcation in Figure 13b resembles the smooth saddle-node bifurcation in Figure 13a and we will call it therefore a discontinuous saddle-node bifurcation.

5.4. TRANSCRITICAL BIFURCATION

First, we consider the scalar smooth system

$$\dot{x} = f(x, \mu) = \mu x - x^2 \tag{5.7}$$

with the two fixed points $x = 0$ and $x = \mu$. The Jacobian of (5.7), $\underline{J}(x, \mu) = \mu - 2x$, has the single eigenvalue $\lambda = \mu$ at $x = 0$ and $\lambda = -\mu$ at $x = \mu$.

The static bifurcation, shown in Figure 14a, is a transcritical bifurcation point at which two branches exchange stability. The function $f(x, \mu)$ is depicted in Figure 14b for $\mu = -1$, $\mu = 0$ and $\mu = 1$. The function has two distinct zeros for $\mu \neq 0$, where one is always in the origin. At the bifurcation point ($\mu = 0$), the two zeros coincide to one double zero. The two zeros exchange stability when the bifurcation point is passed. At a continuous transcritical bifurcation point, $f_{,\mu}$ does belong to the range of the matrix $\underline{J}$. The matrix $\left[\underline{J} | f_{,\mu}\right]$ has rank $n - 1$ at $(x, \mu) = (0, 0)$. A second branch therefore crosses the bifurcation point which makes the continuation problem non-unique.

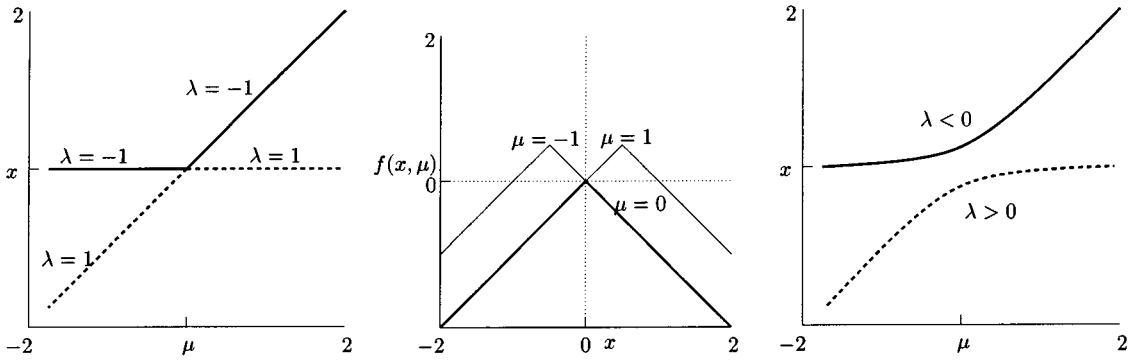

Figure 15. Transcritical bifurcation, discontinuous.

We now study the following non-smooth system:

$$\dot{x} = f(x, \mu) = \left|\frac{1}{2}\mu\right| - \left|x - \frac{1}{2}\mu\right|. \tag{5.8}$$

This non-smooth system approximates the parabola in Figure 14b by a piecewise-linear curve (a tent) as is depicted in Figure 15b. The lines are bold where the curves overlap each other.

The non-smooth system (5.8) has the same fixed points as the smooth system (5.7), $x = 0$ and $x = \mu$. From inspection of the bifurcation diagram depicted in Figure 15a we see that a static bifurcation (in the sense of Definition 5.1) exists at $(x, \mu) = (0, 0)$ as the number of fixed points changes (the change is 2–1–2). The bifurcation of the non-smooth system depicted in Figure 15a is similar to the transcritical bifurcation in Figure 14a. The generalized Jacobian of (5.8) is $\underline{\tilde{J}}(x, \mu) = -\operatorname{Sgn}(x - (1/2)\mu)$ and is set-valued at $(x, \mu) = (0, 0)$. The generalized Jacobian has the eigenvalues

$$\begin{aligned} &\lambda = -1 \quad \text{at } x = 0 \text{ if } \mu < 0, \qquad \lambda = 1 \quad \text{at } x = \mu \text{ if } \mu < 0, \\ &\lambda = 1 \quad \text{at } x = 0 \text{ if } \mu > 0, \qquad \lambda = -1 \quad \text{at } x = \mu \text{ if } \mu > 0. \end{aligned}$$

At the point $(x, \mu) = (0, 0)$ the eigenvalue is set-valued, $\lambda = [-1, 1]$. Where for the smooth transcritical bifurcation the eigenvalue passed the origin, the set-valued eigenvalue of the non-smooth system 'jumps' over the imaginary axis through the origin. For this reason, we will call the point $(x, \mu) = (0, 0)$ a discontinuous bifurcation point (Figure 15a). Because the structure of the branches around the discontinuous bifurcation point resembles the structure of the transcritical bifurcation we will call this bifurcation a discontinuous *transcritical* bifurcation.

The fixed point $(x, \mu) = (0, 0)$ is located on the intersection of two hyperplanes $\mu = 0$ and $x - (1/2)\mu = 0$ in the (x, μ) space. Two parameters, q_1 and q_2, are needed for a linear approximation. The first parameter, q_1, will be varied to satisfy the condition $\det(\underline{\tilde{J}}(0, 0)) = 0$ and the second parameter, q_2, will be varied to ensure that $[\underline{\tilde{J}}(0, 0) | \underset{\sim}{\tilde{f}}_{,\mu}(0, 0)]$ has rank $n - 1$.

The linear approximation $\underline{\tilde{J}}$ of the Jacobian at $(x, \mu) = (0, 0)$ takes the form

$$\underline{\tilde{J}}(0, 0) = \{-2q_1 + 1, \forall\, 0 \le q_1 \le 1\}, \tag{5.9}$$

which becomes singular at $q_1 = 1/2$. Furthermore,

$$\tilde{f}_{,\mu}(x, \mu) = \frac{1}{2}\operatorname{Sgn}(\mu) + \frac{1}{2}\operatorname{Sgn}\left(x - \frac{1}{2}\mu\right), \tag{5.10}$$

which is set-valued at the bifurcation point. We therefore construct a linear approximation

$$\begin{aligned}\tilde{f}_{,\mu}(0,0) &= \left\{\frac{1}{2}(2q_2-1)+\frac{1}{2}(2q_1-1), \forall\, 0\le q_1\le 1, \forall\, 0\le q_2\le 1\right\},\\ &= \{q_2+q_1-1, \forall\, 0\le q_1\le 1, \forall\, 0\le q_2\le 1\}. \end{aligned} \tag{5.11}$$

The matrix $[\underline{\tilde{J}}(0,0) \mid |\tilde{f}_{,\mu}(0,0)]$ has rank $n-1$ at $q_1 = 1/2$, $q_2 = 1/2$. Because of the non-smoothness of the problem it is awkward to conclude that the continuation problem is non-unique as for the smooth case but a resemblance exists.

If we smoothen the non-smooth system (5.8) with a particular arctangent function

$$\dot{x} \approx \frac{1}{\pi}\arctan\left(\frac{1}{2}\varepsilon\mu\right)\mu - \frac{2}{\pi}\arctan\left(\varepsilon\left(x-\frac{1}{2}\mu\right)\right)\left(x-\frac{1}{2}\mu\right) \approx \frac{2}{\pi}\varepsilon(\mu x - x^2),$$

the resulting bifurcation will be a continuous transcritical bifurcation for all ε as can be seen from the expansion around the bifurcation point ($x = 0$, $\mu = 0$). The smoothened system can be transformed to the standard normal form with the time transformation $\tau = \varepsilon t$.

However, not every smoothing function gives a transcritical bifurcation. Consider for instance the following non-symmetric smoothing:

$$\begin{aligned}\left|\frac{1}{2}\mu\right| &\approx \frac{2}{\pi}\arctan\left(\frac{1}{2}\varepsilon\mu\right)\frac{1}{2}\mu+\frac{1}{\varepsilon},\\ \left|x-\frac{1}{2}\mu\right| &\approx \frac{2}{\pi}\arctan\left(\varepsilon\left(x-\frac{1}{2}\mu\right)\right)\left(x-\frac{1}{2}\mu\right),\end{aligned} \tag{5.12}$$

which gives

$$\dot{x} \approx \frac{2}{\pi}\left(\varepsilon(\mu x - x^2)+\frac{1}{\varepsilon}\right) \tag{5.13}$$

for $|x| \ll 1$ and $\varepsilon \gg 1$. Equation (5.13) has two branches in the bifurcation diagram for varying μ but the branches do not intersect (Figure 15c). No bifurcation exists for (5.13).

5.5. Pitchfork Bifurcation

We consider the smooth system

$$\dot{x} = f(x,\mu) = \mu x + \alpha x^3, \tag{5.14}$$

where the constant α will be taken as $\alpha = \pm 1$. There is one fixed point for $\mu/\alpha \ge 0$ and are three fixed points for $\mu/\alpha < 0$,

$$\begin{aligned} &x = 0 \qquad \text{trivial point},\\ &x = \pm\sqrt{-\frac{\mu}{\alpha}} \ \text{ for } \frac{\mu}{\alpha} < 0.\end{aligned}$$

The Jacobian $\underline{J} = \mu + 3\alpha x^2$ has the single eigenvalues

$$\begin{aligned} &\lambda = \mu, \qquad \text{at } x = 0,\\ &\lambda = -2\mu, \ \text{ at } x = \pm\sqrt{-\frac{\mu}{\alpha}} \text{ for } \frac{\mu}{\alpha} < 0.\end{aligned}$$

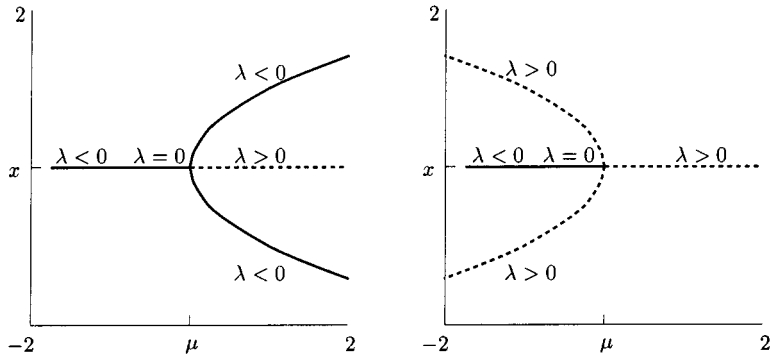

Figure 16. Pitchfork bifurcation, smooth.

For $\alpha = -1$ there is a supercritical pitchfork bifurcation (Figure 16a) and for $\alpha = 1$ a subcritical pitchfork bifurcation (Figure 16b). At a continuous pitchfork bifurcation point, $f_{,\mu}$ does belong to the range of the matrix $\underline{J}$ (cf. theorem 3.1 in [30]). The matrix $[\underline{J}|f_{,\mu}]$ has rank $n - 1 = 0$ at $(x, \mu) = (0, 0)$ which is consistent with the fact that two branches intersect at the bifurcation point.

We now study the following non-smooth system:

$$\dot{x} = f(x, \mu) = -x + \left|x + \frac{1}{2}\mu\right| - \left|x - \frac{1}{2}\mu\right|. \tag{5.15}$$

System (5.15) has the fixed points $x = 0$ (trivial point) and $x = \pm\mu$ for $\mu > 0$. From inspection of the bifurcation diagram (Figure 17a) we observe that a static bifurcation (in the sense of Definition 5.1) exists at $(x, \mu) = (0, 0)$ as the number of fixed points changes (the change is 1–1–3).

The generalized Jacobian of (5.15)

$$\tilde{\underline{J}}(x, \mu) = -1 + \mathrm{Sgn}\left(x + \frac{1}{2}\mu\right) - \mathrm{Sgn}\left(x - \frac{1}{2}\mu\right)$$

has the single eigenvalues

$$\begin{aligned}
&\lambda = -3, \ \text{at } x = 0, \quad \mu < 0,\\
&\lambda = 1, \quad \text{at } x = 0, \quad \mu > 0,\\
&\lambda = -1, \ \text{at } x = \pm\mu, \ \mu > 0
\end{aligned}$$

and is set-valued at $(x, \mu) = (0, 0)$. As there are two hyperplanes where the vector field is discontinuous, we need two parameters for a linear approximation of the Jacobian at $(x, \mu) = (0, 0)$,

$$\begin{aligned}
\tilde{\underline{J}}(0, 0) &= \{-1 + (-2q_1 + 1) - (-2q_2 + 1), \forall\, 0 \le q_1 \le 1, \forall\, 0 \le q_2 \le 1\}\\
&= \{2(q_2 - q_1) - 1, \forall\, 0 \le q_1 \le 1, \forall\, 0 \le q_2 \le 1\},
\end{aligned} \tag{5.16}$$

which becomes singular at $q_2 - q_1 = 1/2$. Furthermore,

$$\tilde{f}_{,\mu}(x, \mu) = \frac{1}{2}\,\mathrm{Sgn}\left(x + \frac{1}{2}\mu\right) + \frac{1}{2}\,\mathrm{Sgn}\left(x - \frac{1}{2}\mu\right), \tag{5.17}$$

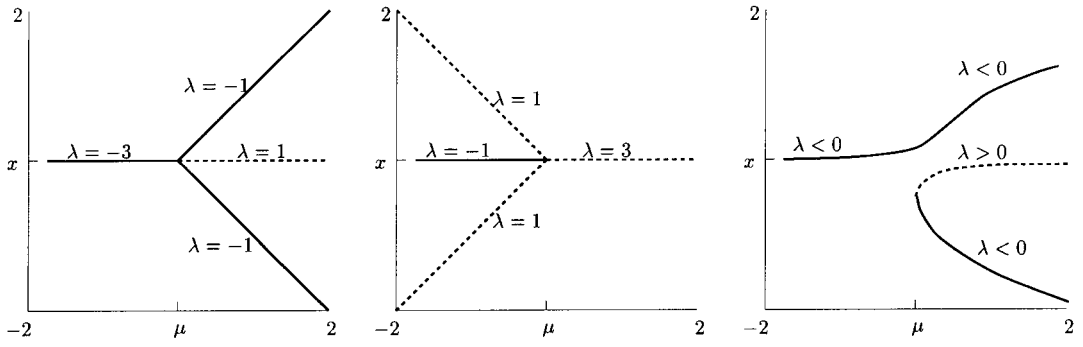

(a) supercritical (b) subcritical (c) Non-symmetric smoothing.

Figure 17. Pitchfork bifurcation, discontinuous.

which is set-valued at the bifurcation point. We therefore construct a linear approximation

$$\begin{aligned}\tilde{f}_{,\mu}(0,0) &= \left\{\frac{1}{2}(2q_1-1)+\frac{1}{2}(2q_2-1), \forall\, 0\le q_1\le 1, \forall\, 0\le q_2\le 1\right\}\\ &= \{q_1+q_2-1, \forall\, 0\le q_1\le 1, \forall\, 0\le q_2\le 1\}. \end{aligned} \tag{5.18}$$

The matrix $\left[\underline{\tilde{J}}(0,0)|\,\tilde{f}_{,\mu}(0,0)\right]$ has rank $n-1$ at $q_1=\frac{3}{4}$, $q_2=\frac{1}{4}$. The continuation problem is clearly non-unique as can be seen from the bifurcation diagram (Figure 17a). But to conclude this from the rank of $[\underline{\tilde{J}}(0,0)|\,\tilde{f}_{,\mu}(0,0)]$ seems awkward because of the non-smoothness of the problem.

The bifurcation diagram is shown in Figure 17a for the discontinuous supercritical pitchfork bifurcation of system (5.15). We call the bifurcation discontinuous because the eigenvalue 'jumps' over the imaginary axis. The discontinuous bifurcation is classified as a discontinuous *pitchfork* bifurcation because it resembles the continuous pitchfork bifurcation. Similarly, the system

$$\dot{x} = f(x,\mu) = x + \left|x+\frac{1}{2}\mu\right| - \left|x-\frac{1}{2}\mu\right| \tag{5.19}$$

exhibits a discontinuous subcritical pitchfork bifurcation (Figure 17b).

We smoothen the non-smooth system (5.15) with a particular arctangent function and apply a Taylor series expansion around ($x=0$, $\mu=0$)

$$\begin{aligned}\dot{x} &= -x + \left|x+\frac{1}{2}\mu\right| - \left|x-\frac{1}{2}\mu\right|\\ &\approx -x + \frac{2}{\pi}\arctan\left(\varepsilon\left(x+\frac{1}{2}\mu\right)\right)\left(x+\frac{1}{2}\mu\right)\\ &\quad -\frac{2}{\pi}\arctan\left(\varepsilon\left(x-\frac{1}{2}\mu\right)\right)\left(x-\frac{1}{2}\mu\right)\\ &\approx \left(-1+\frac{4}{\pi}\varepsilon\mu\right)x - \frac{8}{3\pi}\varepsilon^3\mu x^3. \end{aligned}$$

The resulting bifurcation is a continuous pitchfork bifurcation with the bifurcation point at ($x = 0$, $\mu = \pi/(4\varepsilon)$). The bifurcation point of the smoothened system therefore approaches the origin as ε is increased.

However, not every smoothing function gives a pitchfork bifurcation. Consider for instance the following non-symmetric smoothing:

$$\begin{aligned}\left|x + \frac{1}{2}\mu\right| &\approx \frac{2}{\pi}\arctan\left(\varepsilon\left(x + \frac{1}{2}\mu\right)\right)\left(x + \frac{1}{2}\mu\right) + \frac{1}{\varepsilon},\\ \left|x - \frac{1}{2}\mu\right| &\approx \frac{2}{\pi}\arctan\left(\varepsilon\left(x - \frac{1}{2}\mu\right)\right)\left(x - \frac{1}{2}\mu\right),\end{aligned} \tag{5.20}$$

which gives

$$\dot{x} \approx \left(-1 + \frac{4}{\pi}\varepsilon\mu\right)x - \frac{8}{3\pi}\varepsilon^3\mu x^3 + \frac{1}{\varepsilon} \tag{5.21}$$

for $|x| \ll 1$ and $\varepsilon \gg 1$. System (5.21) has two branches close to the origin in the bifurcation diagram for varying μ, but the branches do not intersect (Figure 17c). Only a saddle-node bifurcation exists for (5.21).

5.6. Hopf Bifurcation

At a Hopf bifurcation point the fixed point looses its stability and a periodic solution is born (or vice-versa). First, we consider the smooth planar system

$$\begin{aligned}\dot{x}_1 &= \mu x_1 - \omega x_2 + (\alpha x_1 - \beta x_2)(x_1^2 + x_2^2),\\ \dot{x}_2 &= \omega x_1 + \mu x_2 + (\beta x_1 + \alpha x_2)(x_1^2 + x_2^2),\end{aligned} \tag{5.22}$$

where μ, ω, α and β are constants. We will study the the fixed points and periodic solutions of system (5.22) for different values of μ. This system has a fixed point $\underline{x} = [x_1, x_2]^{\mathrm{T}} = [0, 0]^{\mathrm{T}}$ for all values of μ and the Jacobian matrix of the linearized system around the fixed point is

$$\underline{J} = \begin{bmatrix} \mu & -\omega \\ \omega & \mu \end{bmatrix}$$

with the eigenvalues $\lambda_1 = \mu - i\omega$ and $\lambda_2 = \mu + i\omega$. For $\mu < 0$ the fixed point is asymptotically stable. When μ is increased to $\mu = 0$ the fixed point becomes non-hyperbolic, and for $\mu > 0$ the fixed point becomes unstable. By using the transformation

$$x_1 = r\cos\theta \quad \text{and} \quad x_2 = r\sin\theta \tag{5.23}$$

we transform (5.22) into

$$\dot{r} = \mu r + \alpha r^3, \tag{5.24}$$

$$\dot{\theta} = \omega + \beta r^2. \tag{5.25}$$

The trivial fixed point of (5.24) corresponds to the fixed point of (5.22), and the nontrivial fixed point ($r \neq 0$) of (5.24) corresponds to a periodic solution of (5.22). In the latter case, r is the amplitude and $\dot{\theta}$ is the frequency of the periodic solution that is created by the Hopf bifurcation. The transformation (5.23) therefore transforms the Hopf bifurcation into the

pitchfork bifurcation. The bifurcation diagram for the transformed system (5.24) is identical to Figure 16 where x should be replaced by r.

We now study the following non-smooth system

$$\begin{aligned}
\dot{x}_1 &= -x_1 - \omega x_2 + \frac{x_1}{\sqrt{x_1^2+x_2^2}}\left(\left|\sqrt{x_1^2+x_2^2}+\frac{1}{2}\mu\right| - \left|\sqrt{x_1^2+x_2^2}-\frac{1}{2}\mu\right|\right),\\
\dot{x}_2 &= \omega x_1 - x_2 + \frac{x_2}{\sqrt{x_1^2+x_2^2}}\left(\left|\sqrt{x_1^2+x_2^2}+\frac{1}{2}\mu\right| - \left|\sqrt{x_1^2+x_2^2}-\frac{1}{2}\mu\right|\right),
\end{aligned} \tag{5.26}$$

which is dependent on the parameters μ and ω. We will study the fixed points and periodic solutions of system (5.26) for different values of μ. The non-smooth system (5.26) has the same fixed point as the smooth system with the same stability. We transform the system (5.26) with the transformation (5.23) into

$$\dot{r} = -r + \left|r+\frac{1}{2}\mu\right| - \left|r-\frac{1}{2}\mu\right|, \tag{5.27}$$

$$\dot{\theta} = \omega. \tag{5.28}$$

The one-dimensional system (5.27) is identical to the non-smooth system (5.15) exposing a discontinuous pitchfork bifurcation. The scenario for the transformed system (5.27) is identical to Figure 17.

5.7. Hopf-Pitchfork Bifurcation

Consider the non-smooth continuous system

$$\begin{aligned}
\dot{x}_1 &= x_2,\\
\dot{x}_2 &= -x_1 + |x_1+\mu| - |x_1-\mu| - x_2 - |x_2+\mu| + |x_2-\mu|.
\end{aligned} \tag{5.29}$$

System (5.29) has the fixed points $(x_1, x_2) = (0, 0)$ (trivial point) and $(x_1, x_2) = (\pm 2\mu, 0)$ for $\mu > 0$. The Jacobian matrix at the trivial branch jumps at $\mu = 0$ from $\underline{J}(0,0)^{\mathrm{tr}}_{-}$ to $\underline{J}(0,0)^{\mathrm{tr}}_{+}$.

$$\underline{J}(0,0)^{\mathrm{tr}}_{-} = \begin{bmatrix} 0 & 1 \\ -3 & 1 \end{bmatrix}, \quad \mu < 0, \quad \lambda = \frac{1}{2} \pm i\frac{1}{2}\sqrt{11}, \tag{5.30}$$

$$\underline{J}(0,0)^{\mathrm{tr}}_{+} = \begin{bmatrix} 0 & 1 \\ 1 & -3 \end{bmatrix}, \quad \mu > 0, \quad \lambda = -1\frac{1}{2} \pm \frac{1}{2}\sqrt{13} \approx \{0.30, -3.30\}. \tag{5.31}$$

The trivial fixed point is therefore an unstable focus for $\mu < 0$ and a saddle for $\mu > 0$. The Jacobian matrix on the non-trivial branches is

$$\underline{J}(\pm 2\mu, 0)^{\mathrm{non}} = \begin{bmatrix} 0 & 1 \\ -1 & -3 \end{bmatrix}, \quad \mu > 0, \quad \lambda = -1\frac{1}{2} \pm \frac{1}{2}\sqrt{5} \approx \{-0.38, -2.62\}. \tag{5.32}$$

Fixed points on the non-trivial branches are therefore stable nodes. The jump of the Jacobian on the trivial branch can be expressed as

$$\tilde{\underline{J}}(0,0)^{\mathrm{tr}} = \{(\underline{J}(0,0)^{\mathrm{tr}}_{+} - \underline{J}(0,0)^{\mathrm{tr}}_{-})q + \underline{J}(0,0)^{\mathrm{tr}}_{-}, \forall\, 0 \le q \le 1\}. \tag{5.33}$$

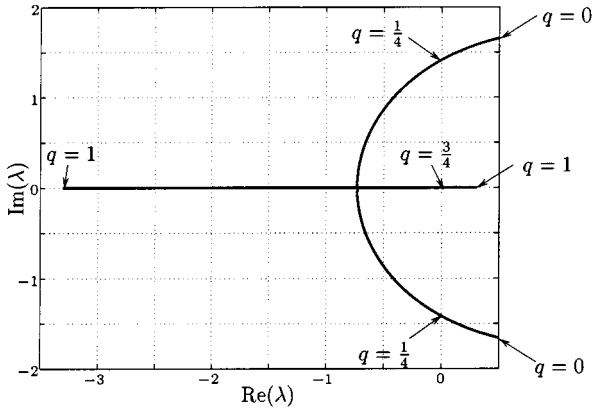

Figure 18. Path of the eigenvalues of $\underline{\tilde{J}}(0,0)^{\mathrm{tr}}$.

The eigenvalues of the convex combination $\underline{\tilde{J}}(0,0)^{\mathrm{tr}}$ are plotted for $0 \leq q \leq 1$ (Figure 18). We observe that the eigenvalues of the convex combination cross the imaginary axis twice. At $q = 1/4$ a pair of complex conjugated eigenvalues passes the imaginary axis and at $q = 3/4$ a single eigenvalue passes the origin.

With the transformation

$$y_1 = \frac{x_1}{\mu}, \quad y_2 = \frac{x_2}{\mu} \tag{5.34}$$

we can transform system (5.29) for $\mu < 0$ to

$$\begin{aligned} \dot{y}_1 &= y_2, \\ \dot{y}_2 &= -y_1 - |y_1 + 1| + |y_1 - 1| - y_2 + |y_2 + 1| - |y_2 - 1| \end{aligned} \tag{5.35}$$

and for $\mu > 0$ to

$$\begin{aligned} \dot{y}_1 &= y_2, \\ \dot{y}_2 &= -y_1 + |y_1 + 1| - |y_1 - 1| - y_2 - |y_2 + 1| + |y_2 - 1|. \end{aligned} \tag{5.36}$$

The transformed systems are independent of μ for $\mu \neq 0$. Fixed points and periodic solutions of (5.35) and (5.36) are after a back-transformation with (5.34) also fixed points and periodic solutions of system (5.29). The location of the fixed points of system (5.29) scale therefore with μ. But also all periodic solutions of system (5.29) scale with μ. This means that the shape of a periodic solution of (5.29) does not change for varying μ, but the size of the periodic solution scales with μ. The period time is independent of μ. The bifurcation diagram of system (5.29) is depicted in Figure 19a. Branches of fixed points are indicated by black lines and periodic branches by grey lines. Stable branches are indicated by solid lines and unstable branches by dashed lines. Fixed points were found analytically and the periodic solution was found numerically. The point $(x_1, x_2, \mu) = (0, 0, 0)$ is a bifurcation point where two branches of fixed points bifurcate from the trivial branch and also one periodic solution. This bifurcation behaviour is consistent with the path of the eigenvalues 'during' the jump (Figure 18). The two crossings with the imaginary axis would suggest a combination of a Hopf and a static bifurcation. This is indeed the case because a periodic branch and other

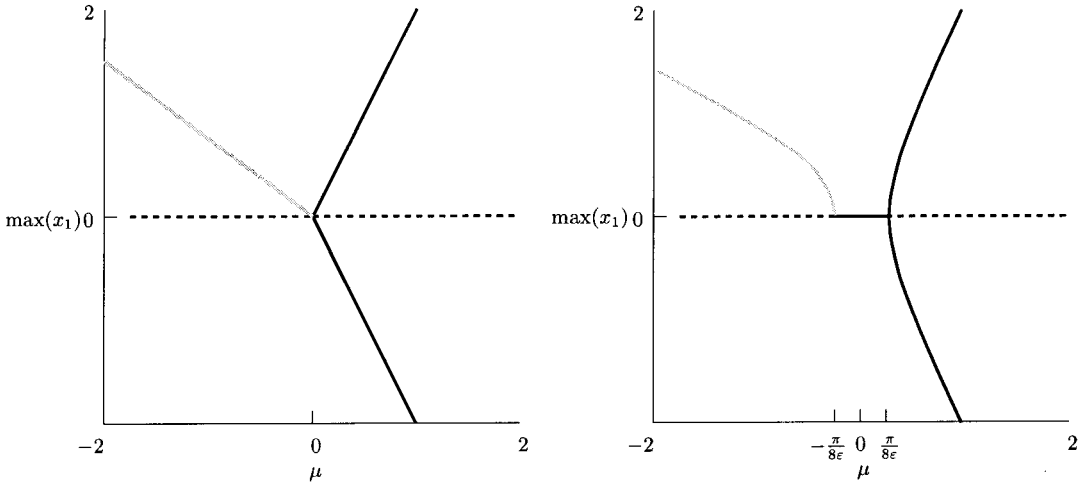

(a) Non-smooth system. (b) Smooth approximating system.

Figure 19. Bifurcation diagrams.

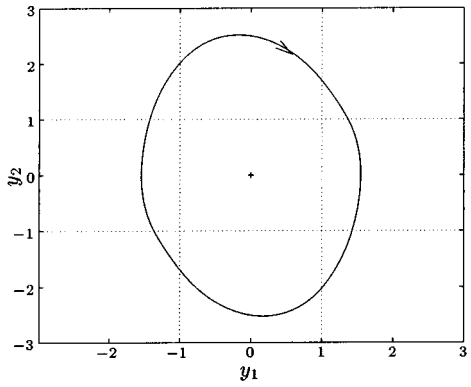

Figure 20. Periodic solution.

branches of fixed points are created at the bifurcation point. The magnitude $\max(x_1)$ varies linearly in μ for all branches as was expected from the transformation. The period time of the periodic solution is $T = 4.03$ s and is independent of μ. The stable periodic solution in the transformed coordinates (5.34) is depicted in Figure 20 together with the unstable fixed point (denoted by '+') and the lines $y_1 = \pm 1$, $y_2 = \pm 1$ on which the vector field is non-smooth.

We now study the smooth approximating system

$$\begin{aligned}
\dot{x}_1 &= x_2, \\
\dot{x}_2 &= -x_1 + \frac{2}{\pi}\arctan(\varepsilon(x_1+\mu))(x_1+\mu) - \frac{2}{\pi}\arctan(\varepsilon(x_1-\mu))(x_1-\mu) \\
&\quad - x_2 - \frac{2}{\pi}\arctan(\varepsilon(x_2+\mu))(x_2+\mu) + \frac{2}{\pi}\arctan(\varepsilon(x_2-\mu))(x_2-\mu). \qquad (5.37)
\end{aligned}$$

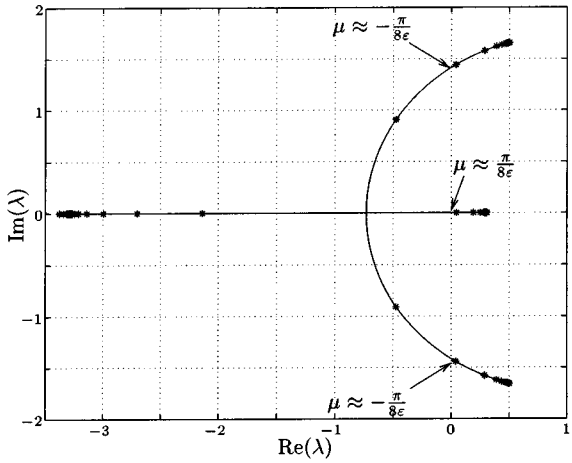

Figure 21. Path of the eigenvalues of the approximating system.

The system can be expanded in a Taylor series around $x_1 = x_2 = 0$

$$\begin{aligned} \dot{x}_1 &= x_2, \\ \dot{x}_2 &\approx \left(-1 + \frac{8}{\pi}\varepsilon\mu\right) x_1 - \frac{64}{3\pi}\varepsilon^3\mu x_1^3 + \left(-1 - \frac{8}{\pi}\varepsilon\mu\right) x_2 + \frac{64}{3\pi}\varepsilon^3\mu x_2^3. \end{aligned} \tag{5.38}$$

The smooth approximating system (5.37) also has the trivial branch of fixed points $(x_1, x_2) = (0, 0)$. The location of the eigenvalues on the trivial branch are computed numerically (with $\varepsilon = 10$) for varying μ. The eigenvalues are plotted in the complex plane in Figure 21 for some values of μ (indicated by *) together with the eigenvalue-path of the convex combination (Figure 18), which is indicated by a solid line. The eigenvalues of the smooth approximating system seem to be almost located on the eigenvalue-path of the convex combination of the non-smooth system. The trivial branch of the approximating system also undergoes a Hopf bifurcation and a pitchfork bifurcation but at different values of μ. The bifurcation diagram of the smooth approximating system is sketched in Figure 19b. The Hopf bifurcation is approximately located at $\mu = -\pi/(8\varepsilon)$ and the pitchfork bifurcation approximately at $\mu = \pi/(8\varepsilon)$. The two bifurcations approach each other for increasing ε.

5.8. Discussion

For each of the classical continuous bifurcations a discontinuous bifurcation was found. Also a discontinuous bifurcation was observed in Section 5.7 which was not a direct counterpart of a classical continuous bifurcation. However, the discontinuous bifurcation can be looked upon as the combination of two continuous bifurcations. The qualitative behaviour of the bifurcation is (in this particular case) simply the combination of the behaviour of a Hopf and a pitchfork bifurcation. In Section 6 we will encounter a combined flip-fold bifurcation of a periodic solution that behaves like a flip and fold bifurcation but also shows behaviour not covered by a flip or fold bifurcation separately. We are therefore not confident that the behaviour of a multiple crossing bifurcation of a fixed point is always simply the combination of behaviour of continuous bifurcations.

The discontinuous bifurcations in the previous examples were all accompanied by a jump of an eigenvalue (or pair) over the imaginary axis. The conclusion that a bifurcation exists

was taken from *inspection* of the bifurcation diagram. If there is a change in the number of fixed points for a certain parameter value then there is a bifurcation at this parameter value according to Definition 5.1. We also observed that a 'jump' exists of the eigenvalue over the imaginary axis. Although it is intuitively appealing to state that at a bifurcation an eigenvalue (or pair of them) *must* 'jump' or pass the imaginary axis, we do not have mathematical proof for this.

The discontinuous bifurcations of the preceding examples were classified by comparing their nature with a certain type of continuous bifurcation. If at a discontinuous bifurcation the change of fixed points is the same as for a certain type of continuous bifurcation, then the discontinuous bifurcation can be regarded as the discontinuous counterpart of that type of continuous bifurcation. We observed that all discontinuous static bifurcations expose a jump of an eigenvalue through the origin, like for the continuous static bifurcations. For the discontinuous Hopf bifurcation, a pair of eigenvalues jumps through the imaginary axis, consistent with the continuous Hopf bifurcation. The example in Section 5.7 exposes a discontinuous bifurcation point at which a branch of periodic solutions as well as a branch of fixed points bifurcate. The set-valued eigenvalues cross the imaginary axis twice, suggesting a Hopf and a static bifurcation. Although we cannot classify this discontinuous multiple-crossing bifurcation as a discontinuous counterpart of a continuous bifurcation, we can still look upon the discontinuous bifurcation as a combination of two continuous bifurcations and classify it as such. Whether we can classify the discontinuous bifurcation by inspecting the crossing of the eigenvalue with the imaginary axis is not proven although it seems intuitively correct. A smoothened version of a non-smooth system does in general not expose the same bifurcation as the non-smooth system.

From the preceding discussion we raise two conjectures.

CONJECTURE 5.1. *A necessary condition for the existence of a discontinuous bifurcation of a fixed point of a non-smooth continuous system is a 'jump' of an eigenvalue (or pair of them) over the imaginary axis, i.e. the path of the set-valued eigenvalue(s) passes the imaginary axis.*

A discontinuous bifurcation point would according to Conjecture 5.1 be structurally unstable in the sense that the set-valued eigenvalue contains a value on the imaginary axis.

CONJECTURE 5.2. *A discontinuous bifurcation of a fixed point of a non-smooth continuous system may be classified by inspecting the point(s) where the path of the set-valued eigenvalue (or pair of eigenvalues) crosses the imaginary axis.*

Remarks. Conjecture 5.2 suggest that we can classify a discontinuous bifurcation *if* it exists. The conjecture does not give a condition for a bifurcation. The conjecture also suggests that we can classify a double-crossing bifurcation as the combination of two continuous bifurcations, like for the Hopf-pitchfork bifurcation, because it exposes the behaviour of both continuous bifurcations. However, the bifurcation can still show features not covered by the two continuous bifurcation separately.

Hence, we keep some scepsis concerning Conjectures 5.1 and 5.2. One can argue that it might be possible that a double-crossing bifurcation is the combination of two bifurcations that cancel each other out. A smooth approximation of a non-smooth system could show

two saddle-node bifurcations (turning the branch in opposite directions) which collide in the limiting case. The bifurcation diagram would then look in the limiting case like a hysteresis point (Figure 11). The non-smooth system, showing a double intersection of a set-valued eigenvalue with the origin, might then have no bifurcation at all and would be a non-smooth counterpart of a hysteresis point. Conjecture 5.1 suggest therefore a *necessary* condition for a discontinuous bifurcation and not a sufficient condition. If indeed a discontinuous bifurcation exists, then Conjecture 5.2 suggests that we can classify the discontinuous bifurcation by inspecting the crossing point(s) of the set-valued eigenvalues with the imaginary axis.

These conjectures are raised from observations and agree with one's intuition as they are generalizations of theorems for continuous bifurcations in smooth systems. The conjectures will be assumed to hold in the remainder of this paper keeping in mind that there exists no mathematical proof that they are correct.

Periodic solutions can be looked upon as fixed points on a Poincaré map. The generalization of eigenvalues for fixed points are Floquet multipliers for periodic solutions. If the above conjectures are correct, then we can expect a discontinuous bifurcation of a periodic solution if a Floquet multiplier (or pair of them) jumps through the unit circle. The type of discontinuous bifurcation of a periodic solution could then be inferred from the crossing point of the path of the eigenvalue with the unit circle. We will discuss bifurcations of periodic solutions in Section 6. The results on discontinuous bifurcations of periodic solutions will be compared with discontinuous bifurcations of fixed points in non-smooth continuous systems (Conjectures 5.1 and 5.2).

6. Bifurcations of Periodic Solutions

In this section we will study periodic solutions of Filippov systems (Section 2), under influence of a single parameter. The set of right-hand sides is discontinuous on one or more hyper-surfaces and is assumed to be linearly bounded. An example of such a system is

$$\dot{\underset{\sim}{x}}(t) = \underset{\sim}{f}(t, \underset{\sim}{x}(t), \mu) = \begin{cases} \underset{\sim}{f}_-(t, \underset{\sim}{x}(t), \mu), & \underset{\sim}{x} \in V_-, \\ \underset{\sim}{f}_+(t, \underset{\sim}{x}(t), \mu), & \underset{\sim}{x} \in V_+, \end{cases} \tag{6.1}$$

with

$$\begin{aligned} V_- &= \{\underset{\sim}{x} \in \mathbb{R}^n \mid h(\underset{\sim}{x}(t), \mu) < 0\}, \\ \Sigma &= \{\underset{\sim}{x} \in \mathbb{R}^n \mid h(\underset{\sim}{x}(t), \mu) = 0\}, \\ V_+ &= \{\underset{\sim}{x} \in \mathbb{R}^n \mid h(\underset{\sim}{x}(t), \mu) > 0\}. \end{aligned} \tag{6.2}$$

The system depends on a single parameter μ. Also the indicator function h is in general dependent on μ, which implies dependence on μ for the hyper-surface Σ and the spaces V_- and V_+. Discontinuous systems of this type can be extended to differential inclusions by means of the method proposed by Filippov (Section 2). The resulting differential inclusion has a set-valued map $\underset{\sim}{F}(t, \underset{\sim}{x}, \mu)$ which is upper semi-continuous, convex, closed, non-empty and linearly bounded. Existence of the solution to the IVP is therefore guaranteed. Uniqueness, however, is not guaranteed.

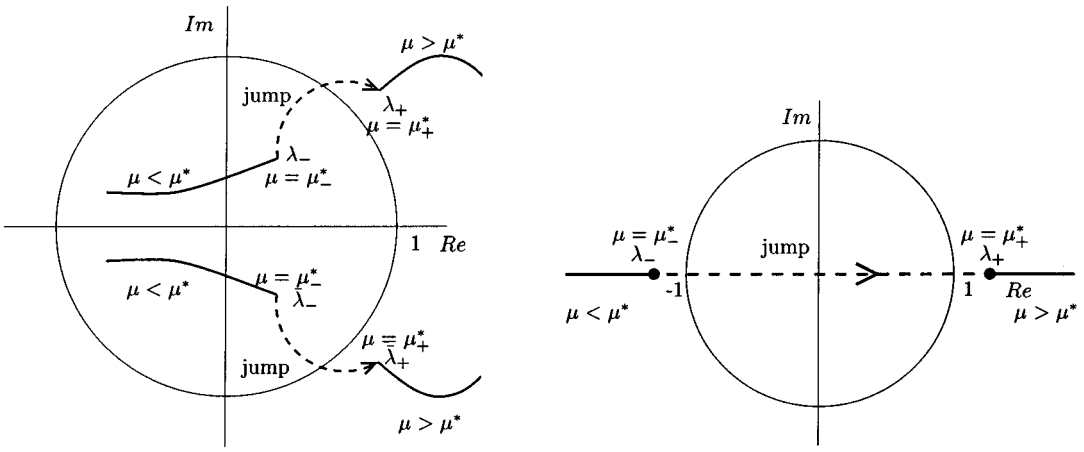

Figure 22. Discontinuous bifurcation.

6.1. Bifurcations in Smooth Systems

In Section 5, bifurcations of fixed points were discussed. A periodic solution can be regarded as a fixed point of a Poincaré map P on a Poincaré section. The results on bifurcations of fixed points are therefore useful for the investigation of bifurcations of periodic solutions. The stability of a periodic solution is determined by its Floquet multipliers λ_i $(i = 1, \ldots, n)$, which are the eigenvalues of the fundamental solution matrix $\underline{\Phi}(T + t_0, t_0)$.

Like for fixed points, different definitions for a bifurcation of a periodic solution exist. We will take Definition 5.1 as definition for a bifurcation of periodic solutions. According to Definition 5.1, a point is a bifurcation point of a periodic solution if the number of periodic solutions change for a varying system parameter. One can also give a definition of a bifurcation of a periodic solution based on topological equivalence of the phase portrait, like Definition 5.3. We will discuss in Section 6.9 the difference between these definitions when they are applied to periodic solutions of discontinuous Filippov systems.

A bifurcation of a periodic solution of a smooth system occurs if a Floquet multiplier (or pair of them) passes through the unit circle under variation of a system parameter.

6.2. Discontinuous Bifurcation: The Basic Idea

Examples of non-smooth continuous systems in Section 5 showed discontinuous bifurcations of fixed points when an eigenvalue jumps over the imaginary axis. In a similar way, we can expect a discontinuous bifurcation of a periodic solution when a Floquet multiplier jumps through the unit circle under influence of a parameter. The basic idea is depicted in Figure 22a. The Floquet multipliers jump at a critical value of the parameter $\mu = \mu^*$ from λ_- and $\bar{\lambda}_-$ to λ_+ and $\bar{\lambda}_+$. The path of the jump is obtained from a convex combination of the fundamental solution matrices before and after the jump. The path of the Floquet multipliers crosses the unit circle. We presume that this causes a discontinuous bifurcation of a periodic solution (in this case a discontinuous Neimark–Sacker bifurcation). Remark that also other jumps are possible as was explained in Section 5 about fixed points (see Figures 12). Like for fixed points also multiple crossings of Floquet multipliers through the unit circle are possible. In Figure 22b a

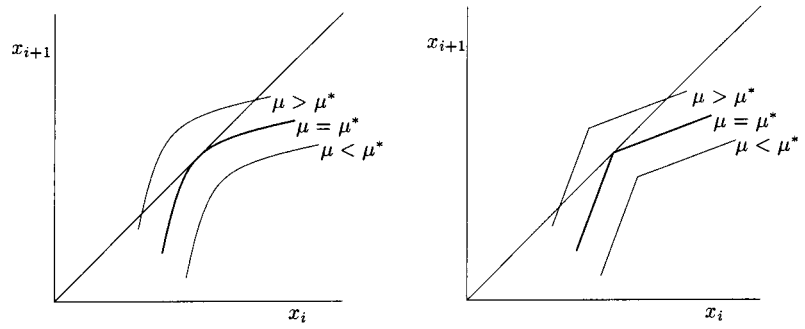

(a) Continuous (b) Discontinuous

Figure 23. Poincaré map at a fold bifurcation.

jump of a real-valued Floquet multiplier is shown which jumps from a value smaller than -1 to a value greater than $+1$ thereby crossing the unit circle twice. It crosses the unit circle at the points -1, involving a flip bifurcation, and at the point $+1$, involving a fold bifurcation. The discontinuous bifurcation is therefore a combination of a fold and a flip bifurcation. We will discuss an example of this type of combined fold–flip bifurcation in Section 6.8.

The idea of a discontinuous bifurcation of a periodic solution, at which a Floquet multiplier jumps through the unit circle, is similar to the 'C-bifurcations' in the work of Feigin [16] and di Bernardo et al. [9, 10]. Feigin classifies C-bifurcations on the number of real-valued eigenvalues of the Poincaré map (see Section 6.3) that are smaller than -1 or larger than $+1$, but does not take complex eigenvalues into account. The classification embraces only the discontinuous fold and flip bifurcation, the combined fold–flip bifurcation and the smooth transition (which is not a bifurcation in the sense of Definition 5.1) [10]. The possibility of a discontinuous symmetry-breaking bifurcation or other discontinuous bifurcations were not mentioned. Non-classical bifurcations of non-smooth discrete mappings were also addressed by [38]. Discontinuous bifurcations are based on jumps in the Floquet multipliers which are essentially the same as the derivatives of the Poincaré map. The 'C-bifurcations' are therefore also discontinuous bifurcations (except for the smooth transition). In this paper it is explained how the discontinuous bifurcations come into being through jumps of the fundamental solution matrix. It is shown that the fundamental solution matrix can jump if a periodic solution touches a non-smooth hyper-surface of discontinuity. The jumps are expressed in saltation matrices which can be found analytically. Furthermore, the path of the Floquet multipliers during the jump is calculated by means of linear approximation. The path of the eigenvalues of the Poincaré map at a C-bifurcation remains on the real axis whereas the Floquet multipliers at a discontinuous bifurcation can be complex conjugated.

6.3. The Poincaré Map

We can elucidate the relation between continuous bifurcations and discontinuous bifurcations even more by studying the Poincaré map [40].

The Poincaré map at a fold bifurcation (Figure 23) has no intersection points with the diagonal $x_{i+1} = x_i$ for $\mu < \mu^*$. The map is tangent to the diagonal for $\mu = \mu^*$. For $\mu > \mu^*$ the map has two intersection points, which correspond to periodic solutions of the dynamical system. Two periodic solutions are therefore created/destroyed at $\mu = \mu^*$, which

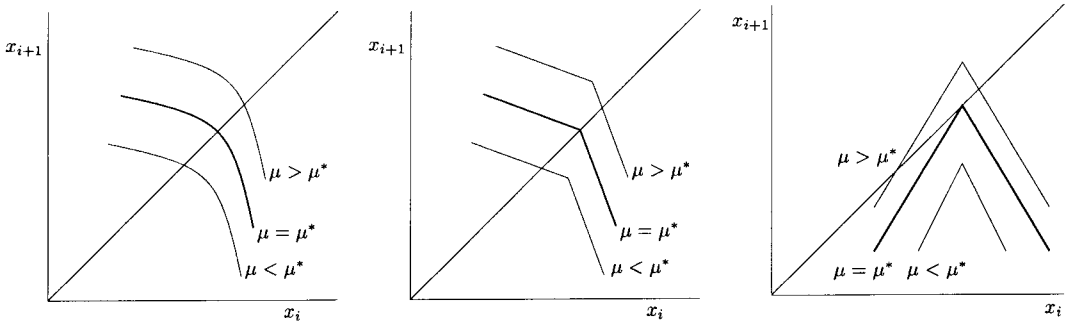

(a) Continuous flip bifurcation

(b) Discontinuous flip bifurcation

(c) Tent map

Figure 24. Poincaré map at a flip bifurcation and the tent map.

is consequently a fold bifurcation. The map at a continuous fold bifurcation, stemming from a smooth system, is smooth and is tangent to the diagonal $x_{i+1} = x_i$, i.e. the slope is $+1$. The map at a discontinuous fold bifurcation, stemming from a discontinuous system, is non-smooth and touches the diagonal with its tip. One limb of the non-smooth map has a slope smaller than $+1$ and the other limb larger than $+1$. The derivative of the map therefore jumps from a value smaller than $+1$ to a value larger than $+1$. The Floquet multiplier is directly related to the derivative of the map.

The map at a continuous flip bifurcation (Figure 24a), stemming from a smooth system, crosses the diagonal with a slope -1. The map at a discontinuous flip bifurcation (Figure 24b), stemming from a discontinuous system, is non-smooth and crosses the diagonal with its tip. One limb of the non-smooth map has a slope smaller than -1 and the other larger than -1. The derivative of the map therefore jumps from a value smaller than -1 to a value larger than -1.

The map at a discontinuous fold bifurcation and the one at a discontinuous flip bifurcation were explained above, but the example of Figure 22b shows a discontinuous bifurcation which is a combination of a flip and a fold as the Floquet multiplier jumps from $\lambda < -1$ to $\lambda > +1$. As the slope of the Poincaré map is directly related to the Floquet multiplier, the map should be non-smooth having two limbs where one has a slope larger than $+1$ and the other a slope smaller than -1. This map is depicted in Figure 24c and appears to be the tent map. This type of bifurcation, with an underlying tent map, will be encountered in Section 6.8.

6.4. Intersection of Hyper-Surfaces of Discontinuity

In Section 3 we elaborated how fundamental solution matrices of discontinuous systems can jump as the trajectory crosses a hyper-surface of discontinuity. Jumps of the Jacobian of fixed points are presumed to lead to discontinuous bifurcations when an eigenvalue (or pair) crosses the imaginary axis, as was outlined in Section 5. The question arises: can jumps in the fundamental solution matrix cause discontinuous bifurcations of periodic solutions?

We consider the following scenario (Figure 25a). The hyper-surface Σ defines a discontinuity and divides the state-space in the two subspaces V_+ and V_-. The vector field is discontinuous on Σ, i.e. $\underset{\sim}{f}_- \neq \underset{\sim}{f}_+$, but Σ itself is smooth. Assume that a system has one periodic solution that changes under influence of a parameter μ. For a value $\mu < \mu^*$ the periodic solution is denoted by periodic solution I. Periodic solution I does not cross Σ. If we

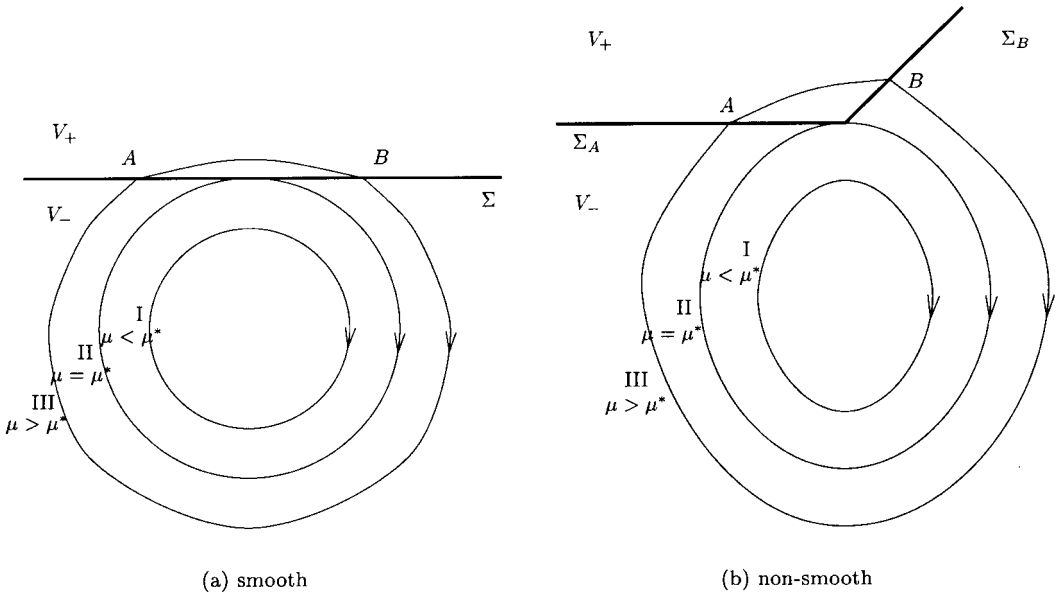

Figure 25. Double intersection of a hyper-surface.

increase the parameter μ to $\mu = \mu^*$, then the periodic solution changes to periodic solution II. Periodic solution II is tangent at one point to Σ. If we increase μ even more to $\mu > \mu^*$, then the period solution becomes periodic solution III which crosses Σ twice at points A and B. Let us assume that periodic solution I comes infinitely close to Σ (without crossing it) and that periodic solution III stays an infinitely small time in V_+ but crosses Σ twice. The periodic solutions I and III are therefore (almost) identical, but the fundamental solution matrix of periodic solution III will jump twice with saltation matrices $\underline{S}_A$ and $\underline{S}_B$. The crossings occur at $t_A = t_B = t_\Sigma$ as periodic solution III stays an infinitely small time in V_+. We can now express the fundamental solution matrix $\underline{\Phi}_{\text{III}}$ into $\underline{\Phi}_{\text{I}}$

$$\underline{\Phi}_{\text{III}}(T + t_0, t_0) = \underline{\Phi}_{\text{I}}(T + t_0, t_0 + t_\Sigma)\underline{S}_B\underline{S}_A\underline{\Phi}_{\text{I}}(t_\Sigma + t_0, t_0). \tag{6.3}$$

However, from (3.18) and (3.19) we conclude that $\underline{S}_B = \underline{S}_A^{-1}$, for non-singular $\underline{S}_A$ and $\underline{S}_B$. The fundamental solution matrix of periodic solution III is therefore identical to the one of periodic solution I, $\underline{\Phi}_{\text{III}}(T + t_0, t_0) = \underline{\Phi}_{\text{I}}(T + t_0, t_0)$. This scenario, in which a single smooth hyper-surface is crossed twice, can consequently not lead to a bifurcation of a periodic solution if $\underline{S}_A$ is non-singular. The singular case arises in sliding mode problems (for instance in Section 6.6).

The preceding scenario did not lead to a bifurcation because the saltation matrix over a smooth hyper-surface is equal to the inverse of the saltation matrix in opposite direction over the same hyper-surface at that point. We will study a second scenario which is depicted in Figure 25b. The hyper-surface Σ is now non-smooth and consists of two parts Σ_A and Σ_B. The periodic solution III enters V_+ by crossing Σ_A at point A and leaves V_+ by crossing Σ_B at point B. The saltation matrix $\underline{S}_A$ is (in general) not equal to $\underline{S}_B^{-1}$. Consequently, the fundamental solution matrix of periodic solution III is not identical to the one of periodic solution I. Therefore, at $\mu = \mu^*$, the fundamental solution matrix over the period time $\underline{\Phi}_{\text{II}}(T + t_0, t_0)$ will jump from $\underline{\Phi}_{\text{I}}(T + t_0, t_0)$ to $\underline{\Phi}_{\text{III}}(T + t_0, t_0)$. We combine the two saltation matrices $\underline{S}_{BA} = \underline{S}_B\underline{S}_A$. From Section 4.1 we know that the theory of linear approximation also applies

to the saltation matrix. Therefore, the combined saltation matrix can also be approximated linearly,

$$\underline{\tilde{S}}_{BA} = \underline{I} + q(\underline{S}_{BA} - \underline{I}), \quad 0 \leq q \leq 1. \tag{6.4}$$

We introduce the *generalized fundamental solution matrix* $\underline{\tilde{\Phi}}$ at $\mu = \mu^*$ which is the closed convex hull of $\underline{\Phi}_{\mathrm{I}}$ and $\underline{\Phi}_{\mathrm{III}}$,

$$\begin{aligned} \underline{\tilde{\Phi}} &= \overline{\mathrm{co}}\{\underline{\Phi}_{\mathrm{I}}(T + t_0, t_0), \underline{\Phi}_{\mathrm{III}}(T + t_0, t_0)\} \\ &= \{q(\underline{\Phi}_{\mathrm{III}}(T + t_0, t_0) - \underline{\Phi}_{\mathrm{I}}(T + t_0, t_0)) + \underline{\Phi}_{\mathrm{I}}(T + t_0, t_0), \forall\, 0 \leq q \leq 1\}. \end{aligned} \tag{6.5}$$

The generalized fundamental solution matrix (6.5) is the set-valued fundamental solution matrix of periodic solution II. In fact, (6.5) defines *how* the fundamental solution matrix of the periodic solution 'jumps' from $\underline{\Phi}_{\mathrm{I}}$ to $\underline{\Phi}_{\mathrm{III}}$ if μ is increased from $\mu < \mu^*$ to $\mu > \mu^*$. From the set-valued generalized fundamental solution matrix we can obtain the set-valued Floquet multipliers. We can look upon $\mathrm{eig}(\underline{\tilde{\Phi}})$ together with (6.5) as if it gives a path of Floquet multipliers 'during' the jump as q is varied from 0 to 1.

A Floquet multiplier can jump from inside the unit circle to outside the unit circle under influence of a parameter μ. Similar to a discontinuous bifurcation of a fixed point we presume that such a jump of a Floquet multiplier causes a discontinuous bifurcation of a periodic solution. Where the Floquet multiplier crosses the unit circle during its jump is determined by $\underline{\tilde{\Phi}}$. The jumping Floquet multiplier can also jump from outside the unit circle to another point outside the unit circle in the complex plane. Similar to our treatment of fixed points, we presume that the existence of a bifurcation depends on the path of the Floquet multiplier during its jump. It could have jumped from one point to the other without passing through the unit circle (which would imply no bifurcation) or it could have passed through the unit circle twice. We presume that the latter case causes a discontinuous bifurcation which is the combination of two bifurcations. If the generalized Jacobian determines the existence and type of discontinuous bifurcation of fixed points (i.e. if Conjectures 5.1 and 5.2 hold), then the generalized fundamental solution matrix determines of the existence and type of bifurcation of periodic solutions.

The discontinuous vector field can also be approximated in a smooth way, with a 'stiffness' depending on the accuracy of approximation. We concluded in Section 5 that the discontinuous bifurcation of a fixed point may vanish if the vector field is approximated by a smooth vector field. This problem probably also exists for bifurcations of periodic solutions. Floquet multipliers of smooth systems do not jump but move 'fast' when the trajectory is passing through a 'stiff' part of the vector field. A smooth approximation which preserves the existence of the bifurcation will yield a continuous path of the Floquet multipliers through the unit circle. A smooth approximation which does not preserve the existence of the bifurcation will yield two unconnected branches that come close to each other. To each branch belongs a continuous path of Floquet multipliers which does not necessarily cross the unit circle.

Some numerical examples in the following sections show discontinuous bifurcations of periodic solutions. The bifurcation diagrams in Sections 6.5 to 6.8 were calculated with a path-following technique based on the shooting algorithm (implemented in MATLAB).

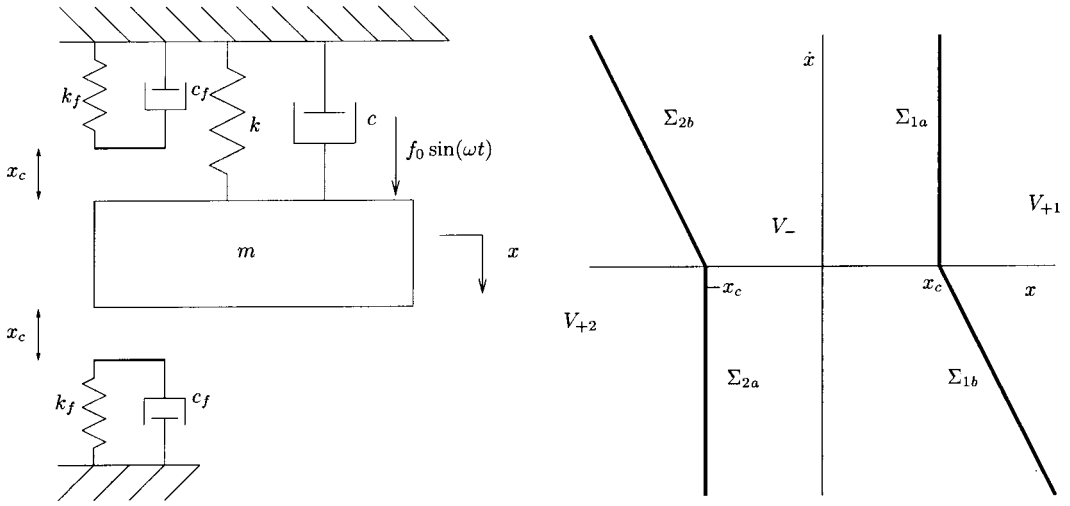

(a) model (b) subspaces

Figure 26. Trilinear system.

6.5. Fold Bifurcation; Trilinear Spring System

In this section we will treat a system that exposes a discontinuous fold bifurcation. The forced oscillation of a damped mass on a spring with cubic term leads to the Duffing equation [23]. The Duffing equation is the classical example where the backbone curve of the harmonic peak is bended and two folds (also called turning point bifurcations) are born. In our example, we will consider a similar mass-spring-damper system, where the cubic spring is replaced by a trilinear spring. Additionally, trilinear damping is added to the model. The trilinear damping will turn out to be essential for the existence of a *discontinuous* fold bifurcation.

The model is very similar to the model of Natsiavas [35, 36] but the transitions from contact with the support to no contact are different from those in the model of Natsiavas. The model of Natsiavas switches as the position of the mass passes the contact distance (in both transition directions). In our model, contact is made when the position of the mass passes the contact distance (for growing $|x|$), and contact is lost when the contact force becomes zero.

We consider the system depicted in Figure 26a. The model is similar to the discontinuous support of Example II in Section 3.4 but now has two supports on equal contact distances x_c. The supports are first-order systems which relax to their original state if there is no contact with the mass. If we assume that the relaxation time of the supports is much smaller than the time interval between two contact events, we can neglect the free motion of the supports. It is therefore assumed that the supports are at rest at the moment that contact is made. This is not an essential assumption but simplifies our treatment as the system reduces to a second-order equation.

The second-order differential equation of this system is

$$m\ddot{x} + C(\dot{x}) + K(x) = f_0 \sin(\omega t), \tag{6.6}$$

where

$$K(x) = \begin{cases} kx, & [x, \dot{x}]^{\mathrm{T}} \in V_-, \\ kx + k_f(x - x_c), & [x, \dot{x}]^{\mathrm{T}} \in V_{+1}, \\ kx + k_f(x + x_c), & [x, \dot{x}]^{\mathrm{T}} \in V_{+2}, \end{cases} \tag{6.7}$$

is the trilinear restoring force and

$$C(\dot{x}) = \begin{cases} c\dot{x}, & [x, \dot{x}]^{\mathrm{T}} \in V_-, \\ (c + c_f)\dot{x}, & [x, \dot{x}]^{\mathrm{T}} \in V_{+1} \cup V_{+2}, \end{cases} \tag{6.8}$$

is the trilinear damping force. The state-space is divided into three subspaces V_-, V_{+1} and V_{+2} (Figure 26b). If the mass is in contact with the lower support, then the state is in space V_{+1}

$$V_{+1} = \{[x, \dot{x}]^{\mathrm{T}} \in \mathbb{R}^2 \mid x > x_c, k_f(x - x_c) + c_f\dot{x} \geq 0\},$$

whereas if the mass is in contact with the upper support, then the state is in space V_{+2}

$$V_{+2} = \{[x, \dot{x}]^{\mathrm{T}} \in \mathbb{R}^2 \mid x < -x_c, k_f(x + x_c) + c_f\dot{x} \leq 0\}.$$

If the mass is not in contact with one of the supports, then the state is in space V_- defined by

$$V_- = \{[x, \dot{x}]^{\mathrm{T}} \in \mathbb{R}^2 \mid [x, \dot{x}]^{\mathrm{T}} \notin (V_{+1} \cup V_{+2})\}.$$

We define the indicator functions $h_{1a}(x, \dot{x})$ and $h_{1b}(x, \dot{x})$ as

$$h_{1a} = x - x_c, \quad h_{1b} = k_f(x - x_c) + c_f\dot{x}. \tag{6.9}$$

The hyper-surface Σ_1 between V_- and V_{+1} consists of two parts Σ_{1a} and Σ_{1b}. The part Σ_{1a} defines the transition from V_- to V_{+1} because contact is made when x becomes larger than x_c

$$\Sigma_{1a} = \{[x, \dot{x}]^{\mathrm{T}} \in \mathbb{R}^2 \mid h_{1a}(x, \dot{x}) = 0, h_{1b}(x, \dot{x}) \geq 0\}. \tag{6.10}$$

The part Σ_{1b} is defined by the indicator equation which defines the transition from V_{+1} back to V_- as contact is lost when the support-force becomes zero (the support can only push, not pull on the mass)

$$\Sigma_{1b} = \{[x, \dot{x}]^{\mathrm{T}} \in \mathbb{R}^2 \mid h_{1a}(x, \dot{x}) \geq 0, h_{1b}(x, \dot{x}) = 0\}. \tag{6.11}$$

Similarly, the hyper-surface Σ_2 between V_- and V_{+2} consists of two parts Σ_{2a} and Σ_{2b} defined by the indicator equations

$$h_{2a}(x, \dot{x}) = x + x_c, \quad h_{2b}(x, \dot{x}) = k_f(x + x_c) + c_f\dot{x}. \tag{6.12}$$

Like we have done in Section 3.4, we can construct the saltation matrices. The saltation matrices are of course similar to those of Section 3.4

$$\underline{S}_{1a} = \underline{S}_{2a} = \begin{bmatrix} 1 & 0 \\ -\dfrac{c_f}{m} & 1 \end{bmatrix}, \quad \underline{S}_{1b} = \underline{S}_{2b} = \underline{I}. \tag{6.13}$$

The hyper-surfaces Σ_1 and Σ_2 are non-smooth. The saltation matrices are not each others inverse, $\underline{S}_{1a} \neq \underline{S}_{1b}^{-1}$ and $\underline{S}_{2a} \neq \underline{S}_{2b}^{-1}$. According to Section 6.2 we now have all the ingredients for the existence of a discontinuous bifurcation.

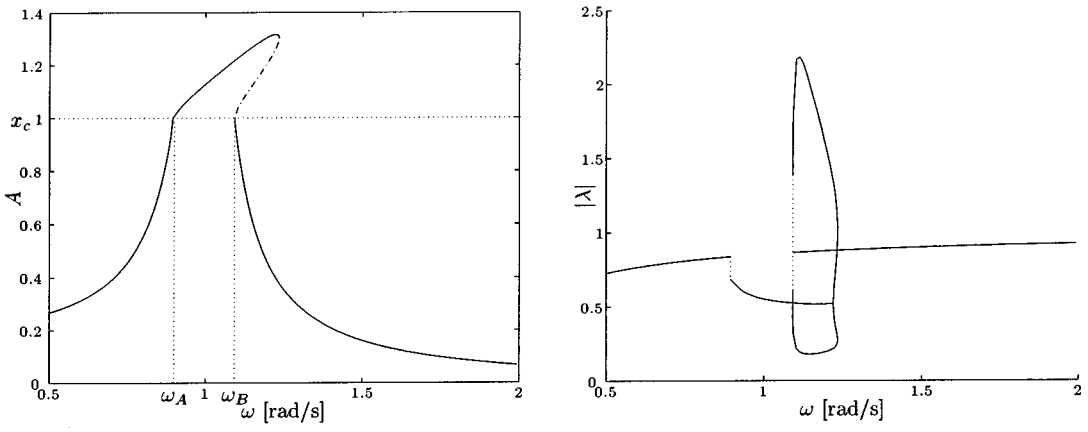

(a) Response diagram

(b) Floquet multipliers

Figure 27. Trilinear spring system.

The response diagram of the trilinear system is shown in Figure 27a for varying forcing frequencies with the amplitude A of x on the vertical axis. Stable branches are indicated by solid lines and unstable branches by dashed-dotted lines. The parameter values are given in Appendix A.2.

There is no contact with the support for amplitudes smaller than x_c and the response curve is just the linear harmonic peak. For amplitudes above x_c there will be contact with the support, which will cause a hardening behaviour of the response curve. The backbone curve of the peak bends to the right like the Duffing system with a hardening spring. The amplitude becomes equal to x_c twice at $\omega = \omega_A$ and $\omega = \omega_B$, on both sides of the peak, and corners of the response curve can be seen at these points. The orbit touches the corners of Σ_1 and Σ_2 for $A = x_c$, like solution II in Figure 25b. The Floquet multipliers can therefore jump at those points. The magnitude of the Floquet multipliers is shown in Figure 27b. The two Floquet multipliers are complex conjugate for $A < x_c$ (and therefore have the same magnitude). The pair of Floquet multipliers jump at $\omega = \omega_A$ but do not jump through the unit circle. From the numerical calculations depicted in Figure 27a it follows that no bifurcation exist (in the sense of Definition 5.1) at $\omega = \omega_A$. However, at $\omega = \omega_B$ the complex pair jumps to two distinct real multipliers, one with a magnitude bigger than one. One of those Floquet multipliers therefore jumps through the unit circle. A bifurcation is observed in Figure 27a at $\omega = \omega_B$ (one periodic solution exists for $\omega < \omega_B$ and three periodic solutions co-exist for $\omega > \omega_B$). We presume that this bifurcation is caused by the jump of the Floquet multiplier through the unit circle. The path of the Floquet multipliers on the jump is obtained by the generalized fundamental solution matrix (6.5). One Floquet multiplier crosses $+1$. The observed bifurcation resembles a continuous fold bifurcation of a smooth system. The bifurcation at $\omega = \omega_B$ at which the Floquet multiplier jumps through $+1$ is therefore called a *discontinuous fold bifurcation*.

Damping of the support is essential for the existence of this discontinuous fold bifurcation. For $c_f = 0$, all saltation matrices would be equal to the identity matrix and the corner between Σ_{1a} and Σ_{1b} would disappear (and also between Σ_{2a} and Σ_{2b}); therefore no discontinuous bifurcation could take place and the fold bifurcation would be continuous (see also Example 3.4). The model of Natsiavas [35, 36] did not contain a *discontinuous* fold bifurcation because the transitions were modeled such that $\underline{S}_{1a} = \underline{S}_{1b}^{-1}$ and $\underline{S}_{2a} = \underline{S}_{2b}^{-1}$.

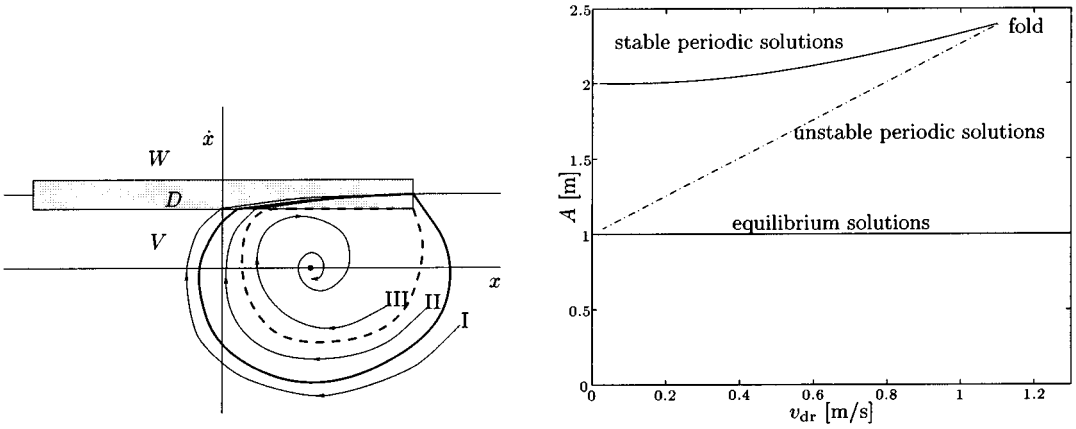

(a) Phase plane (b) Bifurcation diagram

Figure 28. Stick-slip system.

6.6. INFINITELY UNSTABLE PERIODIC SOLUTIONS

In Section 6.5 we studied the discontinuous fold bifurcation, where a Floquet multiplier jumped through the unit circle, through $+1$, to a finite value. In this section we will study a discontinuous fold bifurcation where the Floquet multiplier jumps to infinity (crossing $+1$). This results in periodic solutions with a Floquet multiplier at infinity, which we will call *infinitely unstable periodic solutions*.

We consider again the stick-slip system of Section 3.3 depicted in Figure 5a, but now for positive damping $c > 0$. The equilibrium solution of system (3.21) is given by

$$\underline{x}_{eq} = \begin{bmatrix} \dfrac{F_{\text{slip}}}{k} \\ 0 \end{bmatrix} \tag{6.14}$$

and is stable for positive damping ($c > 0$).

The model also exhibits stable periodic stick-slip oscillations. In Section 3.3 it was shown that the saltation matrix for the transition from slip to stick is given by (3.25)

$$\underline{S}_{\alpha} = \begin{bmatrix} 1 & 0 \\ 0 & 0 \end{bmatrix},$$

which is singular. The fundamental solution matrix will therefore also be singular. The periodic solution has two Floquet multipliers, of which one is always equal to one as the system is autonomous. The singularity of the fundamental solution matrix implies that the remaining Floquet multiplier has to be equal to zero, independent of any system parameter. The Floquet multipliers of the stable periodic solution of this system are therefore $\lambda_1^{\text{stable}} = 1$ and $\lambda_2^{\text{stable}} = 0$.

The stable periodic solution is sketched in the phase plane in Figure 28a (bold line). The equilibrium position is also stable and indicated by a dot. The space D is enlarged in Figure 28a to make it visible but is infinitely thin in theory and is taken very thin in numerical calculations. We assume that the thickness of D in the numerical calculations is small enough to yield the same qualitative behaviour as the theoretical infinitely thin space D.

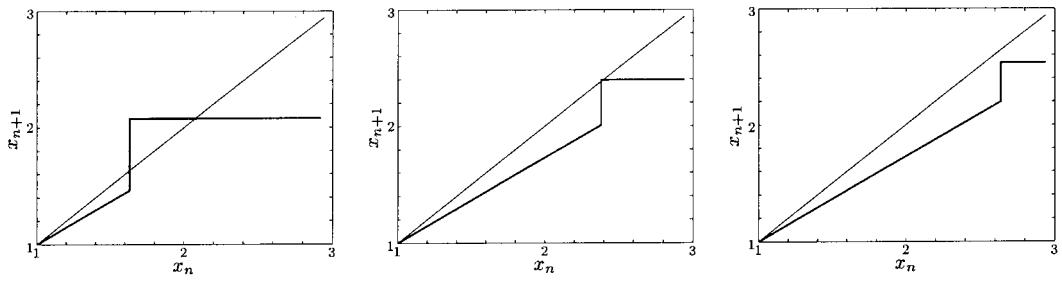

(a) $v_{\mathrm{dr}} = 0.5$ m/s (b) $v_{\mathrm{dr}} = 1.1$ m/s (c) $v_{\mathrm{dr}} = 1.3$ m/s

Figure 29. Poincaré maps of the stick-slip system.

A trajectory outside the stable periodic solution, like solution I in Figure 28a, will spiral inwards to the stable periodic solution and reach the stick-phase D. The stick-phase will bring the trajectory exactly on the stable periodic solution as it is infinitely small. Every point in D is therefore part of the basin of attraction of the stable periodic solution.

Trajectory II starts inside the stable periodic solution and spirals around the equilibrium position and hits D whereupon it is on the stable periodic solution. But a trajectory inside the stable periodic solution might also spiral around the equilibrium position and not reach the stick phase D (trajectory III). It will then be attracted to the equilibrium position.

A trajectory inside the stable periodic solution can therefore spiral outwards to the stable periodic solution, like trajectory II, or inwards to the equilibrium position (trajectory III). Consequently, there must exist a boundary of attraction between the two attracting limit sets. This boundary is the unstable periodic solution sketched by a dashed line in Figure 28a. The boundary of attraction is partly along the border between D and V because trajectories in D will attract to the stable periodic solution and just outside D to the equilibrium position. The unstable periodic solution is therefore defined by the trajectory in V which hits the border of D tangentially and by a part along the border of D and V. The part of the unstable periodic solution along the border of D is therefore a sliding mode along a discontinuity as discussed in Section 2. The trajectory on either side of the sliding mode is repulsing from it. It is therefore a repulsion sliding mode. The trajectory starting from a point on a repulsion sliding mode is not unique as was discussed in Section 2. Non-uniqueness causes one Floquet multiplier to be at infinity because a trajectory may drift away from the periodic solution without any initial disturbance from the periodic solution. The unstable periodic solution is therefore infinitely unstable. As the periodic solution is infinitely unstable, it is not possible to calculate it in forward time. However, calculation of the periodic solution in backward time is possible. The repulsion sliding mode in forward time will turn into an attraction sliding mode in backward time. Information about where the trajectory came from is therefore lost through the attraction sliding mode. In other words: the saltation matrix of the transition from V to D during backward time is singular. The fundamental solution matrix will therefore be singular in backward time because it contains an attraction sliding mode. The Floquet multipliers of the unstable periodic solution in backward time are therefore 1 and 0. The Floquet multipliers in forward time must be their reciprocal values. The second Floquet multiplier is therefore infinity, $\lambda_1^{\mathrm{unstable}} = 1$ and $\lambda_2^{\mathrm{unstable}} = \infty$, which of course must hold for an infinitely unstable periodic solution.

The bifurcation diagram of the system is shown in Figure 28b with the velocity of the belt v_{dr} as parameter and the amplitude A of x on the vertical axis. The equilibrium branch

and the stable and unstable periodic branches are depicted. The unstable branch is of course located between the stable periodic branch and the equilibrium branch as can be inferred from Figure 28a. The stable and unstable periodic branches are connected through a fold bifurcation point. The second Floquet multiplier jumps from $\lambda = 0$ to $\lambda = \infty$ at the bifurcation point, and therefore through $+1$ on the unit circle. We will call this bifurcation therefore a discontinuous fold bifurcation. The fold bifurcation occurs when v_{dr} is such that a trajectory which leaves the stick phase D, transverses V, and hits D tangentially (like the unstable periodic solution). The stable and unstable periodic solutions coincide at this point. Note that there exists again a corner of hyper-surfaces at this point as in Figure 25b. The saltation matrices are not each others inverse, $\underline{S}_\alpha \underline{S}_\beta \neq \underline{I}$, which is essential for the existence of a discontinuous bifurcation. Moreover $\underline{S}_\alpha$ is singular.

Three Poincaré maps are depicted in Figure 29 for different values of v_{dr}; before, at and after the bifurcation point. The Poincaré section is chosen as $\Omega = \{\underset{\sim}{x} \in \mathbb{R}^2 \mid x \geq F_{\mathrm{slip}}/k, \dot{x} = 0\}$. The three intersection points of the Poincaré map with the diagonal in Figure 29a indicate the equilibrium position at $x = 1$ and the unstable and stable periodic solutions. The slope of the Poincaré map at the intersection points of the periodic solutions is equal to the second Floquet multiplier, which is consistent with $\lambda_2^{\mathrm{stable}} = 0$ and $\lambda_2^{\mathrm{unstable}} = \infty$. The Poincaré map of Figure 29b touches the diagonal with its tip similar to the Poincaré map of the discontinuous fold bifurcation in Figure 23. The stable and unstable periodic solutions disappeared in Figure 29c as is shown in Figure 28b.

A similar model was studied in [51] with a very accurately smoothed friction curve. The stable branch was followed for increasing v_{dr} but the fold bifurcation could not be rounded to proceed on the unstable branch. As the unstable branch is infinitely unstable for the discontinuous model, it is extremely unstable for the smoothed approximating model. The branch can therefore not be followed numerically in forward time if the friction model is approximated accurately.

The stable branch in Figure 28b was followed in forward time up to the bifurcation point. The path-following algorithm was stopped and restarted in backward time to follow the unstable branch.

This section showed that infinitely unstable periodic solutions come into being through repulsion sliding modes. Filippov theory turns out to be essential for the understanding of infinitely unstable periodic solutions. Infinitely unstable periodic solutions and their branches can be found through backward integration. Smoothing of a discontinuous model is not sufficient to obtain a complete bifurcation diagram as infinitely unstable branches cannot be found.

6.7. Symmetry-Breaking Bifurcation; Forced Vibration with Dry Friction

The second type of bifurcation of a periodic solution which will be studied is the *symmetry-breaking bifurcation*. Suppose a non-autonomous time-periodic system has the following symmetry property (also called *inversion symmetry*)

$$\underset{\sim}{f}(t, \underset{\sim}{x}) = -\underset{\sim}{f}\left(t + \frac{1}{2}T, -\underset{\sim}{x}\right), \tag{6.15}$$

where T is the period. If $\underset{\sim}{x}_1(t) = \underset{\sim}{x}(t)$ is a periodic solution of the system, then also $\underset{\sim}{x}_2(t) = -\underset{\sim}{x}(t + (1/2)T)$ must be a periodic solution. The periodic solution is called *symmetric* if $\underset{\sim}{x}_1(t) = \underset{\sim}{x}_2(t)$ and asymmetric if $\underset{\sim}{x}_1(t) \neq \underset{\sim}{x}_2(t)$. When a Floquet multiplier passes through the

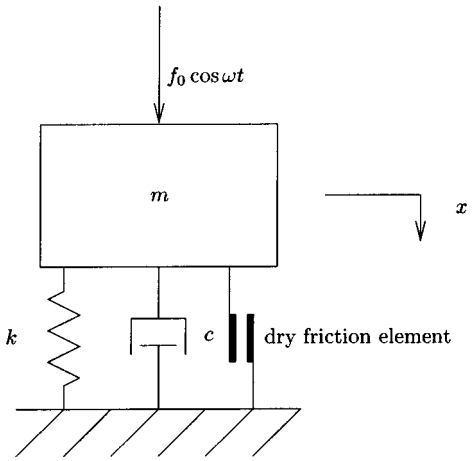

Figure 30. Forced vibration with dry friction.

unit circle at $+1$, the associated bifurcation depends on the nature of the periodic solution prior to the bifurcation. Suppose that the periodic solution prior to the bifurcation is a symmetric periodic solution. Then, if the bifurcation breaks the symmetry of the periodic solution, it is called a symmetry-breaking bifurcation [47].

We will show in this section that the continuous symmetry-breaking bifurcation has a discontinuous counterpart. Consider the forced vibration of the system depicted in Figure 30. The mass is supported by a spring, damper and dry friction element. The parameter values are given in Appendix A.3. The equation of motion reads as

$$m\ddot{x} + c\dot{x} + kx = f_{\text{fric}}(\dot{x}, x) + f_0 \cos \omega t \tag{6.16}$$

with the friction model

$$f_{\text{fric}}(\dot{x}, x) = \begin{cases} -F_{\text{slip}} \operatorname{sgn}(\dot{x}), & \dot{x} \neq 0 \ \text{ slip}, \\ \min(|F_{\text{ex}}|, F_{\text{stick}}) \operatorname{sgn}(F_{\text{ex}}), & \dot{x} = 0 \ \text{ stick}, \end{cases} \tag{6.17}$$

where $F_{\text{ex}} = kx - f_0 \cos \omega t$. The system (6.16) has been analyzed numerically with the switch-model as in Section 3.3 and in [31]. It can be verified that the system (6.16) has the symmetry property (6.15).

The bifurcation diagram of this system (Figure 31a) shows two branches with periodic solutions. Branch I is unstable between the points A and B. Branch II bifurcates from branch I at point A and B. For large amplitudes, the influence of the dry friction element will be much less than the linear elements. Near the resonance frequency, $\omega_{\text{res}} = \sqrt{k/m} = 1$ [rad/s], branch I will therefore be close to the harmonic resonance peak of a linear one degree-of-freedom system. We first consider periodic solutions on branch I at the right side of point B. The velocity of the mass $\dot{x}$ becomes zero at two instances of time during one oscillation (as do linear harmonic oscillations). The mass does not come to a stop during an interval of time. In other words: the oscillation contains no *stick event* in which the periodic solution passes the stick phase. The number of stick events on a part of a branch is indicated by numbers (0,1,2) in Figure 31a. The Floquet multipliers on this part of branch I are complex (Figure 31b). The system therefore behaves 'almost linearly'. All the periodic solutions on branch I are symmetric.

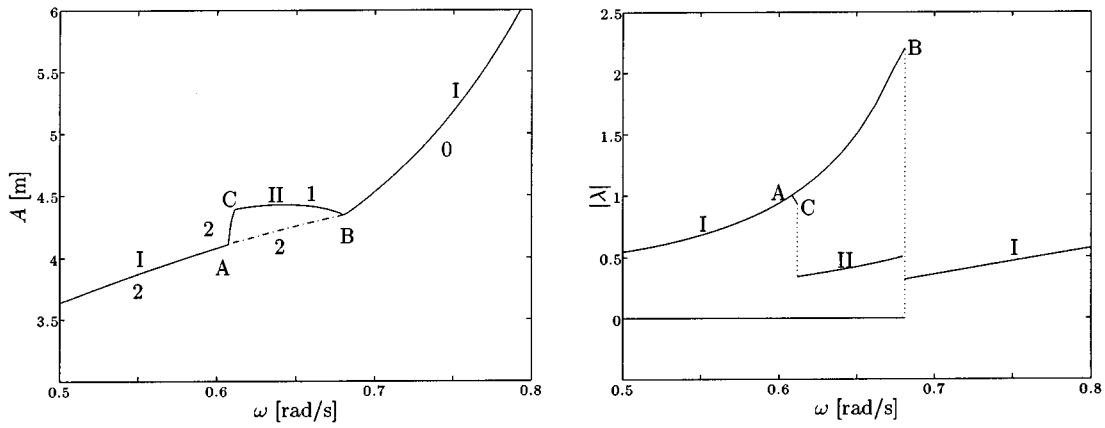

(a) bifurcation diagram (b) Floquet multipliers

Figure 31. Forced vibration with dry friction.

If this part of branch I with 'almost linear' symmetric periodic solutions is followed to frequencies below ω_{res}, then bifurcation point B is met. At bifurcation point B, the symmetric branch I becomes unstable and a second branch II with asymmetric periodic solutions is created. In fact, on the bifurcated asymmetric branch two distinct periodic solutions $\underset{\sim}{x}_1(t) \neq \underset{\sim}{x}_2(t)$ exist, which have the same amplitude. The periodic solutions on branch I left of point B contain two stick events per cycle. The periodic solutions on branch II between the points B and C contain one stick event, and they contain two stick events between the points A and C . The existence of a stick event during the oscillation causes one Floquet multiplier to be equal to zero. Points B and C are points where stick events are created/destroyed, which cause the Floquet multipliers to be set-valued (they jump). A set-valued Floquet multiplier at B passes $+1$. The bifurcation at point B resembles a continuous symmetry-bifurcation and is therefore called a *discontinuous symmetry-breaking bifurcation.* We presume that a discontinuous symmetry-breaking bifurcation is always associated with a jump of a Floquet multiplier through $+1$.

Branch II encounters a jump of the Floquet multipliers at point C but the set-valued Floquet multipliers remain within the unit circle. We observe that point C is not a bifurcation point but the path of branch II is non-smooth at C due to the jump of the Floquet multipliers.

The asymmetric branch meets the symmetric branch again at point A. The Floquet multipliers pass $+1$ without a jump and point A is therefore a continuous symmetry-breaking bifurcation. No new stick events are created at point A because all branches have two stick events per cycle. Remark that the branch I behaves smooth at bifurcation A and non-smooth at bifurcation B.

6.8. Flip Bifurcation; Forced Stick-slip System

Another type of bifurcation of a periodic solution is the *flip bifurcation* which is characterized by a Floquet multiplier which is passing through the unit circle at -1. A new type of discontinuous bifurcation will be studied in this section which occurs in a forced stick-slip system taken from Yoshitake and Sueoka [53]. The discontinuous bifurcation is a combination of a continuous fold and flip bifurcation. The system is identical to the stick-slip system of Section 3.3 (Figure 5a) without linear damping and a different friction model. Additionally,

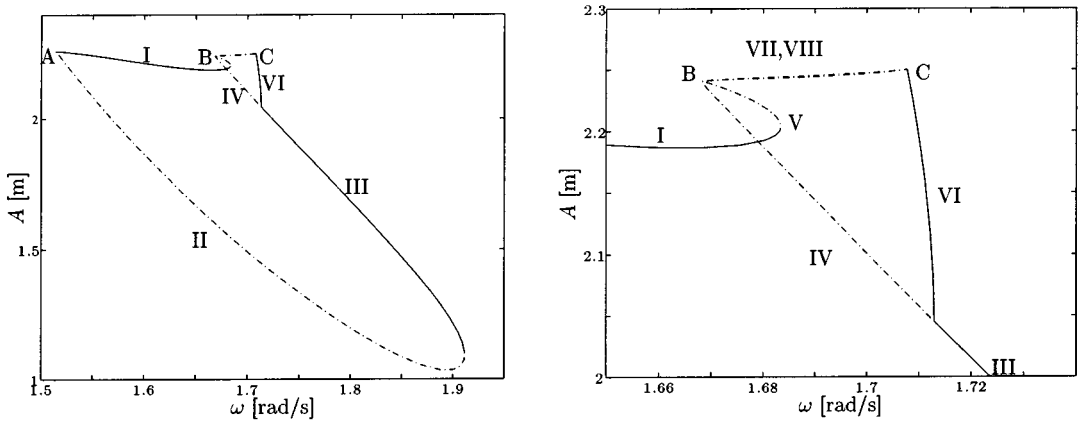

Figure 32. Bifurcation diagram of the forced stick-slip system.

the mass is forced periodically. The parameter values are given in Appendix A.4. The equation of motion reads as

$$m\ddot{x} + kx = f_{\text{fric}}(v_{\text{rel}}, x) + f_0 \cos \omega t \tag{6.18}$$

with $v_{\text{rel}} = \dot{x} - v_{\text{dr}}$. The friction model reads as

$$f_{\text{fric}}(v_{\text{rel}}, x) = \begin{cases} -\alpha_0 \operatorname{sgn}(v_{\text{rel}}) + \alpha_1 v_{\text{rel}} - \alpha_3 v_{\text{rel}}^3, & v_{\text{rel}} \neq 0 \quad \text{slip} \\ \min(|F_{\text{ex}}|, \alpha_0) \operatorname{sgn}(F_{\text{ex}}), & v_{\text{rel}} = 0 \quad \text{stick} \end{cases} \tag{6.19}$$

where $F_{\text{ex}} = kx - f_0 \cos \omega t$. This model has been analyzed numerically with the switch-model as in Section 3.3 and in [31], which resulted in Figures 32 to 34.

The resonance curve of this model has been published by [53] for $0.2 \leq \omega \leq 4$. The 1/2-subharmonic closed resonance curve is of special interest and depicted in Figure 32a and a part is enlarged in Figure 32b. The real part of the largest Floquet multiplier (in magnitude) is depicted in Figure 33. All Floquet multipliers are real except on a part of branch III. Stable branches of periodic solutions are denoted by solid lines and unstable branches by dashed-dotted lines. Jumps of the Floquet multiplier (set-valued Floquet multipliers) are denoted by dotted lines.

The 1/2-subharmonic closed resonance curve possesses several discontinuous and continuous bifurcations. Branches I-V are period-2 solutions, branches VI and VII are period-4, and branch VIII is period-8. A discontinuous fold bifurcation at point A connects the stable branch I to the unstable branch II and its largest Floquet multiplier jumps through $+1$ (similar to the discontinuous fold bifurcation in Section 6.5). The stable branch I folds smoothly into branch V and stability is exchanged. At point B, the unstable branch V is folded into the unstable branch IV *without exchanging stability*. The set-valued Floquet multiplier at point B crosses the unit circle twice as it jumps from $\lambda > 1$ on branch V to $\lambda < -1$ on branch IV, thereby crossing the points $+1$ and -1 on the unit circle (Figure 22b). In Section 6.2 we presumed that such a 'multiple-crossing' jump of a Floquet multiplier causes a bifurcation which is a combination of a fold and a flip bifurcation. The fold action of the bifurcation is clear as the branch is folded. A conventional continuous flip bifurcation causes a period-doubled branch to bifurcate from the main branch. Branches IV and V are period-2 and branch VII emanates indeed from point B and is period-4. The bifurcation at point B therefore also shows a flip

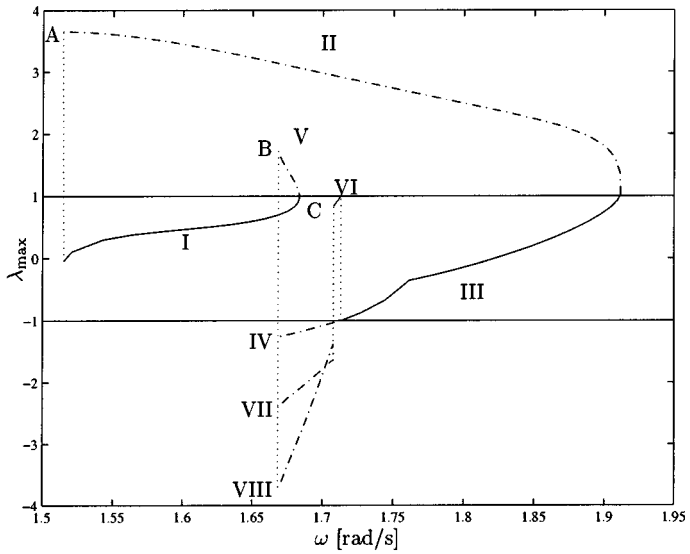

Figure 33. Floquet multiplier.

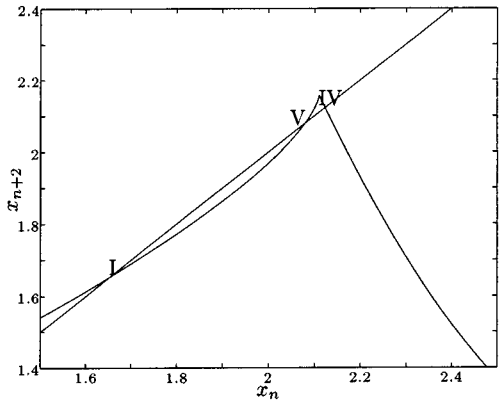

Figure 34. Poincaré map ($\omega = 1.67587$ [rad/s]).

action. But branch VIII also bifurcates from B and is period-8. This is not in conformity with the bifurcation theory for smooth systems.

A better understanding of the phenomenon can be obtained by looking at the Poincaré map depicted in Figure 34. Remark that the map has indeed the *tent structure* of Figure 24c. In fact, the 'full' Poincaré map is a mapping from $\mathbb{R}^2$ to $\mathbb{R}^2$ which cannot easily be visualized. Instead, a section of this map is depicted with the displacement $x_n = x(nT)$, where $T = 2\pi/\omega$, on the abscissa and the displacement after two periods x_{n+2} on the ordinate (because we study period-2 oscillations). The velocity $\dot{x}_n$ is iterated with a Newton-Raphson method to be equal to $\dot{x}_{n+2}$. Fixed points of this reduced map are periodic solutions with period-2 (or period-1) as holds $x(nT) = x((n+2)T)$ and $\dot{x}(nT) = \dot{x}((n+2)T)$. The map is calculated for $\omega = 1.67587$ [rad/s] which is just to the right of the bifurcation point B. It can be seen that there are three fixed points which corresponds to the periodic solutions at the branches I, IV and V. The map exposes a peak between the fixed points IV and V. Although this is a section of a higher-dimensional map, the 'full' map will also contain a tent structure.

The *tent map* has been studied thoroughly in literature [44]. The tent map is the non-smooth piece-wise linear version of the logistic map (both non-invertible). The logistic map is smooth and leads to a cascade of period-doublings which is a well known route to chaos. The distance between two succeeding period-doublings is finite for the logistic map. For the tent map however, infinitely many period-doublings occur at the same bifurcation value which leads directly to chaos.

The results on the tent map could explain the behaviour at the bifurcation point B. The tent structure in the Poincaré map suggests that there are infinitely many period-doublings. This would result in an infinite number of other unstable branches starting from point B (period-8, 16, 32 ...). A period-8 branch (VIII) starting from point B was indeed found beside the 'expected' period-4 branch (VII). The infinitely many other branches become more unstable as their period-doubling number increases and the branches become closely located to each other which makes it difficult to find them numerically. These facts agree with the analytical results on the tent map.

How do we classify the discontinuous bifurcation at point B? The discontinuous bifurcation is not a direct counterpart of a continuous bifurcation. In the sequel we will call this bifurcation a discontinuous fold–flip bifurcation because it resembles both bifurcations. The name is not completely satisfactory because branch VIII and the possibly infinitely many branches that are created at the discontinuous bifurcation point is resembled neither by a continuous fold nor by a continuous flip bifurcation.

The branches VII and VIII connect bifurcation point B with bifurcation point C. The Floquet multiplier at point C jumps from inside the unit circle to outside the unit circle through -1. We call bifurcation point C a discontinuous flip bifurcation because it resembles a continuous flip bifurcation. Where do those infinitely many branches starting from point B lead to? We can suggest that the infinitely many other unstable branches will probably lead to bifurcation point C. But the Floquet multiplier at C does not seem to pass both $+1$ and -1, but only -1. The Poincaré map at point C will look like Figure 24b and will not expose a tent structure. It is therefore not clear whether the infinitely many other unstable branches will be connected to bifurcation point C. As follows from the tent map, the system will behave chaoticly for ω-values just to the right of point B.

Yoshitake and Sueoka [53] studied the model carefully and showed that the underlying Poincaré map has a tent structure but did not find the branches VII and VIII (or higher period-doublings). Discontinuous fold and flip bifurcations, where the Floquet multipliers jump at the bifurcation point, were found by Yoshitake and Sueoka, a result not found before in literature. However, they did not show how the Floquet multipliers jump which can be explained from saltation matrices and generalized fundamental solution matrices as elaborated in this paper. They classified the region between B and C as chaotic and mentioned the similarity with the bifurcations found by [38]. Nusse and York studied discrete dynamical systems with a tent structure and denoted the discontinuous bifurcations they found by 'border-collision bifurcations'. Their numerical calculations only showed stable solutions. They did not give a method to classify discontinuous bifurcations but conclude their paper that this is still an open question. In this paper it is presumed that the discontinuous bifurcations can at least be partly classified by investigating the generalized Jacobian, the generalized fundamental solution matrix or the generalized derivative of the Poincaré map (Section 4.1).

A discontinuous fold-flip bifurcation was discussed in this section and it was shown that it is related to the one-dimensional tent map. It is suggested that infinitely many branches meet

at the same bifurcation point and these branches are all period-doublings of the branch under bifurcation.

6.9. DISCUSSION

The examples in this section showed that discontinuous bifurcations (in the sense of Definition 5.1) exist of periodic solutions in discontinuous Filippov systems. The conclusion that a point on a branch is a (continuous or discontinuous) bifurcation point was in the preceding examples always drawn from observation of the bifurcation diagram. We call a bifurcation point a discontinuous bifurcation point if it exposes a jump of the Floquet multipliers through the unit circle. Sections 6.5 to 6.8 show a number of bifurcations of periodic solutions in the sense of Definition 5.1. Some of the bifurcations are accompanied by a Floquet multiplier which passes continuously through the unit circle. The branch of periodic solutions at such bifurcation points remains smooth. We classify those bifurcations as continuous bifurcations. Other bifurcation points are accompanied by a Floquet multiplier which crosses the unit circle discontinuously. The branch on such bifurcation points is continuous but non-smooth. We classify those bifurcations as discontinuous bifurcations of periodic solutions because of the discontinuous behaviour of the Floquet multipliers.

It is shown that discontinuous bifurcations of periodic solutions can occur if a periodic solution touches a non-smooth hyper-surface for a critical parameter value. This is clearly illustrated by the example in Section 6.5 which shows a discontinuous fold bifurcation.

All the examples show that a discontinuous bifurcation is always accompanied by a jump of Floquet multiplier(s) through the unit circle. Points at which the Floquet multipliers jumped but remained within the unit circle never occurred to be a bifurcation point. We do not have evidence that a jump of a Floquet multiplier through the unit circle should always be accompanied by a bifurcation. We presume that such a jump is a necessary condition for a bifurcation of a periodic solution (in the sense of Definition 5.1).

Can we classify the bifurcation by inspecting the point(s) where the path of the set-valued Floquet multiplier(s) crosses the unit circle? Sections 6.5, 6.6 and 6.7 show bifurcations which behave qualitatively like fold and symmetry-breaking bifurcations. They are called discontinuous fold or symmetry-breaking bifurcations because they resemble the conventional bifurcation and because of the discontinuous behaviour of the Floquet multipliers. The classification of those bifurcations as fold or symmetry-breaking bifurcations seems consistent with the fact that they are accompanied by a jump of a Floquet multiplier through $+1$. Along the same reasoning, bifurcation points A and C in Figure 32 can be classified as discontinuous fold and flip bifurcations. Bifurcation point B, however, exposes a jump through the unit circle at -1 and $+1$. The latter discontinuous bifurcation is not a direct counterpart of a continuous bifurcation. We will classify this bifurcation as a discontinuous fold–flip bifurcation because it resembles both bifurcations. The classification is not completely satisfactory because branch VIII and the possibly infinitely many branches that are created at the discontinuous bifurcation point resemble neither a continuous fold nor a continuous flip bifurcation. We conclude that a classification, based on the points where the set-valued Floquet multiplier crosses the unit circle, is only *partly* possible.

Definitions 5.1 and 5.3 can be inconsistent when they are applied to periodic solutions of discontinuous Filippov systems. Definition 5.1 is based on a change of the number of fixed points and periodic solutions at a critical value of a parameter of the system. Definition 5.3 is based on a topological change of the phase portrait under variation of a parameter. If we

compare a periodic solution I which is not along an attraction sliding mode with a periodic solution II which is partly along an attraction sliding mode, then we can map every trajectory in the phase plane of periodic solution I to a trajectory in the phase plane of periodic solution II. However, the inverse map (mapping trajectories from II to I) does not exist. Consequently, there is no homeomorphism between the two phase planes. A periodic solution with an attraction sliding mode is therefore topologically different from a periodic solution without a sliding mode. Consider point C in Figure 31a. The point is not a bifurcation point according to Definition 5.1. The number of stick intervals change at this point from 2 to 1. Each stick interval is an attraction sliding mode. Consequently, point C is a bifurcation according to Definition 5.3. The term 'sliding bifurcation' is introduced in [9] for a change of a periodic solution with a sliding mode to a periodic solution without a sliding mode under influence of a parameter. The term 'multi-sliding bifurcation' is introduced for a change in the number of sliding modes. Point C in Figure 31a would according to this definition be a multi-sliding bifurcation. Although not explicitly stated in [9], it seems that a 'sliding bifurcation' is a bifurcation in the sense of Definition 5.3.

The different definitions for a bifurcation can lead to confusion when they are applied to discontinuous systems. This urges for a consensus about what is to be understood by 'bifurcation'. Definition 5.1 seems to be a good candidate as it is very clear from the bifurcation diagram whether or not a point on a branch is a bifurcation point.

In Section 5 we formulated Conjectures 5.1 and 5.2 about existence and classification of bifurcations of fixed points of non-smooth continuous systems. From the preceding discussion we formulate similar conjectures for bifurcations of periodic solutions in discontinuous systems.

CONJECTURE 6.1. *A necessary condition for the existence of a discontinuous bifurcation in the sense of Definition 5.1 of a periodic solution in a discontinuous system is a 'jump' of a Floquet multiplier (or pair of them) through the unit circle, i.e. the path of the set-valued Floquet multiplier(s) passes through the unit circle.*

CONJECTURE 6.2. *A discontinuous bifurcation of a periodic solution of a discontinuous system can be classified by inspecting the point(s) where the path of the set-valued Floquet multipliers (or pair of them) passes through the unit circle.*

Conjecture 6.2 presumes that we can classify bifurcation point B in Figure 32 as a fold–flip bifurcation but we should keep in mind that the bifurcation point shows behaviour not covered by a conventional fold or flip bifurcation separately.

Remark that Conjectures 6.1 and 6.2 are related with Conjectures 5.1 and 5.2 through the Poincaré map.

7. Conclusions

It was shown in this paper that discontinuous vector fields lead to jumps in the fundamental solution matrix if a parameter of the system is varied. It turned out that a double intersection of a non-smooth hyperplane is necessary to cause a jump of the fundamental solution matrix. These jumps may lead to set-valued Floquet multipliers. A discontinuous bifurcation is encountered if a set-valued Floquet multiplier crosses the unit circle. The relation between discontinuous bifurcations of fixed points in non-smooth continuous systems and discontinuous bifurcations of periodic solutions in discontinuous systems was explained. The theory of

Filippov, generalized derivatives and Floquet theory were combined in this paper, which led to new insight in bifurcations in discontinuous systems. We close this paper by stating that the results on periodic solutions of discontinuous systems seem to be consistent with the results on fixed points of non-smooth continuous systems.

Acknowledgments

This project was supported by the Dutch Technology Foundation, STW. The authors are much indebted to the anonymous reviewers for useful comments.

A. Parameter Values

A.1. Stick-Slip System

$k = 1$ N/m, $m = 1$ kg, $v_{\text{dr}} = 0.2$ m/s, $c = 0.1$ Ns/m in Section 6.6,
$F_{\text{slip}} = 1$ N, $\eta = 10^{-4}$ m/s, $F_{\text{stick}} = 2$ N, $c = 0$ Ns/m in Section 3.3.

A.2. Trilinear System

$m = 1$ kg, $c = 0.05$ N/(ms), $k = 1$ N/m, $x_c = 1$ m,
$k_f = 4$ N/m, $c_f = 0.5$ N/(ms), $f_0 = 0.2$ N.

A.3. Forced Vibration with Dry Friction

$m = 1$ kg, $c = 0.01$ N/(ms), $k = 1$ N/m, $f_0 = 2.5$ N,
$F_{\text{slip}} = 1$ N, $F_{\text{stick}} = 2$ N.

A.4. Forced Stick-slip System

$m = 1$ kg, $c = 0$ N/(ms), $k = 1$ N/m, $v_{\text{dr}} = 1$ m/s,
$\alpha_0 = 1.5$ N, $\alpha_1 = 1.5$ Ns/m, $\alpha_3 = 0.45$ Ns^3/m^3, $f_0 = 0.1$ N.

References

1. Aizerman, M. A. and Gantmakher, F. R., 'On the stability of periodic motions', *Journal of Applied Mathematics and Mechanics* **22**, 1958, 1065–1078 (translated from Russian).
2. Andronov, A. A., Vitt, A. A., and Khaikin, S. E., *Theory of Oscillators*, Dover Publications, New York, 1987, Reprint. Originally published Pergamon Press, Oxford, 1966 (translated from Russian).
3. Armstrong-Hélouvry, B., Dupont, P., and Canudas De Wit, C., 'A survey of models, analysis tools and compensation methods for the control of machines with friction', *Automatica* **30**(7), 1994, 1083–1138.
4. Aubin, J. P. and Cellina, A., *Differential Inclusions*, Springer-Verlag, Berlin, 1984.
5. Begley, C. J. and Virgin L. N., 'Impact response under the influence of friction', *Journal of Sound and Vibration* **211**(5), 1998, 801–818.
6. Blazejczyk-Okolewska, B. and Kapitaniak, T., 'Dynamics of impact oscillator with dry friction', *Chaos, Solitons & Fractals* **7**(9), 1996, 1455–1459.
7. Brogliato, B., *Nonsmooth Mechanics*, Springer-Verlag, London, 1999.

8. Clarke, F. H., Ledyaev, Yu. S., Stern, R. J., and Wolenski, P. R., *Nonsmooth Analysis and Control Theory*, Graduate Texts in Mathematics, Springer-Verlag, New York, 1998.
9. di Bernardo, M., Johansson, K., and Vasca F., 'Sliding orbits and their bifurcations in relay feedback systems', in *Proceedings of the 38th Conference on Design & Control*, Phoenix, CD-ROM publication, 1999, pp. 708–713.
10. di Bernardo, M., Feigin, M. I., Hogan, S. J., and Homer, M. E., 'Local analysis of C-bifurcations in n-dimensional piecewise-smooth dynamical systems', *Chaos, Solitons & Fractals* **10**(11), 1999, 1881–1908.
11. Dankowicz, H. and Nordmark, A. B., 'On the origin and bifurcations of stick-slip oscillations', *Physica D* **136**(3–4), 2000, 280–302.
12. Deimling, K. and Szilagyi, P., 'Periodic solutions of dry friction problems', *Zeitschrift für Angewandte Mathematik und Physik* **45**, 1994, 53–60.
13. Elmer, F.-J., 'Nonlinear dynamics of dry friction', *Journal of Physica A: Mathematical and General* **30**(17), 1997, 6057–6063.
14. Eich-Soellner, E. and Führer, C., *Numerical Methods in Multibody Dynamics*, Teubner, Stuttgart, 1998.
15. Fečkan, M., 'Bifurcations of periodic and chaotic solutions in discontinuous systems', *Archivum Mathematicum* **34**, 1998, 73–82.
16. Feigin, M. I., 'The increasingly complex structure of the bifurcation tree of a piecewise-smooth system', *Journal of Applied Mathematics and Mechanics* **59**(6), 1995, 853–863.
17. Filippov, A. F., 'Differential equations with discontinuous right-hand side', *American Mathematical Society Translations, Series 2* **42**, 1964, 199–231.
18. Filippov, A. F., *Differential Equations with Discontinuous Right-Hand Sides*, Mathematics and Its Applications, Kluwer, Dordrecht, 1988.
19. Foale, S. and Bishop, R., 'Bifurcations in impacting oscillations', *Nonlinear Dynamics* **6**, 1994, 285–299.
20. Galvanetto, U. and Knudsen, C., 'Event maps in a stick-slip system', *Nonlinear Dynamics* **13**(2), 1997, 99–115.
21. Génot, F. and Brogliato, B., 'New Results on Painlevé paradoxes', *European Journal of Mechanics A/Solids* **18**, 1999, 653–677.
22. Glocker, Ch., *Dynamik von Starrkörpersystemen mit Reibung und Stößen*, Fortschr.-Ber. VDI Reihe 18, Nr. 182, VDI Verlag, Düsseldorf, 1995.
23. Guckenheimer, J. and Holmes, P., *Nonlinear Oscillations, Dynamical Systems, and Bifurcations of Vector Fields*, Applied Mathematical Sciences, Vol. 42, Springer-Verlag, New York, 1983.
24. Heemels, W. M. H., 'Linear complementarity systems: A study in hybrid dynamics', Ph.D. Thesis, Eindhoven University of Technology, The Netherlands, 1999.
25. Hinrichs, N., Oestreich, M., and Popp, K., 'On the modelling of friction oscillators', *Journal of Sound and Vibration* **216**(3), 1998, 435–459.
26. Ibrahim, R. A., 'Friction-induced vibration, chatter, squeal and, chaos; Part I: Mechanics of contact and friction; Part II: Dynamics and modeling', *ASME Applied Mechanics Reviews* **47**(7), 1994, 209–226, 227–253.
27. Ivanov, A. P., 'Bifurcations in impact systems', *Chaos, Solitons & Fractals* **7**(10), 1996, 1615–1634.
28. Karnopp, D., 'Computer simulation of stick-slip friction in mechanical dynamic systems', *ASME Journal of Dynamic Systems, Measurement and Control* **107**, 1985, 100–103.
29. Kunze, M. and Küpper, T., 'Qualitative bifurcation analysis of a non-smooth friction oscillator model', *Zeitschrift für Angewandte Mathematik und Physik* **48**(1), 1997, 87–101.
30. Kuznetsov, Y. A., *Elements of Applied Bifurcation Theory*, Applied Mathematical Sciences, Vol. 112, Springer-Verlag, New York, 1995.
31. Leine, R. I., Van Campen, D. H., De Kraker, A., and Van den Steen, L., 'Stick-slip vibrations induced by alternate friction models', *Nonlinear Dynamics* **16**(1), 1998, 41–54.
32. Meijaard, J. P., 'A mechanism for the onset of chaos in mechanical systems with motion-limiting stops', *Chaos, Solitons & Fractals* **7**(10), 1996, 1649–1658.
33. Meijaard, J. P., 'Efficient numerical integration of the equations of motion of non-smooth mechanical systems', *Zeitschrift für Angewandte Mathematik und Mechanik* **77**(6), 1997, 419–427.
34. Müller, P. C., 'Calculation of Lyapunov exponents for dynamic systems with discontinuities', *Chaos, Solitons & Fractals* **5**(9), 1995, 1671–1681.
35. Natsiavas, S., 'Periodic response and stability of oscillators with symmetric trilinear restoring force', *Journal of Sound and Vibration* **134**(2), 1989, 315–331.

36. Natsiavas, S. and Gonzalez, H., 'Vibration of harmonically excited oscillators with asymmetric constraints', *ASME Journal of Applied Mechanics* **59**, 1992, 284–290.
37. Nordmark, A. B., 'Universal limit mapping in grazing bifurcations', *Physical Review E* **55**(1), 1997, 266–270.
38. Nusse, H. E. and York, J. A., 'Border-collision bifurcations including "period two to period three" for piecewise smooth systems', *Physica D* **57**, 1992, 39–57.
39. Oancea, V. G. and Laursen, T. A., 'Investigations of low frequency stick-slip motion: Experiments and numerical modelling', *Journal of Sound and Vibration* **213**(4), 1998, 577–600.
40. Parker, T. S. and Chua, L. O., *Practical Numerical Algorithms for Chaotic Systems*, Springer-Verlag, New York, 1989.
41. Peterka, F., 'Bifurcations and transition phenomena in an impact oscillator', *Chaos, Solitons & Fractals* **7**(10), 1996, 1635–1647.
42. Pfeiffer, F. and Glocker, Ch., *Multibody Dynamics with Unilateral Contacts*, Wiley, New York, 1996.
43. Popp, K., Hinrichs, N., and Oestreich, M., 'Dynamical behaviour of a friction oscillator with simultaneous self and external excitation', in *Sādhāna: Academy Proceedings in Engineering Sciences*, Indian Academy of Sciences, Banglore, India, Part 2-4, Vol. 20, 1995, pp. 627–654.
44. Rasband, S. N., *Chaotic Dynamics of Nonlinear Systems*, Wiley International, Chichester, 1990.
45. Reithmeier, E., *Periodic Solutions of Nonlinear Dynamical Systems*, Springer-Verlag, Berlin, 1991.
46. Roxin, E., 'Stability in general control systems', *Journal of Differential Equations* **1**, 1965, 115–150.
47. Seydel, R., *Practical Bifurcation and Stability Analysis; From Equilibrium to Chaos*, Interdisciplinary Applied Mathematics, Springer-Verlag, New York, 1994.
48. Stelter, P., 'Nonlinear vibrations of structures induced by dry friction', *Nonlinear Dynamics* **3**, 1992, 329–345.
49. Stelter, P. and Sextro, W., 'Bifurcations in dynamical systems with dry friction', *International Series of Numerical Mathematics* **97**, 1991, 343–347.
50. Van der Schaft, A. and Schumacher, H., 'Hybrid systems described by the complementarity formalism', in *Hybrid and Real-Time Systems, Proceedings International Workshop, HART'97*, Grenoble, O. Maler (ed.), Springer-Verlag, Berlin, 1997, pp. 403–414.
51. Van de Vrande, B. L., Van Campen, D. H., and De Kraker, A., 'An approximate analysis of dry-friction-induced stick-slip vibrations by a smoothing procedure', *Nonlinear Dynamics* **19**(2), 1999, 157–169.
52. Wiercigroch, M., 'On modelling discontinuities in dynamic systems', *Machine Vibration* **5**, 1996, 112–119.
53. Yoshitake, Y. and Sueoka, A., 'Forced self-excited vibration accompanied by dry friction', in *Applied Nonlinear Dynamics and Chaos of Mechanical Systems with Discontinuities*, M. Wiercigroch and A. de Kraker (eds.), World Scientific, Singapore, 2000 (to appear).